A TWO DIMENSIONAL TEST OF A SINGLE BAY COLD THRUST AUGMENTATION EJECTOR WING

H. G. Streiff, et al

Bell Aerospace Company

Prepared for:

Air Force Flight Dynamics Laboratory

March 1974

DISCLAIMER NOTICE

THIS DOCUMENT IS BEST QUALITY PRACTICABLE. THE COPY FURNISHED TO DTIC CONTAINED A SIGNIFICANT NUMBER OF PAGES WHICH DO NOT REPRODUCE LEGIBLY.

NOTICE

When Government drawings, specifications, or other data are used for any purpose other than in connection with a definitely related Government procurement operation, the United States Government thereby incurs no responsibility nor any obligation whatsoever; and the fact that the government may have formulated, furnished, or in any way supplied the said drawings, specifications, or other data, is not to be regarded by implication or otherwise as in any manner licensing the holder or any other person or corporation, or conveying any rights or permission to manufacture, use, or sell any patented invention that may in any way be related thereto.

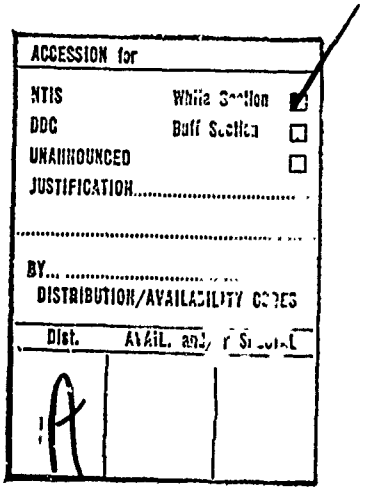

Copies of this report should not be returned unless return is required by security considerations, contractual obligations, or notice on a specific document.

UNCLASSIFIED

Security Classification

AD-779 713

DOCUMENT CONTROL DATA - R & D

(Security classification of title, body of abstract and indexing annotation must be entered when the overall report is classified)

1. ORIGINATING ACTIVITY (Corporate author) Bell Aerospace Company P.O. Box 1 Buffalo, N.Y. 14240	2a. REPORT SECURITY CLASSIFICATION Unclassified 2b. GROUP N/A

3. REPORT TITLE

A TWO DIMENSIONAL TEST OF A SINGLE BAY COLD THRUST AUGMENTATION EJECTOR WING

4. DESCRIPTIVE NOTES (Type of report and inclusive dates)

Final Report

5. AUTHOR(S) (First name, middle initial, last name)

H. G. Streiff
R. Ashby
V. Krishnamoorthy

6. REPORT DATE March, 1974	7a. TOTAL NO. OF PAGES 145	7b. NO. OF REFS 5
8a. CONTRACT OR GRANT NO. F33615-73-C-3128 b. PROJECT NO. 1207 c. d.	9a. ORIGINATOR'S REPORT NUMBER(S) BAC Report No.7500-933010 9b. OTHER REPORT NO(S) (Any other numbers that may be assigned this report) AFFDL-TR-74-4	

10. DISTRIBUTION STATEMENT

This Document is Approved for Public Release; Distribution is Unlimited

11. SUPPLEMENTARY NOTES N/A	12. SPONSORING MILITARY ACTIVITY Air Force Flight Dynamics Lab/FTC Wright Patterson, AFB, Ohio 45433

13. ABSTRACT

A two dimensional model of a single bay cold thrust augmentation ejector wing designed and built by Bell Aerospace Company and utilizing hypermixing nozzles developed by the Aerodynamic Research Laboratory of Wright Patterson Air Force Base was tested both statically and at speed in the Lockheed-Georgia low speed wind tunnel facility. The wing was tested at flap angles of 20 and 30 degrees at airspeeds from 0 to 165 fps and through an angle of attack range of -10 to +30 degrees. The ejector primary pressure ratio was varied from 1.0 to 2.25 and the diffuser area ratio was varied from 1.3 to 2.0.

This report presents a detailed description of the model including its air supply and instrumentation systems, the test facility and data reduction equations and methodology. Also, presented is the detailed run schedule, the data limitations and the resulting plotted data.

DD FORM 1 NOV 68 1473

UNCLASSIFIED

Security Classification

14. KEY WORDS	LINK A		LINK B		LINK C	
	ROLE	WT	ROLE	WT	ROLE	WT
Cold Thrust Augmentation						
Ejector Wing						
2D Wind Tunnel Test						
Single Bay Ejector						
Hypermixing						

TABLE OF CONTENTS

LIST OF FIGURES

LIST OF TABLES

I INTRODUCTION

The Bell Aerospace 2D-CTA single bay ejector wing wind tunnel model was modified for an inlet to nozzle area ratio of approximately 15. The model was tested in the Lockheed-Georgia low speed wind tunnel during the period beginning July 16, 1973 and ending August 1, 1973. The resulting data from that test is presented in this report.

The purpose of the tests was to determine for flap angles of 20 and 30 degrees: (a) The performance of the ejector at static and forward speed conditions; and (b) The aerodynamic characteristics of the wing-ejector combination. The ejector performance data was measured in terms of: (1) static augmentation ratio as a function of primary pressure ratio and diffuser area ratio; (2) ejector gross and net thrust as a function of V_∞, α, diffuser area ratio and primary pressure ratio. The aerodynamic characteristics were obtained for variations of C_L, C_X and $C_{m_{ej}}$ vs α at various δ_e values. The power-off (ejector primary off) effects were also investigated.

The test program was comprised of a total of 60 runs, 39 of these were for a nominal flap angle of 30°, 19 were for flap angle 20° and two were tare runs. The primary test variables and their range of values were;

(a) ejector plenum pressure ratio 1.0 to 2.25
(b) airspeed 0 to 165 fps
(c) ejector diffuser area ratio 1.3 to 2.0
(d) angle of attack -10 to +28 degrees

The flap angle was defined to be the position of the aft flap with respect to the wing chord line. This position was maintained at a fixed angle. The diffusion area ratio was obtained by moving the ejector exit door to the position required to

provide the specified area ratio. Since the thrust vector angle would be approximately the centerline of the ejector diffuser (assuming uniform flow across the ejector) it varies with diffusion area ratio at a given flap angle. The airspeed was measured between the false tunnel walls in close proximity to the model and corrected for tunnel wall and blockage effects. The angle of attack was the angle of the airfoil chord line with respect to horizontal, corrected for tunnel flow angularities and blockage effects. The ejector plenum pressure ratio was the ratio of the total pressure as measured at the center of the hypermixing nozzle plenum and the tunnel atmospheric pressure.

A detailed description of the test facility, model, instrumentation, air supply system and data reduction program is presented in the following sections.

II TEST FACILTIY DESCRIPTION

A. GENERAL

The wind tunnel tests were conducted in the Lockheed-Georgia Company low speed wind tunnel facility. This wind tunnel facility consists of a horizontal single return circuit having two test sections operating at atmospheric pressure. The pertinent details of the two available test sections are summarized in Table I.

TABLE I. FACILITY TEST SECTION CHARACTERISTICS

	V/STOL	LOW SPEED
Size (ft.)	26 wide 30 high 63 long	23.25 wide 16.25 high 43 long
Velocity range (ft/sec)	20.5 to 115	41 to 370
Dynamic pressure range (psf)	0.5 to 40	2 to 160
Total temperature upper limit (^{o}F)	120	120

The low speed test section was used during this program.

B. BALANCE AND MODEL SUPPORT SYSTEM

A six component balance is mounted under each test section and consist of a rigid earth frame, a coupled lift frame, a forces frame, and a moments frame.

Table II lists the design limit loads and the expected accuracy of the longitudinal forces and moments which were of interest during the present investigation. These limits include a model static weight of up to 5000 lb.

TABLE II. FORCE BALANCE LIMIT LOADS AND ACCURACY

	Lift (lbf)	Drag (lbf)	Pitching Moment (lbft)
Limit Load	-5,000 +10,000	-1,500 +3,000	±5,000
Accuracy	±1.0	±0.4	±1.0

Three balance readout sensitivity ranges are also available to provide high resolution for the measurement of small model loads. These ranges are listed in Reference 6.

One-, two-, or three-strut systems are available for use with the balances to support the model and transfer loads to the balances. The struts are generally rendered non-metric by means of wind shields attached to the test section floor.

This program employed the two outside struts of the three strut system and a specially designed pitch actuation system mounted on the left hand strut. The struts were mounted inside false walls which were built inside the wind tunnel. The false walls (discussed in Section III.A) in addition to acting as a wind shield for the support struts and air supply systems became the model end plates necessary for a two-dimensional test.

C. DATA ACQUISITION SYSTEM

The main components of the facility data acquisition system include a CDC 1700 computer, data reading equipment (paper tape and cards), a magnetic tape deck, the computer control typewriter, data printout equipment (line printer and plotters), and the required signal conditioners and amplifiers.

The balance data and model attitude are on digital display. Auxiliary data such as pressure, temperature, and strain gage readings along with wind tunnel parameters may be displayed on 16 digital data channels and 55 analog channels.

In addition, still photographs are available for the collection of qualitative data.

D. AUXILIARY SYSTEMS

Auxiliary air is supplied to the facility via a multistage centrifugal compressor powered by a 4500 h.p. synchronous motor. The system has a capacity of 20 lb/sec up to a total pressure head of 318 psi. The total temperature is approximately 100°F.

An auxiliary electrical system is available to provide a maximum power level of 240 h.p. at voltages up to 400 V.

III MODEL DESCRIPTION

A large two-dimensional wing model was selected for the experimental test portion of this program. It has a span of 76.5", a chord of 60" and its airfoil section is a 747A to 0.4C, 0015-34 to the trailing edge and the whole cambered 2.23%. The wing section is mounted between two metric end plates of 6.5 ft. diameter. The model size was selected from a trade-off between ejector size required for good performance and available wind tunnel facilities suitable for this type testing.

The details of the single bay CTA ejector are shown in Figure 1. The centerline of the ejector mixing bay crosses the wing chord line at the 70% chord station. The centerline of the ejector bay is inclined 30° from the vertical. The ejector is located entirely aft of the 60% chord station. The mixing section width is 5 inches. There are 30 hypermixing nozzles spaced on 2.5 inch centers. The nozzles at each end of the span are placed with their centers 2 inches from the end plates. The plane through the hypermixing nozzle exits is normal to the mixing section centerline The straight-walled, constant area mixing section extends approximately 7 inches below the hypermixing nozzle exit plane. Primary airflow is also introduced into the CTA from 2 slot nozzles running the full span of the wing. One slot nozzle is at the top of the forward side of the inlet and the other is located at the bottom of the aft side of the mixing section.

The inlet slot height is controlled by spacing washers held in place by screws. The mean slot height is 0.020 inches and is maintained by 51 evenly spaced washers, each 0.3125 inches in diameter.

The slot located at the bottom of the aft side of the mixing section has a height of 0.050 inches. A similar slot is located at the flap top surface and is used to control the flow over the wing at large flap angles. This slot was sealed during this test program.

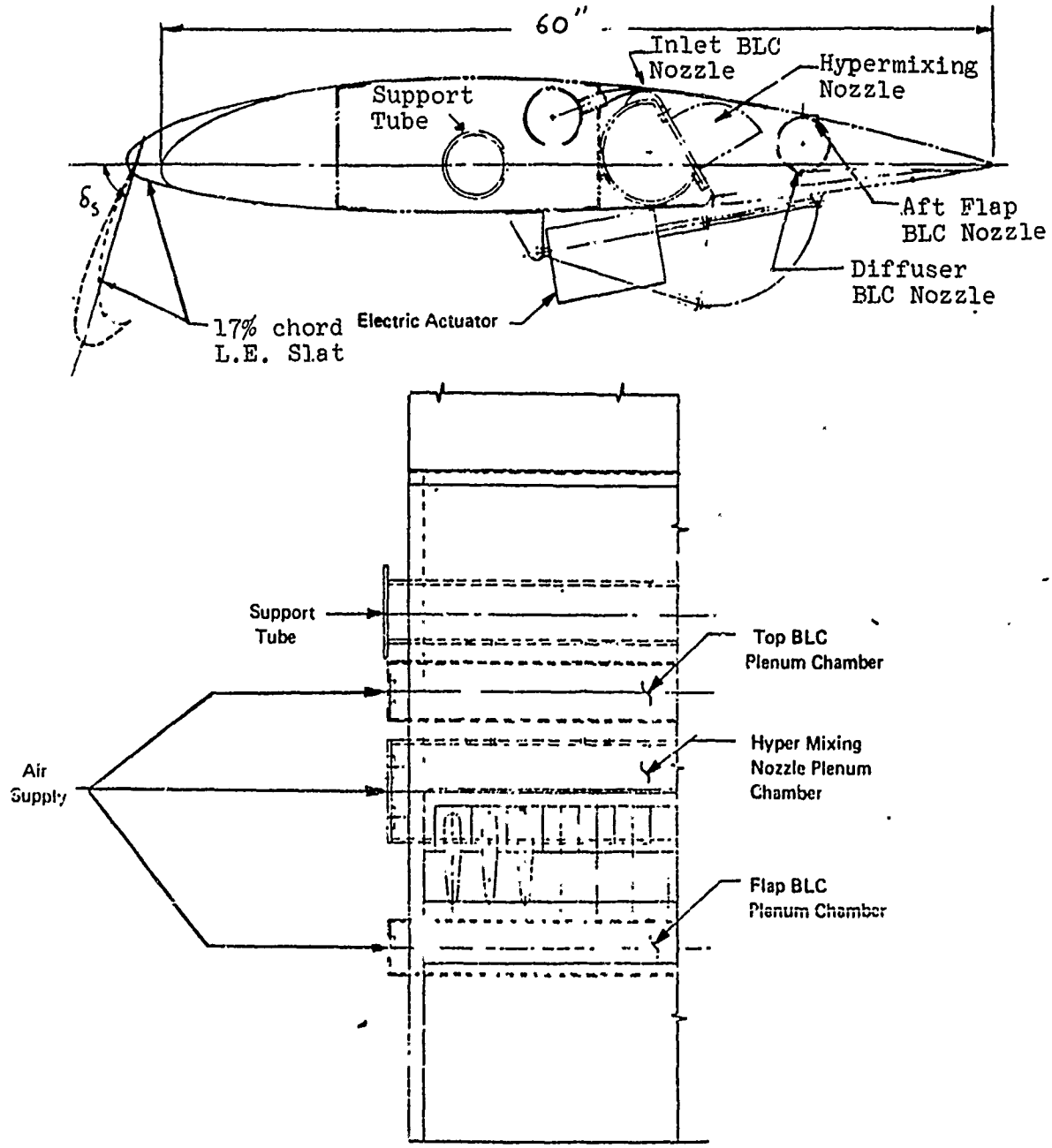

FIGURE 1. CTA 2D MODEL

The plenum chambers, which feed the nozzles, have been made large enough to insure that the internal airflow mach number will be 0.25 and less at the primary nozzle inlets.

The ratio of the inlet area to the effective exit area of the primary nozzles was between 18:1 and 19:1. Appendix B presents a detailed description of the nozzle area ratio, and its determination.

The flap system is composed of an aft flap which is similar to any conventional simple flap and a forward flap which is hinged at the ejector bay exit forward wall. The forward flap when closed is the bay exit door and when deflected forms the ejector forward diffuser wall. The aft flap when deflected forms the ejector aft diffuser wall. The forward flap was designed to be remotely controlled and infinitely variable from zero degrees to 90 degrees. The aft flap is variable in fixed increments to 90 degrees. Provisions for settings of 0, 20, 30, 35, 45, and 60 degrees are currently available. The flap angle was defined to be the position of the aft flap with respect to the wing chord line. This position was maintained at a fixed angle. The diffusion area ratio was obtained by moving the ejector exit door to the position required to provide the specified area ratio. Since the thrust vector angle would be approximately the centerline of the ejector diffuser (assuming uniform flow across the ejector) it varies with diffusion area ratio at a given flap angle.

A leading edge slat was provided which could be positioned at either a 45 or 60 degree angle. During this program all slats on tests were with the slat at the 60° position.

Figures 2 and 3 are front and rear views of the model mounted in the wind tunnel. In these pictures the leading edge slat is installed and the ejector bay is open in a 30° flap setting condition. The 14 pressure rakes visible in Figure 3 were used for determining the ejector exit velocity, the augmented thrust and the augmentation ratio. The rakes are described in more detail in Section V.

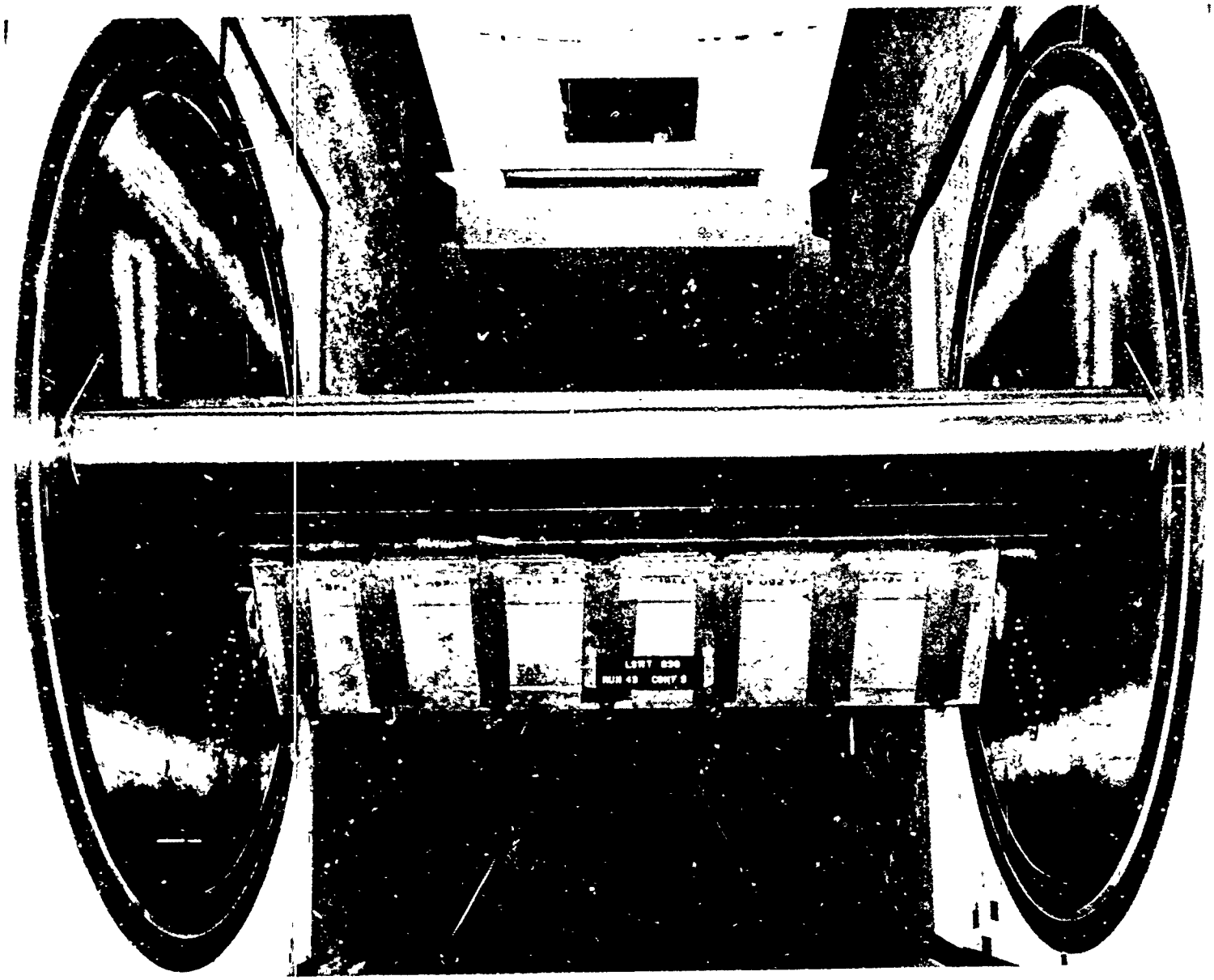

FIGURE 2. CTA 2D MODEL FWD VIEW

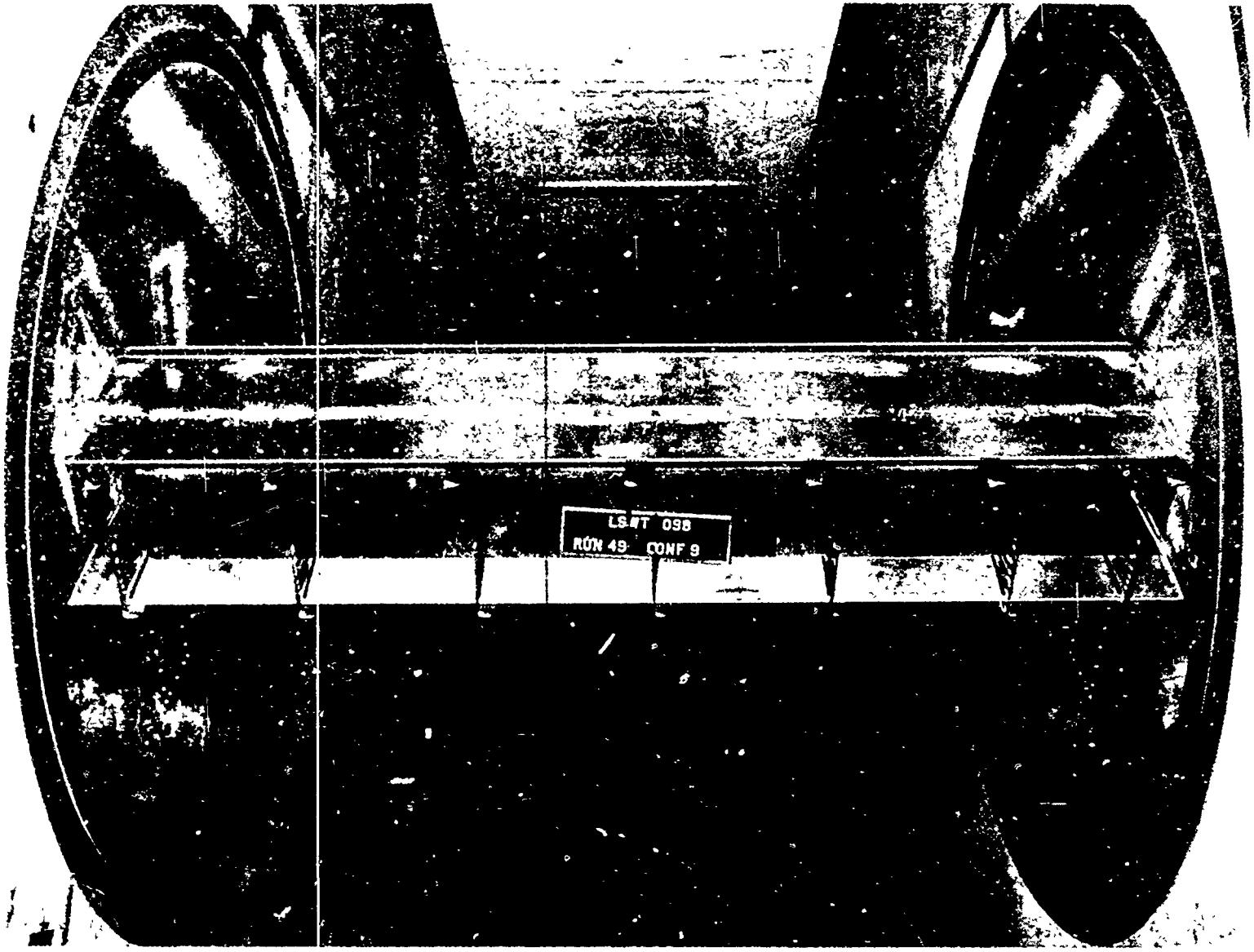

FIGURE 3. CTA 2D MODEL AFT VIEW

To enhance the two-dimensional qualities of the test the 6.5 ft. diameter metric end plates had eight boundary layer control nozzles (4 each) inserted at strategic positions along the wing chord. The nozzles extend from the wing surface upwards and are located approximately 10%, 50% and 75% chord stations and inside the ejector bay at the hypermixing nozzle exit plane. These nozzles blow tangential to the end plate surface to remove the boundary layer at the wing-end plate intersection.

For the wind tunnel test phase of the program the two-dimensional aspects of the model were completed by mounting the wing section and metric end plates between two large nonmetric wall sections built inside the tunnel. Figure 4 shows the model mounted between these false walls. The walls completely spanned the tunnel from floor to ceiling (16.25 ft) and were 28 feet long from leading edge to trailing edge. The model support struts, model ducting and model instrumentation were all located inside these walls so that no airloads were transmitted to the balance because of them.

FIGURE 4. CTA 2D MODEL W.T. INSTALLATION

IV INSTRUMENTATION

The test section dynamic pressure head was computed from the average total and static pressures as measured by 2 total pressure probes and 10 static taps which were located approximately 12 ft. upstream of the model between the false walls.

The model's auxiliary air mass flow rates were monitored by means of orifices mounted in the main air line, the flap air line, the top inlet air line, the end wall air line and the floor blowing air line. A schematic of the air supply system is shown in Figure 5. Static pressure taps positioned on each side of the orifices provided pressures used in the computations of the mass flow rates.

The angle of the ejector bottom door was monitored by means of a rotary potentiometer mounted at the door's hinge point.

The ejector nozzle conditions were measured using total pressure probes located at the closed end of the inlet boundary layer control and flap plenum chambers and through total pressure probes located in the left entrance, right entrance and center of the hypermixing plenum chamber. The mixing section exit pressures were measured by two sets of rakes (five probes each rake, one for total and one for static pressure measurements) positioned as shown in Figure 6 and 7.

The end plate boundary layer control slot nozzles were monitored by measuring the pressure in each slot plenum.

Ejector exit conditions were measured by means of 14 pressure rakes mounted as shown in Figure 3. The locations of these rakes are shown in Figure 14. Seven of these rakes were suspended from the flap while the remainder were mounted from the door. The upper and lower rakes which were mounted at centerline (B.L.0.0) of the model each consisted of six pitot static probes. The remaining six upper rakes contained five total probes and one pitot static probe while all the probes of the six remaining bottom door rakes were of the total pressure variety.

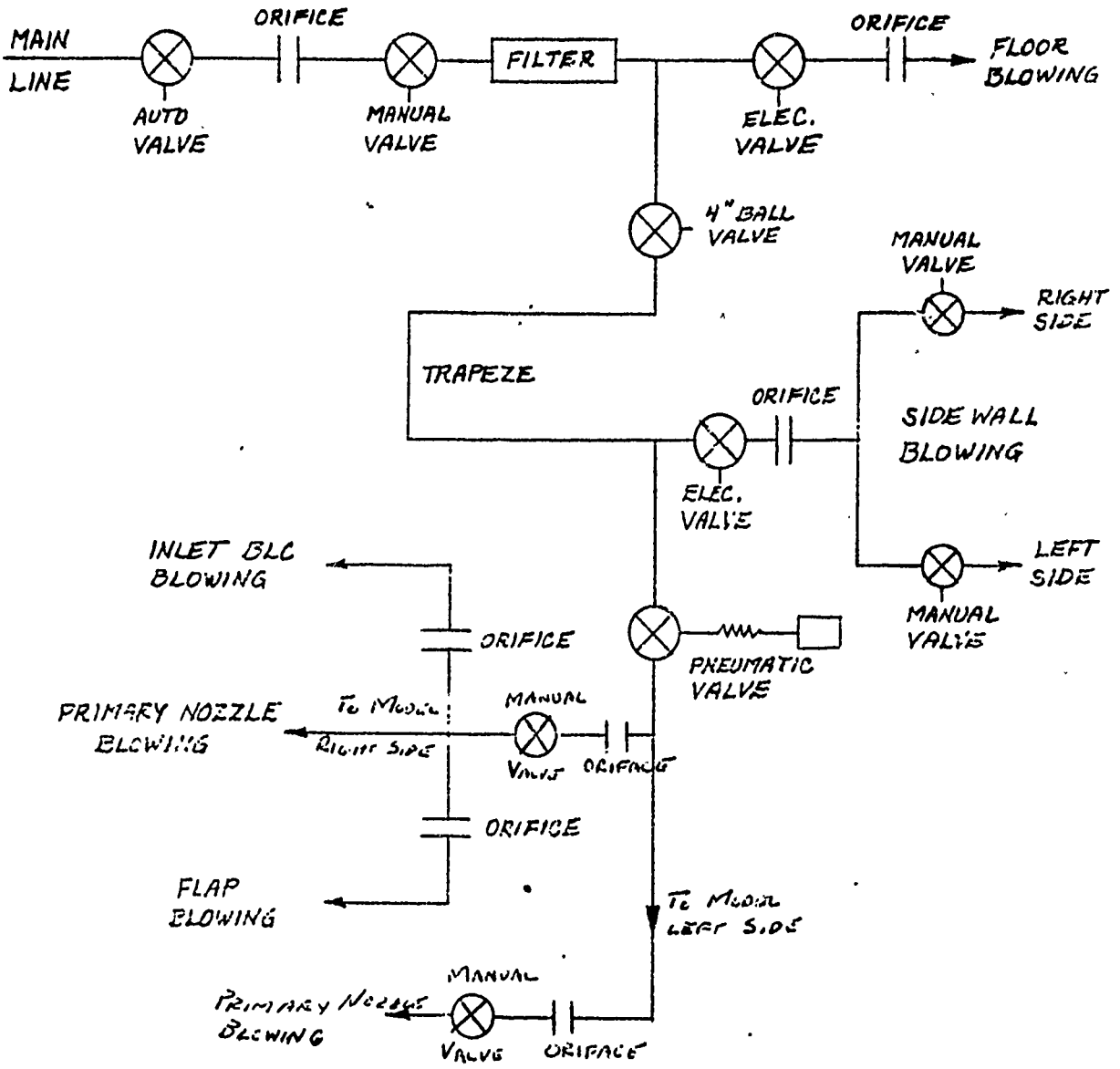

FIGURE 5. SCHEMATIC OF MODEL AIR SUPPLY SYSTEM

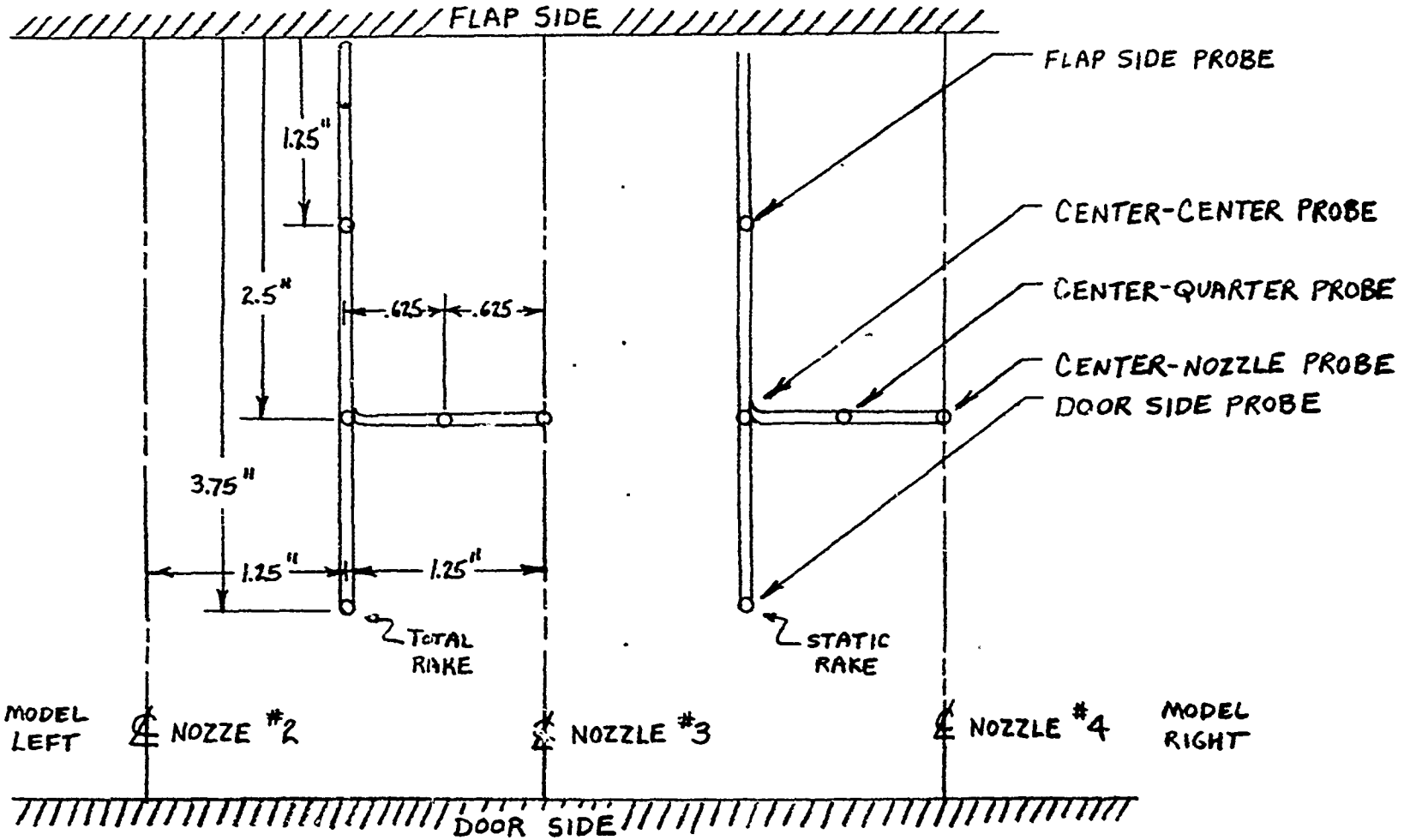

FIGURE 6 PLAN VIEW, MIXING SECTION RAKES

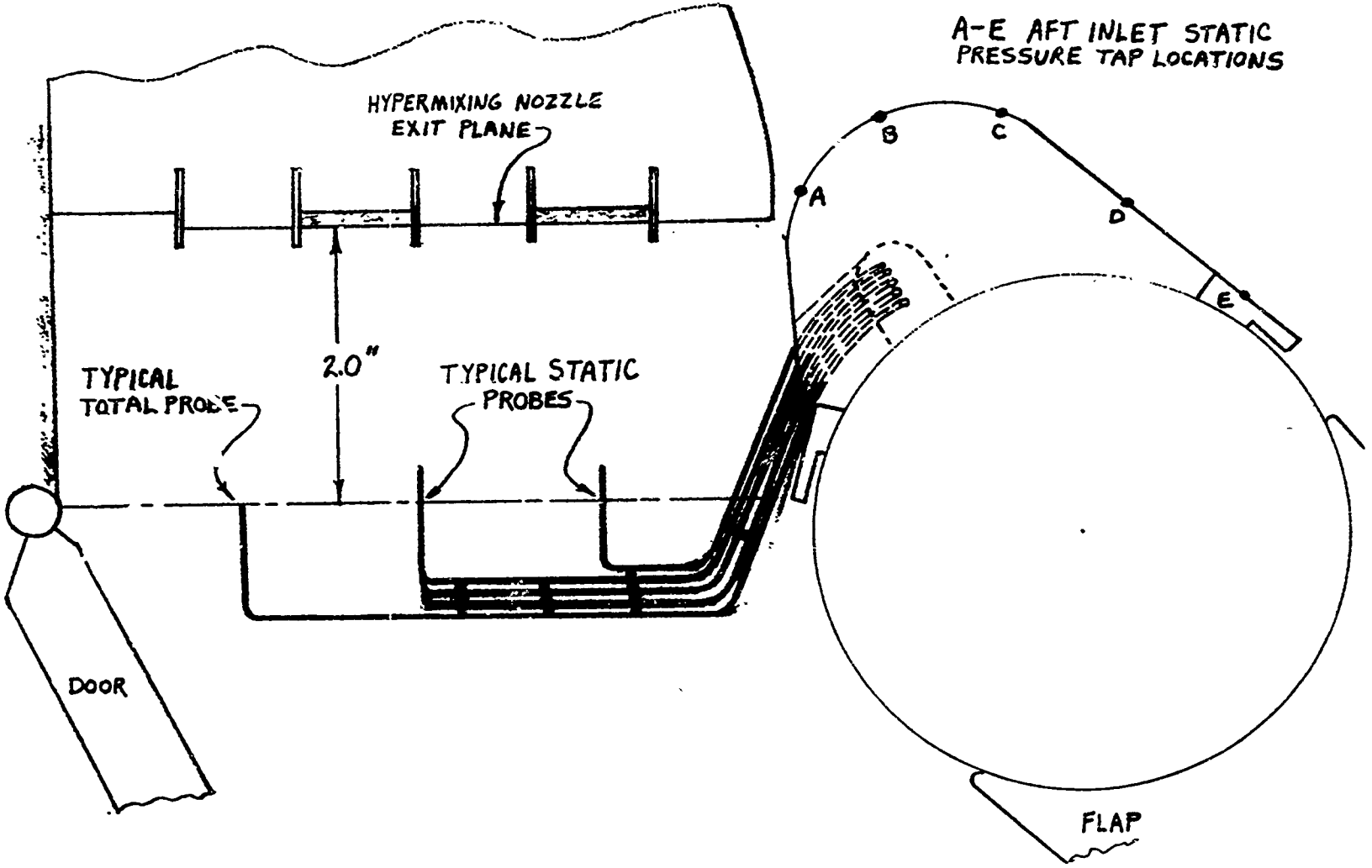

FIGURE 7 SIDE VIEW, MIXING SECTION RAKE

A typical upper rake is shown in Figure 8. The ports of the total probes were bevelled internally approximately 30 degrees to minimize the effects of misalignment of the fixed probes with respect to the airstream velocity vectors. Figure 16.16 of Reference 1 indicates that approximately 15 degrees of misalignment is possible with this type of port with no significant error.

A 21 port boundary layer rake and 16 port static pressure board were installed on the floor under the model to measure test parameters in the vicinity of the floor. Table III gives pertinent dimensions of both the boundary layer rake and floor static pressure board.

The main balance is a null type system, and the six-component forces and moments are measured on precision weighbeams. Each weighbeam is balanced by moving a jockey weight along the length of each beam. The position of the jockey weight on each weighbeam which indicates the balance loads is determined by an optical encoder. Encoder output is converted to the appropriate signals for entry into the Data Acquisition System (D.A.S.).

Wing chordwise pressure distribution was measured by 30 static pressure taps located around the wing outer surfaces at the 25 inch span station. The chordwise location of each pressure tap is given in Section V.

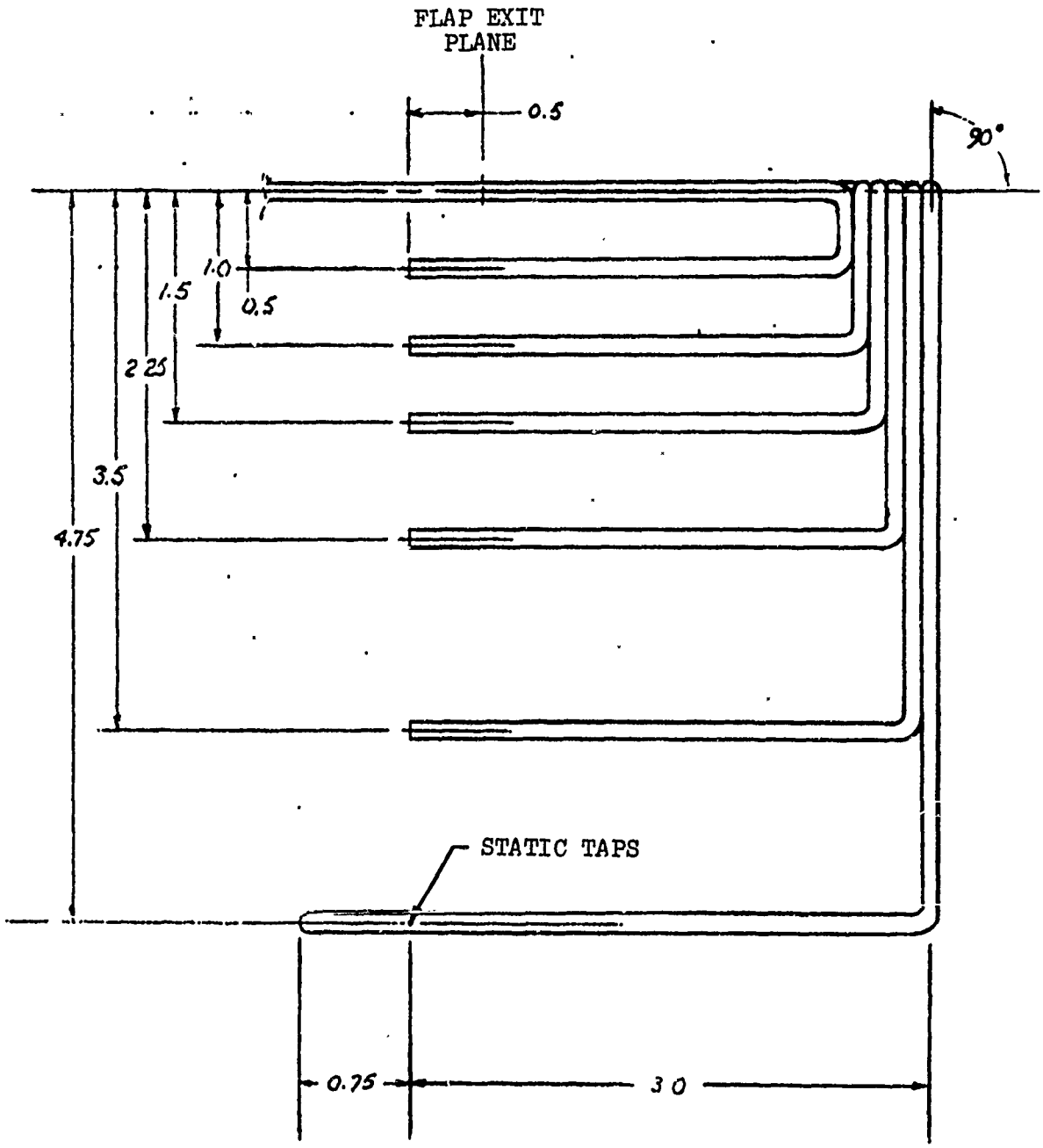

FIGURE 8. TYPICAL UPPER RAKE CONFIGURATION

TABLE III

BOUNDARY LAYER RAKE AND FLOOR STATIC BOARD

Orifice Locations - Boundary Layer Rake

Orifice	Inches Above Floor	Orifice	Inches Above Floor
1	0.500	12	6.000
2	1.000	13	7.000
3	1.500	14	8.000
4	2.000	15	9.000
5	2.500	16	10.000
6	3.000	17	11.000
7	3.500	18	12.000
8	4.000	19	14.000
9	4.500	20	16.000
10	5.000	21	18.000
11	5.500		

Orifice Locations - Floor Static Board

Orifice	End Wall	Surface	X, Z Location, Feet
1, 12	South, North	Stream Side	-8, 5
2, 13			-11, -1
3, 14			-8, -1
4, 15			-5, -1
5, 16			-8, -5
6, 17		Back Side	-11, -1
7, 18			-8, -1
8, 19		Stream Side	6, -1
9, 20			11, -1
10, 21		Back Side	6, -1
11, 22			11, -1

Note: Positive directions are up and downstream.

V DATA REDUCTION

Six-component external main balance, test section freestream, and model pressure data were reduced on-line during the test as-well-as off-line after the test using standard FORTRAN reduction programs for the on-site Control Data Corporation 1700 computer. Wind tunnel corrections accounting for balance interactions, weight tares, trapeze tares, end plate tares, wind tunnel wall effects, and freestream flow angularities were applied to the data.

A. CORRECTIONS TO TEST DATA

The reduced aerodynamic and propulsive data were tabulated according to the format presented on Table IV. The aerodynamic data are presented in the data listing in both the corrected and uncorrected forms. The uncorrected data is tabulated on page 1 of the reduced data format. It is a compilation of the tunnel instrumentation readout corrected only for tare parameters with no test section blockage or flow irregularities included. The corrected data is tabulated on page 3 of the reduced data format. This data, in addition to having the usual corrections for model weight, trapeze, and end wall blowing tares applied to the balance force and moment readout, was also corrected for tunnel curvature and blockage effects.

The test section dynamic pressure and velocity were corrected for model blockage and wake blockage for the power-off (no blowing through primary hypermixing nozzles) condition; only model blockage corrections were applied to the power-on case. These corrections are given in Reference 2 and are listed below for convenience.

$$q_{o\ corr} = q_{o\ uncorr}\ (1 + 2\epsilon) \qquad (1)$$

where $\epsilon = \epsilon_{s.b.} + \epsilon_{w.b.}$

$$\epsilon_{s.b.} = \frac{K_1 \times \text{Model Volume}}{C^{3/2}}$$

$K_1 = 0.74$ for wing spanning tunnel breadth

Model volume = wing volume only

= 0.7 x wing thickness x wing chord x wing span

C = tunnel cross sectional area within end walls
- area due to displacement thickness around the perimeter of the test section.

$$\varepsilon_{w.b.} = \frac{1}{4} \frac{C}{h} \cdot C_{d_{uncorr}}$$

C = wing chord
h = tunnel height
C_d = uncorrected drag coefficient

The corrections for test section velocity and model Reynolds number will be

$$V_{corr} = V_{uncorr} (1 + \varepsilon) \tag{2}$$

$$RN_{corr} = RN_{uncorr} (1 + \varepsilon) \tag{3}$$

The conventional stream line curvature corrections will be applied to the power-off and power-on test data. These corrections are

$$\alpha_{corr} = \alpha_{uncorr} + \frac{57.3\sigma}{2\pi} C_{l_{uncorr}} + 4 Cm_{\frac{1}{4}uncorr} \tag{4}$$

$$C_{\ell\ corr} = C_{\ell\ uncorr} (1 - \sigma - 2\varepsilon) \tag{5}$$

$$C_{m_{\frac{1}{4}corr}} = C_{m_{\frac{1}{4}}\ uncorr} (1 - 2\varepsilon) + \frac{\sigma C_{\ell_{corr}}}{4} \tag{6}$$

$$C_{d_{corr}} = C_{d_{uncorr}} (1 - 3\varepsilon_{s.b.} - 2\varepsilon_{w.b.}) \tag{7}$$

where $\sigma = (\frac{\pi^2}{48}) (c/h)^2$

Note that in equations (5), (6) and (7), $\varepsilon_{w.b.}$ is made zero when correcting power-on test data.

The corrections for Ram drag and ejector exit momentum coefficients are

$$(\text{Ram drag})_{corr} = \text{Entrained flow rate} \times V_{corr}$$

$$C\mu_{corr} = \frac{\text{ejector gross thrust}}{Q_{o_{corr}} \times S_{ref}}$$

where S_{ref} = wing plan area

The inlet slot and flap upper surface slot momentum coefficients are corrected as follows:

$$C\mu \text{ inlet slot (corr)} = \frac{\text{momentum through inlet slot}}{Q_{o_{corr}} \times S_{ref}}$$

$$C\mu \text{ flap (corr)} = \frac{\text{momentum through flap upper surface slot}}{Q_{o_{corr}} \times S_{ref}}$$

The uncorrected and corrected results of a typical test (Run No. 75) are shown in figures 9 to 11. Solid blockage correction increases the dynamic head of the main stream. The wake blockage is substantially altered by the jet exit momentum and when conventional wake blockage correction is applied, it decreases the value of the free stream dynamic pressure. The blockage effects are reflected in the value of C_μ obtained in the test.

The induced stream line curvature over the wing chord and alterations to the curvature of the jet sheet are to be considered in any two dimensional jet-blowing model tests. In the absence of any available wall corrections, conventional corrections are applied. The lift curve slope is essentially the same, and for a specified α lowest C_l value is obtained when solid blockage and curvature corrections are applied. The same corrections produce lower nose down moment and lower thrust for C_1 values of interest.

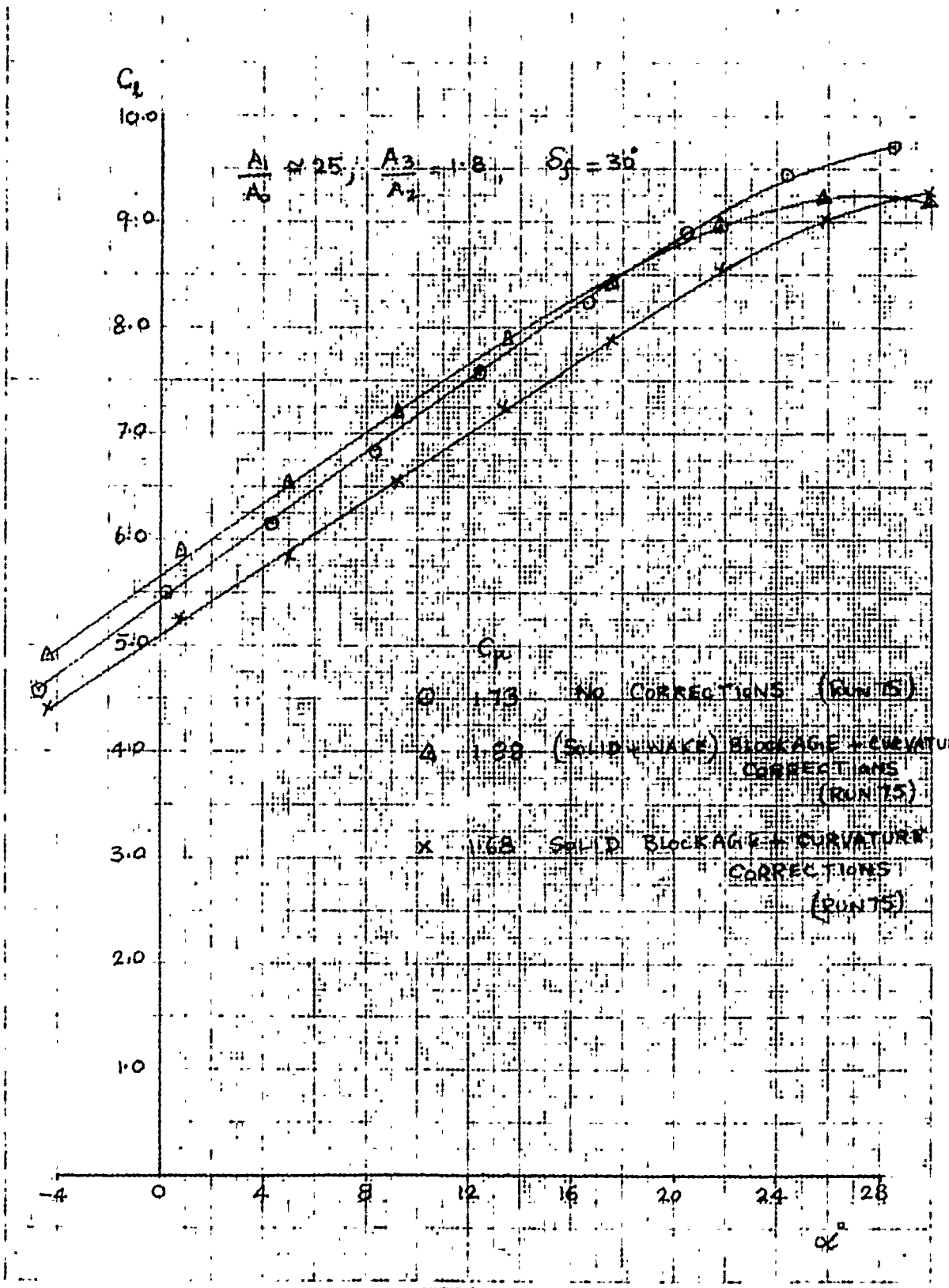

FIGURE 9. C_l VS α, EFFECT OF VARIOUS TUNNEL CORRECTIONS

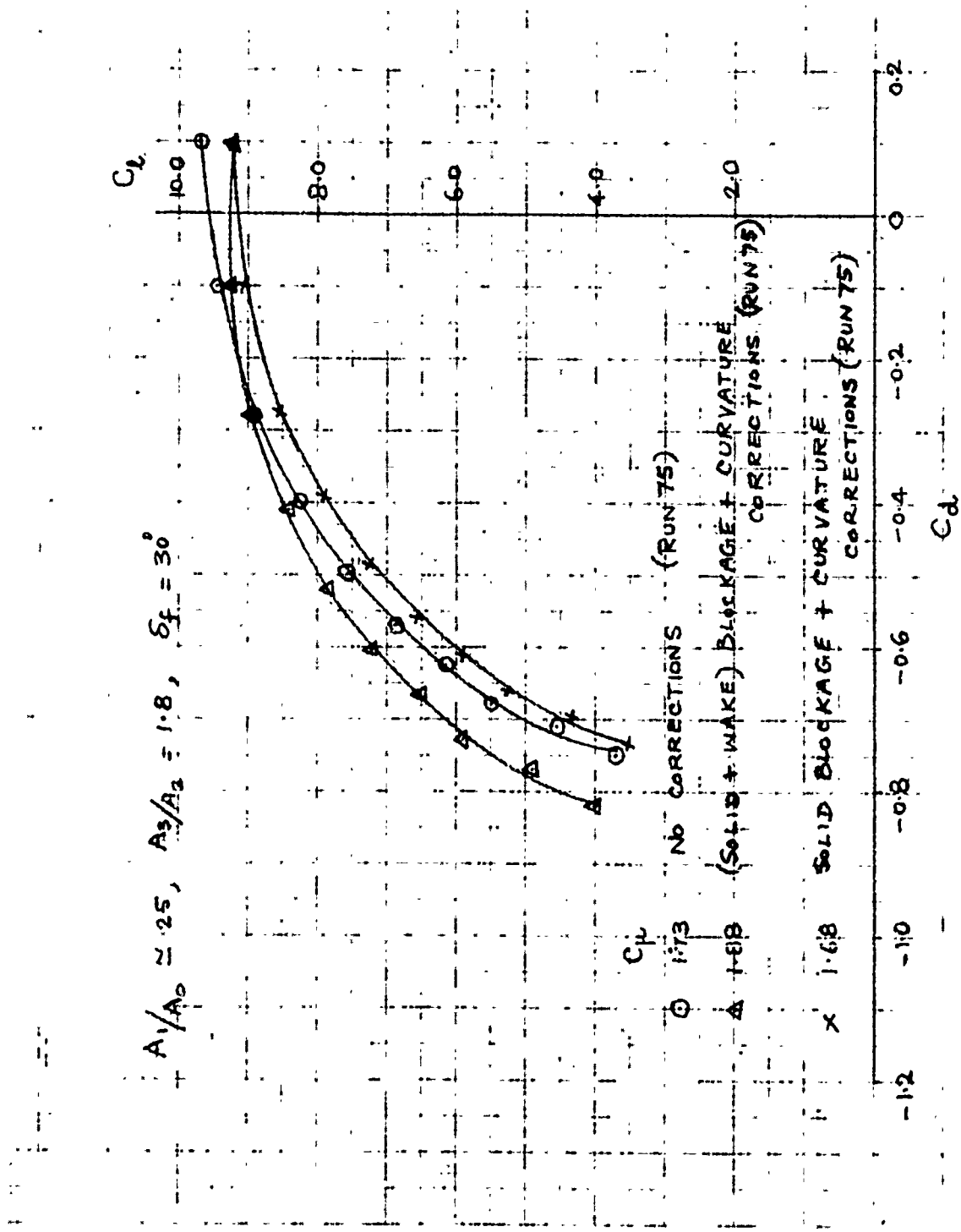

FIGURE 10. C_d VS C_ℓ, EFFECT OF VARIOUS TUNNEL CORRECTIONS

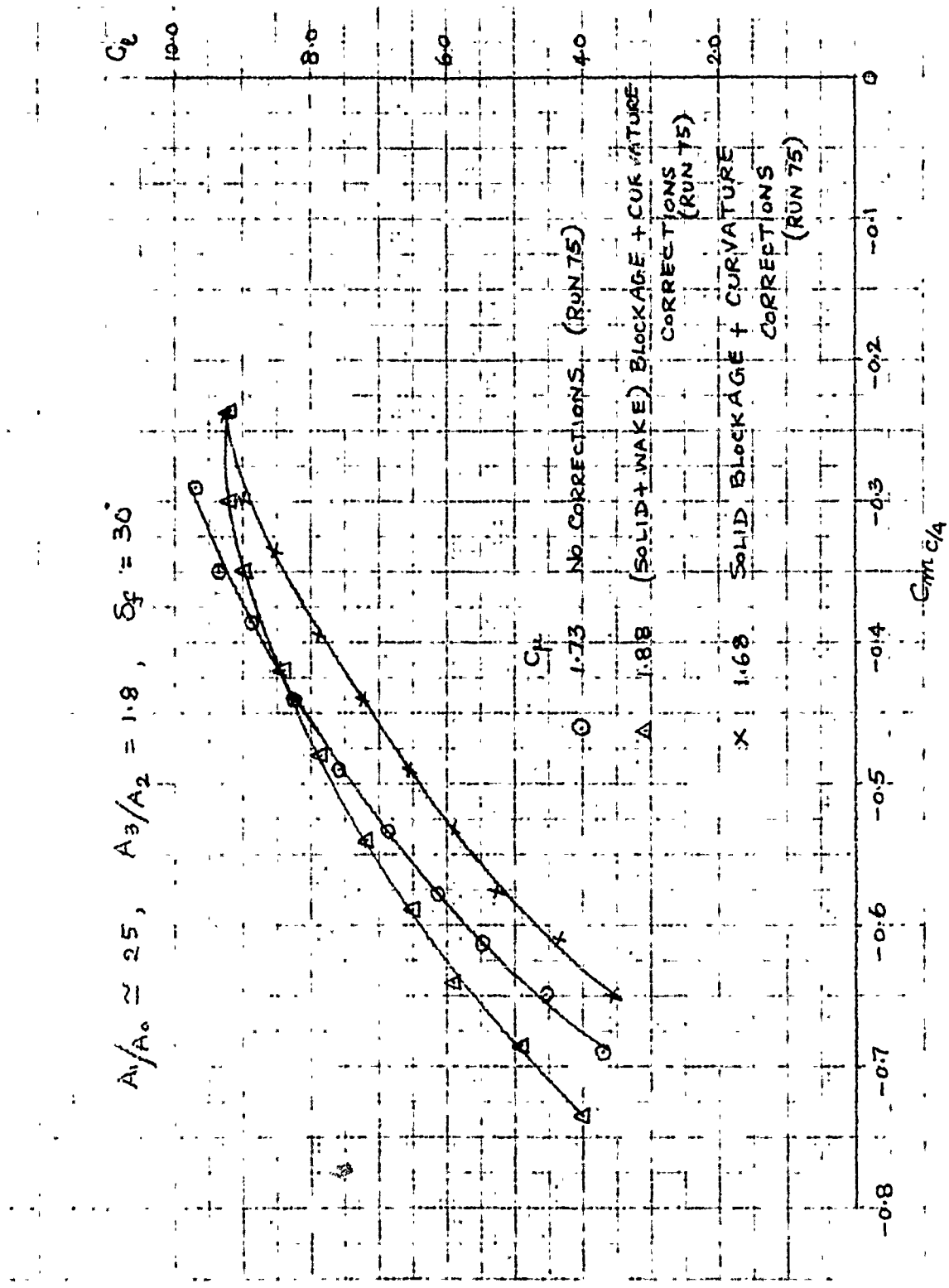

FIGURE 11. $C_{m_{C/4}}$ VS C_ℓ, EFFECT OF VARIOUS TUNNEL CORRECTIONS

B. DATA METHODS, TABULATION AND FORMAT

A detailed description of the data tabulation format together with the equations and methods required for developing each data item is presented in this section. The page and line listing given in parenthesis following each data item refers to those listed on the sample format data sheets presented in Table IV.

1. Title Section (page 1, lines 1-6)

This section identifies the data but contains no data. The date in the title block is the date on which the data was reduced, not the date the run was made. The entire program was assigned the test number 108 by Lockheed.

The runs are numbered consecutively. Run number 1 is the trapeze tare run and run number 2 is the boundary layer control end blowing tare run. Run number 3 is the first actual wing section test run. The configuration number identifies which set of primary nozzles are on the model. Configuration 1 designates the FDL nozzle set.

2. Model Attitude and Free Stream Data (page 1, lines 7-11)

The information on this line is as follows:

PT = Test Point, a point within the run at which data is taken.

ALPHA= Model angle of Attack, the angle the airfoil chord line makes with the tunnel horizontal. This is a geometric alpha. The aerodynamic corrected alpha is shown in another section.

QO = Tunnel free stream dynamic pressure, measured between the model end walls 10.5 ft forward of the basic airfoil leading edge (approx. 2 chord lengths) QO is based on VO.

VO = The average tunnel free stream velocity. It is the arithmetic average of two pitot-static probes.

RN = Model Reynolds number

PO = Tunnel test section free stream static pressure

TO = Tunnel test section free stream static temperature

TABLE IV. SAMPLE FORMAT DATA SHEETS

REPORT LSRI 108
MODEL CTOL- 2D
DATE 05 SEP 75
PAGE 8- 7

TEST ID. RUN 49 C F 2

MODEL ATTITUDE AND FREESTREAM DATA

PT	ALPHA (DEG)	QO (PSF)	VO (FPS)	RN (10-6)	PO (PSFA)	TO (DEG-R)	VJ (FPS)	VR (FPS)
3	7.33	.67	24.7	.703	2036.0	541.5	23.6	25.6

MAIN BALANCE DATA

	CL	CD	CM	RESULTANT (LBS)	THETA (DEG)	XCHORD (IN)
WING SECTION	326.0820	-305.9812	-299.6029			
END PL TARE (LBS)	28.1	-21.8	-63.7			
FLAP THRUST	0	0	0			
EJECTOR THRUST	326.1	-309.0	-299.6	449.2	-46.5	11.03

MASS FLOW DATA

	T (DEG-R)	P (PSFA)	DP (PSF)	W (LB/S)	PERCENT	PRIMARY SPLIT	HYPER SPLIT
TUNNEL MAIN	558.3	20736.27	295.25	10.43	100.0		
MODEL RIGHT		14550.69	1870.16	5.97			
MODEL LEFT		14342.68	1149.45	3.30			
MODEL END		10715.00	1168.78	1.57			
TUNNEL FLOOR		2637.61	.00	.00			
DISCREPANCY					3.6		
INLET PLENUM		3957.61	310.1	.83		8.9	
FLAP PLENUM		3903.32	323.63	.99		20.4	
RIGHT HYP PLENUM				3.25			49.7
LEFT HYP PLENUM				3.30			50.3
TOTAL HYP PLENUM				6.55		70.7	

EJECTOR PLENUM DATA

	PT (PSFA)	PR (PT/PO)	AO (IN-2)	MACH NO.	VEL (FPS)	PS (PSIA)	PT-PS (PSI)	PT-PO (PSI)	AOH/30= .366 IN-2 AOT = .109 FT-2	
INLET PLENUM	3773.4	1.809	1.44					11.41		
FLAP PLENUM	3654.1	1.795	3.31					11.24	A1	=381.57 IN-2
HYP PLENUM CENTER	3815.6	1.874	10.97					12.36	A2	=392.50 IN-2
RIGHT	3815.6			.124	142.90	26.22	.28	12.36	A3	=783.31 IN-2
LEFT	3817.6			.136	157.70	26.17	.31	12.37	A1/AO = 24.27	

END PLOTTING PRESSURE

	PLENUM PRESSURE (PSIA) LEFT	RIGHT
FORWARD SLOT	50.29	52.70
MID-SPAN SLOT	42.32	52.54
AFT SLOT	56.70	54.69
EJECTOR BAY SLOT	22.37	22.12

MIXING SECTION EXIT PRESSURE

	PT (PSFG)	PS (PSFG)
FLAP SIDE	24.7	4.4
CENTER CENTER	7.9	4.4
CENTER QUARTER	.9	-112.8
CENTER NOZZLE	46.4	-75.7
DOOR SIDE	.0	-4.4

TABLE IV. (continued)

REPORT LSNT 108
MODEL CIA- 2D
DATE 05 SEP 73
PAGE B- 8

TEST 108 RUN 49 CONF 2

POINT 3 RAKE DATA

EJECTOR EXIT TEMP(DEG-R)=539.5 LE(IN)=10.24 LR(IN)=10.25 DELD(DEG)=24.0 DELR(DEG)=20.0 A9/A2= 2.00

		FLAP DY= .650	.500	.625	1.000	1.250	1.126	1.126	1.125	.875	.625	.500	DOOR .87=
RIGHT													
DY= 6.25	PT(PSFA)	2066.4	2053.7	2055.9	2062.2	2067.2	2061.6	2069.9	2072.9	2138.7	2158.6	2136.6	2115.9
	PS(PSFA)	2023.0	2023.1	2023.1	2023.0	2023.0	2024.6	2025.0	2024.2	2022.5	2022.3	2022.2	2021.5
	VM(FPS)	199.2	187.2	175.6	189.3	196.9	155.2	202.6	211.0	326.1	333.2	315.1	293.4
	VE(FPS)	166.2	156.8	137.9	154.3	168.3	116.7	175.4	183.1	305.6	333.8	298.3	269.4
DY=14.00	PT(PSFA)	2036.2	2043.1	2048.1	2045.8	2067.6	2049.3	2065.9	2051.6	2090.7	2110.6	2086.3	2078.9
	PS(PSFA)	2024.2	2024.3	2024.3	2024.2	2025.1	2025.8	2026.1	2025.4	2023.7	2023.4	2023.3	2023.0
	VM(FPS)	104.9	131.2	147.5	140.6	219.1	166.4	190.5	154.9	247.5	282.3	240.1	226.1
	VE(FPS)	14.2	80.6	104.9	94.5	216.6	109.8	164.8	119.2	222.9	260.4	213.9	197.5
DY=12.00	PT(PSFA)	2058.2	2073.4	2077.7	2087.2	2091.4	2061.3	2075.2	2072.2	2082.3	2093.1	2105.4	2115.1
	PS(PSFA)	2024.9	2025.1	2025.1	2024.9	2025.8	2026.6	2026.5	2026.1	2024.4	2024.2	2024.1	2023.8
	VM(FPS)	174.2	210.2	219.4	238.6	244.9	178.1	210.1	205.2	230.0	250.9	272.5	269.0
	VE(FPS)	141.9	184.4	194.7	215.8	234.5	151.6	188.8	181.4	205.0	227.7	251.1	248.2
DY=12.00	PT(PSFA)	2021.4	2020.4	2020.3	2020.5	2024.3	2028.1	2048.1	2068.0	2087.8	2095.6	2092.3	2090.0
	PS(PSFA)	2023.2	2023.3	2023.3	2023.2	2024.1	2024.8	2025.2	2024.4	2022.7	2022.5	2022.4	2022.1
	VM(FPS)	.0	.0	.0	.0	14.3	54.6	144.8	199.6	244.0	259.2	255.0	249.5
	VE(FPS)	.0	.0	.0	.0	.0	.0	104.9	170.5	216.9	233.3	226.2	221.6
DY=12.00	PT(PSFA)	2055.6	2060.2	2064.5	2079.4	2083.9	2052.7	2051.9	2066.6	2097.1	2124.2	2114.7	2101.4
	PS(PSFA)	2021.1	2021.2	2021.2	2021.1	2021.9	2022.7	2023.0	2022.3	2020.6	2020.3	2020.2	2019.9
	VM(FPS)	177.8	188.9	199.1	231.2	238.1	191.2	162.7	201.3	264.8	308.4	284.1	273.3
	VE(FPS)	133.5	148.2	160.9	196.7	208.6	155.7	120.3	166.6	235.7	283.1	267.4	263.9
DY=14.00	PT(PSFA)	2072.3	2070.2	2062.1	2084.1	2071.6	2056.1	2062.5	2077.5	2087.9	2113.0	2127.8	2123.6
	PS(PSFA)	2020.2	2020.3	2020.3	2020.2	2021.1	2021.8	2022.2	2021.4	2019.7	2019.5	2019.4	2019.0
	VM(FPS)	218.3	213.7	193.5	241.9	215.1	127.1	192.1	226.6	250.0	292.8	315.2	309.6
	VE(FPS)	181.6	176.3	153.9	209.1	179.9	135.1	155.2	194.2	217.2	264.6	288.8	282.2
DY= 6.25	PT(PSFA)	2080.7	2067.9	2062.2	2082.0	2079.6	2058.0	2067.7	2114.2	2143.2	2133.2	2133.3	2125.8
	PS(PSFA)	2023.7	2023.8	2023.8	2023.7	2024.5	2025.3	2025.6	2024.8	2023.1	2022.9	2022.8	2022.5
	VM(FPS)	228.5	200.9	187.4	231.1	211.7	123.1	196.2	285.7	331.4	317.6	317.9	307.5
	VE(FPS)	201.6	170.3	154.2	204.6	184.8	141.5	169.8	266.5	312.1	297.2	297.3	285.7
LEFT													

AIRFOIL PRESSURE DISTRIBUTION (CP)

PERCENT CHORD	0	1.25	2.5	5	10	15	20	40	55	60
TOP	-3.04	-8.01	-7.15	-6.92	-6.60	-6.17	-6.27	-8.21	-18.18	
BOTTOM		-.79	-.33	-.22	-.12	-2.72	-.14	-.23	-.22	-.25

IN. FROM TE	A	B	C	D	E	16	12	9	6	4	2
TOP FLAP	-362.67	-265.17	-68.97	-10.69	-4.79		-.45	-.22		-.66	
BOTTOM DOOR						-.25	-.23		-.34		-.36

TABLE IV. (continued)

TEST IDN RUN 43 CONF 2

POINT 3 PERFORMANCE DATA

GROSS THRUST AUGMENTATION RATIO (FG/FI)	= 1.622	
NET THRUST AUGMENTATION RATIO ((FG-FR)/FI)	= 1.435	
CMU EJECTOR (FG/QD*SREF) (SREF=31.875 SQ.-FT.)	=435.718	
MASS AUGMENTATION RATIO ((WE-WP)/WP)	= 7.431	
EJECTOR GROSS THRUST (FG)	=435.75 LBS.	
PRIMARY ISENTROPIC THRUST (FI) TOTAL	=299.50 LBS.	
HYDROMIXING	=311.58 LBS.	
INLET SLOT	= 26.27 LBS.	CMU=26.271
DIFFUSER SLOT	= 59.65 LBS.	
FLAP THRUST (ESTIMATED)	= .00 LBS.	CMU= .000
EJECTOR PUMP DRAG (FR) AND RAM DRAG COEF.	= 52.86 LBS.	CD =52.864
PRIMARY PUMP DRAG (FPR)	= 7.11 LBS.	
PRIMARY WEIGHT FLOW (WP)	= 3.24 LBS./SEC.	
EJECTOR EXIT WEIGHT FLOW (WE)	= 28.10 LBS./SEC.	
MEAN EJECTOR EXIT VELOCITY ((G*FG)/WE)	=200.12 FPS	
SYS. NET AUGMENTATION RATIO (FG-FR-FPR)/(FI-FPR)	= 1.436	
STATIC THRUST AUGMENTATION RATIO = FORCE BALANCE	= 1.560	

VO (FPS)	PRN	DELF (DEG)	A1/AC	A3/A2	ALPHI (DEG)	SLOT	TOP SLOT	DIF. SLOT	FLAP SLOT
24.71	1.87	20.00	24.27	2.05	7.33	ON	ON	ON	OFF

DATA CORRECTED FOR STREAM CURVATURE AND BLOCKAGE EFFECTS

ALPHAC (DEG)	CLC	CDC	CMC	QDC (PSF)	PDC (PSF)	VDC (FPS)	RNC (10-6)
7.33	320.0620	-308.9812	-299.6029	.668	2036.01	24.71	.703

CMUC EJECT	CMUC INLET	CMUC FLAP	CDC RAM	FRC (LB)	FPRC (LB)	PRNC
435.748	26.271	.000	52.864	52.86	7.11	1.87

VL = Freestream velocity as determined by a pitot-static tube whose tip is 12.5 ft forward, and 1.67 ft below the basic airfoil 40% chord point. The tube is 1.5 ft from the left end wall.

VR = Free stream velocity as determined by a pitot-static tube whose tip is 12.5 ft forward, and 1.67 ft above the basic airfoil 40% chord point. The tube tip is 1.5 ft from the right endwall.

NOTE: The pitot-static tube locations are presented relative to the model 40% chord point because the model pivots around this point and it serves as a convenient reference point. The values of V, and Q are measured values. Corrected values appear elsewhere in this report.

3. Main Balance Data (page 1, lines 13-21)

In this section up to four lines of data are shown under four column headings. The column headings are defined as follows:

CL = Lift
CD = Drag
CM = Pitching Moment
Resultant = Magnitude of the ejector induced force vector
Theta = Direction of the ejector induced force vector
X chord = Position of the ejector induced force vector

When the tunnel Q is less than 2.0, the lift and drag are given in pounds and the pitching moment is given in foot-pounds. When tunnel Q exceeds 2.0, the lift drag and moment are given in coefficient form.

The first line of data is the wing section lift, drag, and pitching moment. All tares including end blowing tares have been applied.

The second line is a listing of the end blowing tare used in arriving at the wing section data of the previous line, and is always shown in pounds.

The third and fourth lines are printed only when Q is less than 2.0. Line four labeled, flap thrust, is the estimated thrust which is produced by the top of the flap BLC slot. This slot was not used during this test program hence these thrust values are always zero. Line four is the ejector induced thrust and in this test program always equal to the wing section force. The angle theta and the distance XCHORD are printed for all low speed tests, but are only valid for points where angle of attack equals zero. Theta and XCHORD are defined as follows.

$$\theta = \text{Arctan}\left(\frac{\text{Lift}}{\text{Drag}}\right)$$

$$\text{XCHORD} = \frac{\text{Pitching Moment at 25\% chord}}{(\text{resultant force})\ (\sin \theta)}$$

4. Mass flow Data (page 1, lines 22-39)

In this section all the data pertaining to the high pressure air supply mass flows is displayed.

There are seven square edged metering orifices in the high pressure air supply system. These are identified as follows.

Tunnel main, This orifice is located in the main air supply line. All high pressure air used in the test passes this metering station.

Model Right, This orifice meters all air supplied to the right side of the model, exclusive of the end wall blowing air. This air goes to the right manifold and then into the inlet BLC slot plenum tube, the flap BLC plenum tube, and the right end of the hypermixing nozzle plenum tube.

Model Left, This orifice meters all air supplied to the left side of model, exclusive of the end wall blowing air. All air passing this orifice enters the hypermixing nozzle plenum tube.

Model End, This orifice meters all the BLC air supplied to the model endwall slots.

Tunnel Floor, This orifice meters all air supplied to the test section, tunnel floor blowing slot.

Inlet Plenum, After the inlet BLC slot air leaves the right side air manifold, it passes this metering orifice.

Flap Plenum, This orifice installation is similar to the inlet BLC slot orifice installation and meters all air entering the flap tube plenum.

The weight flow through each of the orifices is determined from the measured values of air temperatures (T), orifice upstream static pressure (P) and the static pressure differential (DP) across the orifice plate. The temperature is measured at one station near the main orifice and is assumed to remain constant throughout the system since the high pressure air temperature is near that of the ambient surroundings. The measured temperature, upstream pressure, pressure differential, and reduced weight flowrate (W) are displayed in this section for each of the seven metering orifices. The data was reduced using the following equations recommended in Reference 4.

$$W = .525\ K\ Y\ D^2 \left(\frac{P(DP)}{R\ T}\right)^{\frac{1}{2}},\ LB/SEC$$

where $K \equiv Cd/(1-\beta^4)^{\frac{1}{2}}$

$$Y = 1-(0.41+.35\beta^4)(DP/1.4P)$$

β = D/Dpipe

D = orifice diameter, inches

R = gas constant, ft-lb/lb-°R

The ejector primary weight flowrates were determined from four of the seven orifices. The characteristics of these four are shown in Table V.

TABLE V - PRIMARY ORIFICE CHARACTERISTICS

NAME	TAP LOCATION	D pipe INCHES	D INCHES	β	K EQUATION (Ref. 2)
MODEL LEFT	FLANGE	4.026	2.250	0.559	$K=0.63667(1+(475.28/RN))$ (1)
MODEL RIGHT	FLANGE	4.026	2.650	0.658	$K=0.67130(1+(879.02/RN))$ (1)
INLET PLENUM	D & ½ D	4.321	2.199	0.510	$K=0.62090+(1.471/(RN)^{\frac{1}{2}})$ (1)
FLAP PLENUM	D & ½ D	4.321	3.104	0.720	$K=(0.70994+(3.246/(RN)^{\frac{1}{2}}))(0.985)$ (2)
					(1) AT RN ≥ 30,000
					(2) AT RN ≥ 50,000
					NOTE, RN ≡ PIPE REYNOLDS NO.

The main orifice total weight flow was assigned an arbitrary value of 100 percent. The sum of the weight flows from the other six orifices should equal the weight flowrate through the main orifice. The extent to which this sum did not match the main orifice result is displayed on the data sheet in the Percent column and on the line labeled Discrepancy.

The primary split column displays what percentage of the primary ejector air goes to each of the three types of primary nozzles.

The Hyper split column displays what percentage of the hypermixing nozzle air supply is entering at each end of the plenum tube.

5. Ejector Plenum Data (page 1, lines 40-49)

This section presents primarily the pressure data gathered in the ejector plenums. Five total pressure measurements were made and they are listed in the column marked PT. The pressure tap locations are as follows.

Inlet Plenum = A pressure tap at the dead end of the inlet slot plenum tube.

Flap Plenum = A pressure tap at the dead end of the flap plenum tube.

Hyp Plenum Center = A wall tap located on the hypermixing nozzle plenum tube surface, at midspan.

Hyp Plenum Right, Hyp Plenum Left = Total pressure probes located as shown in Figure 12.

In the third column are the primary nozzle effective areas. The effective areas are computed as follows.

$$AO = \frac{W(T)^{\frac{1}{2}}}{(FFT)}\ (PT)$$

AO = Effective area of the nozzle, inches

W = Measured flowrate through the nozzle, #/sec

T = Primary air supply temperature, °R

PT = Plenum total pressure, PSIA

FFT- Total flow function

where,

$$FFT = \left(\frac{PO}{PT}\right)\left(\frac{2\gamma g}{(\gamma-1)R}\right)^{\frac{1}{2}}\left(\frac{PT}{PO}^{\frac{2(\gamma-1)}{\gamma}} - \frac{PT}{PO}^{\frac{\gamma-1}{\gamma}}\right)^{\frac{1}{2}}$$

PO = Tunnel static pressure

γ = Ratio of specific heats, 1.4

R = Gas constant, 53.3 ft#/#°R

g = Gravity constant, 32.2 ft/sec^2

In the forth and fifth columns the Mach number and velocity of the air at both ends of the hypermixing nozzle plenum are dis-

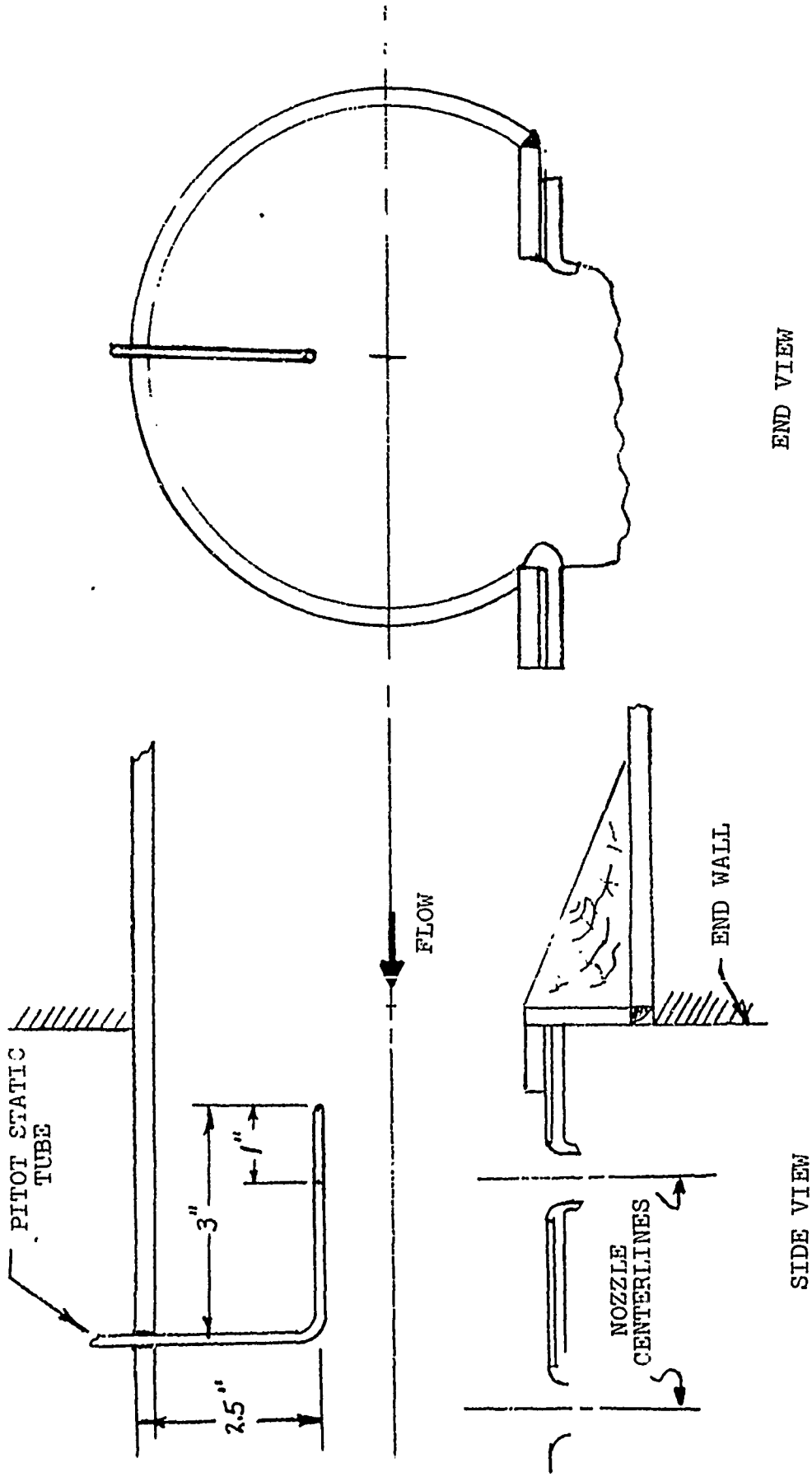

FIGURE 12. HYPERMIXING NOZZLE PLENUM TOTAL PRESSURE PROBES

played. These values are computed as follows

PT = Total pressure reading from pitot-static probe
PS = Static pressure reading from pitot-static probe
T = Supply air total temperature

$TS = T(\frac{PS}{PT})^{\frac{\gamma-1}{\gamma}}$ = static temp at plenum inlet

$AV = (\gamma\ gRT)^{\frac{1}{2}}$ = speed of sound at plenum inlet

$VEL = (\ (2)(Cp)\ (J)\ (g)\ (T-TS)\ )^{\frac{1}{2}}$ = velocity at plenum inlet

MACH NO. = VEL/AV = Mach number at plenum inlet
J = Joule's Constant, 778.3 BTU/FT-LB
Cp = Constant pressure specific heat, 0.24 BTU/lb-°R

In column six are the readings of the static pressure ports on the pitot-static tubes and column seven is the measured difference between the pitot-static tube total and static readings. Column eight is the measured plenum pressures presented as gauge pressures.

Column nine contains five areas and one area ratio. These values are defined as follows:

AOH/30 = The mean effective area of the thirty hypermixing nozzles.
AOT = The total ejector primary effective area.
A1 = The estimated inlet area available to the ejector secondary flow at the hypermixing nozzle exit plane.

$A1 = (5.15)(76.5) - (AOH + AOI)$

where

5.15 = Ejector bay width at hypermixing nozzle exit plane (inches)
76.5 = Ejector bay span, inches
AOH = Effective exit area of thirty hypermixing nozzles
AOI = Effective exit area of the inlet BLC slot

A2 = Ejector mixing section area at end of straight walled mixing section. This area lies in a plane parallel to, and 2.1 inches below the hypermixing nozzles exit plane. The value of 382.5 square inches is a constant for this model and is the 5 inch bay width multiplied by the 76.5 inch bay span.

A3 = The diffuser exit area. This area is defined by LE of item 7 multiplied by the wing span (76.5 in.).

A1/A0 = The inlet secondary to primary area ratio. It was this area ratio which was intended to have a nominal value of 15 to 1 for this test program.

6. End Blowing Pressures and Mixing Section Exit Data (page 1, lines 50-60)

The end blowing pressures are measured at each of the end wall blowing slot plenums and are listed in columns one and two.

The mixing section exit pressures are measured by two sets of rakes positioned as shown in figures 6 and 7.

7. Diffuser Exit Rake Data (page 2, lines 1-42)

This section presents both the measured and computed diffuser exit rake values. These values are listed as follows.

PT = Rake total pressure measurement. These measurements were taken at 84 locations within the diffuser exit.

PS = Rake static pressure measurement or estimate. The static pressures were measured at 18 rake locations and estimated at the remaining 66 locations.

VM = The air velocity at the probe or measuring station

$$VM = \left(64.4\ (PT-PS)\frac{(53.3)(T3)}{PS}\right)^{\frac{1}{2}}$$

where T3 = The measured ejector exit temperature, shown on page 2, line 3 of print-out.

VE = The ultimate diffuser air exit velocity attained when the air static pressure equals ambient. The additional diffusion which takes place beyond the rake probes is assumed to occur with negligible additional total pressure loss.

$$VE = \left(64.4\ (PT-PO)\frac{(53.3)(T3)}{PO}\right)^{\frac{1}{2}}$$

The estimated static pressures are formed as follows. Each probe tip location is designated by the subscripting convention shown below.

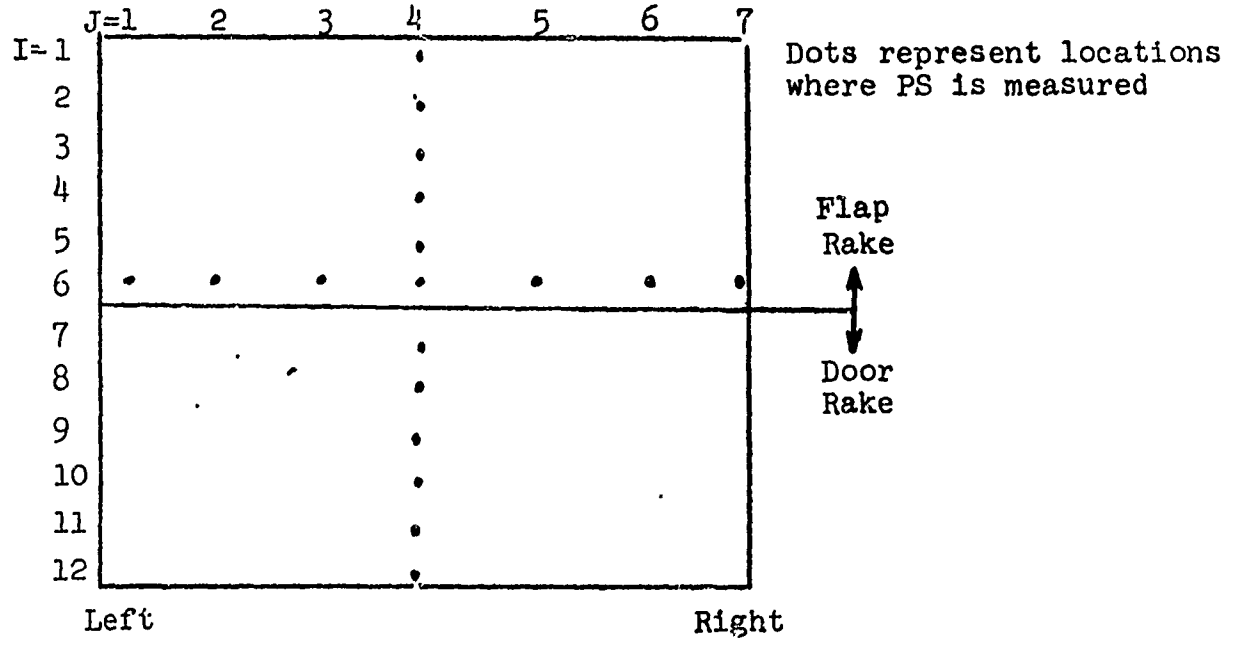

Then,

$$PS\ (I, J) = PS\ (I, 4)\left(\frac{PS(J,6)}{PS(J,4)}\right)$$

Line 3 of this page lists, in addition to the ejector exit temperature, two diffuser exit dimensions, the flap and door position indicator angles, and the diffuser exit (A3) to mixing section (A2) area ratio. The diffuser exit dimensions are defined as follows.

LE = The diffuser exit dimension is used to compute the diffuser exit area (A3). This dimension has been arbitrarily defined as shown in Figure 13.

LM = The exit dimension along which the rake probe readings are assumed to apply. This dimension is also shown in Figure 10.

DELD = The door position angle is a parameter used when conducting the test to aid in setting the door position and is included

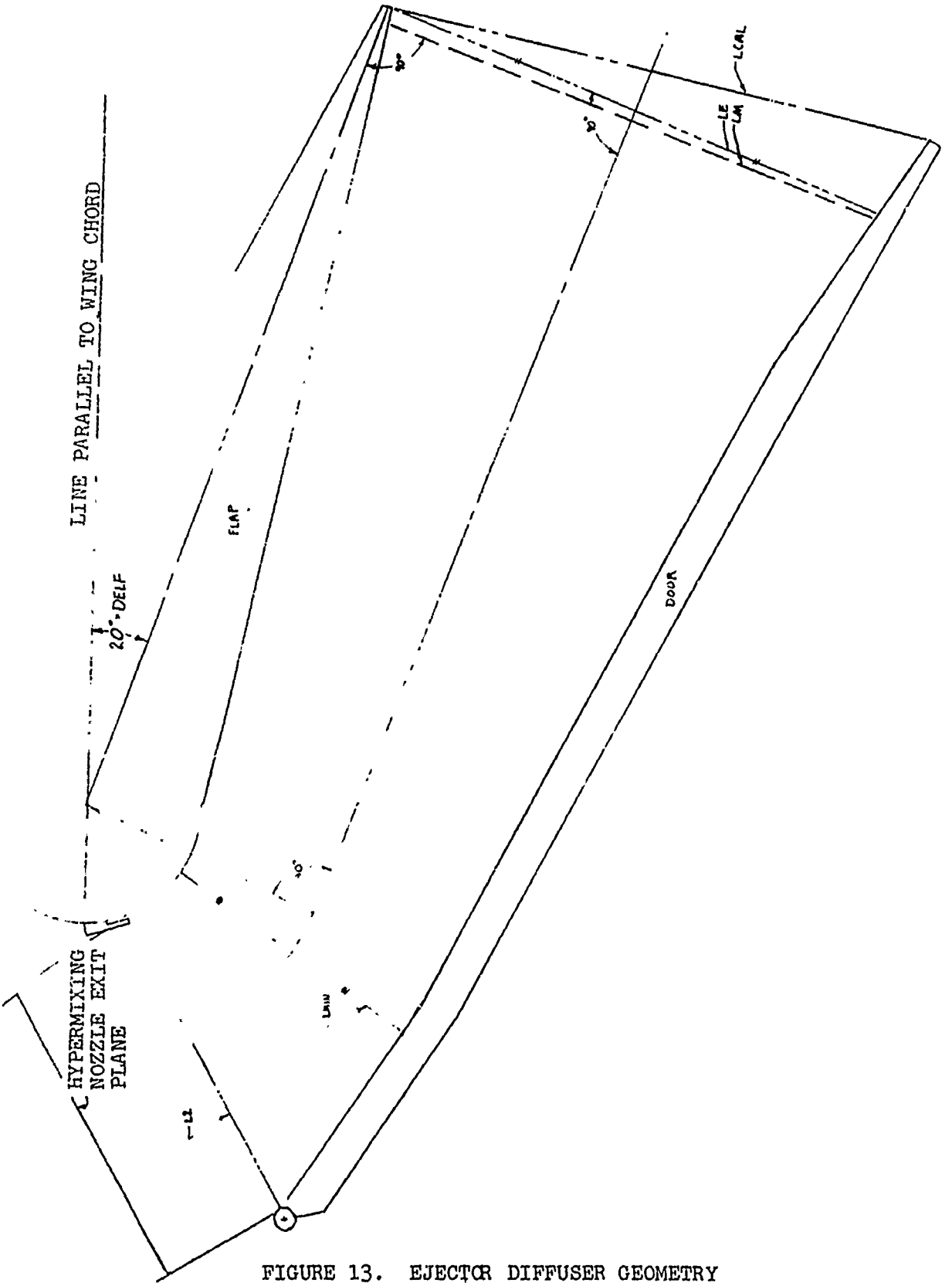

FIGURE 13. EJECTOR DIFFUSER GEOMETRY

in the output for reference only.

DELF = The flap angle is defined as the angle the flap chord line makes with the basic airfoil chord line. This angle is 5° greater than the amount of flap deflection required to achieve it.

A3/A2 = The diffuser exit to mixing section area ratio. This is defined as follows,

$$A3/A2 \equiv LE/5.0$$

Also shown on page 2 are the increments along the span (DY) and the increments (DZ) along the exit dimension (LM), over which each probe reading is assumed to apply. The values of DY are picked so that the probes are near the center of the increment over which they apply. These increments were selected before the tests began and were never changed. The sum of the DY increments is 76.5 inches. The actual location of the rakes within these increments is shown in Figure 14.

The DZ increments for each probe, used in the integration to determine total ejector mass flow, over the distance from mid way between each of the adjacent probes or from the ejector wall and the adjacent probe as shown below.

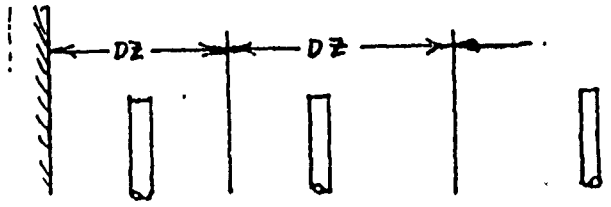

In the case of overlapping rakes the DZ values for any probe on a door rake which falls above the sixth probe on a flap rake is assigned the value of zero. The sum of all the DZ increments equal LM.

8. Airfoil Pressure Distribution (page 2, lines 43-52)

This section displays airfoil surface static pressure. If QO is less than 2.0 the units on these values are PSFG, but if QO exceeds 2.0 the values are in the form of pressure coefficients.

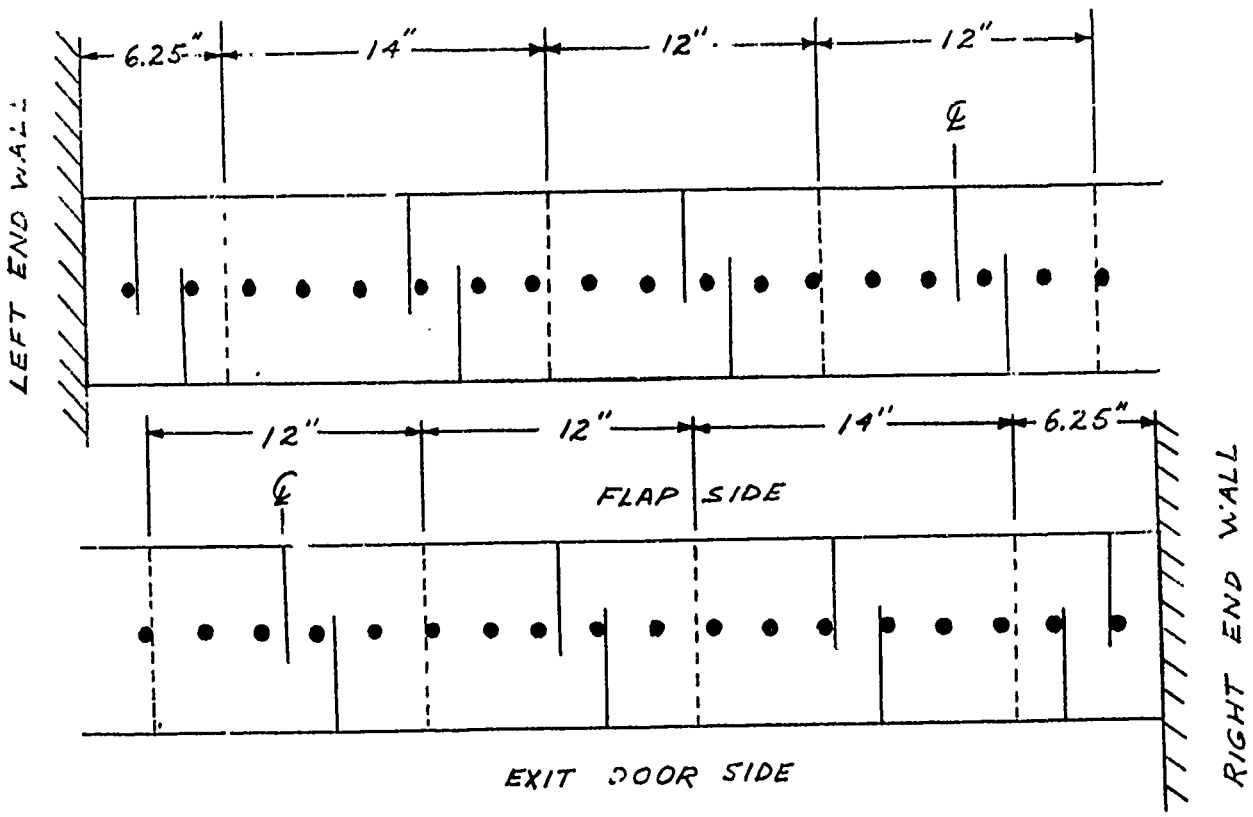

NOTES:

1. Solid vertical lines signify locations of pressure rakes.
2. Dashed vertical lines signify integration elements (DY) covered by each set of pressure rakes.
3. Black dot signifies the location of each hypermixing nozzle
4. Drawing is 1/8 scale

FIGURE 14. EJECTOR EXIT PLANFORM

Figure 15 shows the pressure tap locations as designated in the data printout. Table VI presents these locations in percent of chord of the closed wing. The locations around the airfoil surface are given as a percent chord for taps forward of the 60% chord line. Behind the ejector the pressure tap locations are identified by their distances in inches from the trailing edge of the flap and door respectively. Five locations along the ejector aft inlet are denoted by the letters A through E. These locations are identified on Figure 7.

9. Performance Data (page 3, lines 1, 41)

The following equations are used to produce the performance results presented in this section. The gross thrust augmentation ratio is determined for the two dimensional wing section. The end blowing nozzles, while introducing air into the ejector, are assumed to be doing nothing more than helping maintain the two dimensional character of the flow across the entire wing span. For this reason, the airflow through these nozzles is not considered when the rentropic primary thrust (FI) component of the thrust augmentation ratio is being computed for the two dimensional section. No correction is applied to the gross thrust (FG) as determined by the diffuser exit rakes since these rakes are far enough from the high velocity wall jet flow to be uneffected by it. The reaction force produced by these wall jets must be subtracted from the thrust balance reading however, to determine the wing section contribution to the balance force.

The density at the diffuser exit measuring section, along line LM, is calculated as follows.

$$RHOM(I,J) = PS(I,J)/(53.3)(T3)$$

Next the flowrate through each area increment is computed.

$$W(I,J) = (DZ(I)(DY(J)) \quad (RHOM(I,J)\ (VM(I,J))$$

The total ejector exit mass flowrate and thrust are determined by summing up the values determined for each probe increment.

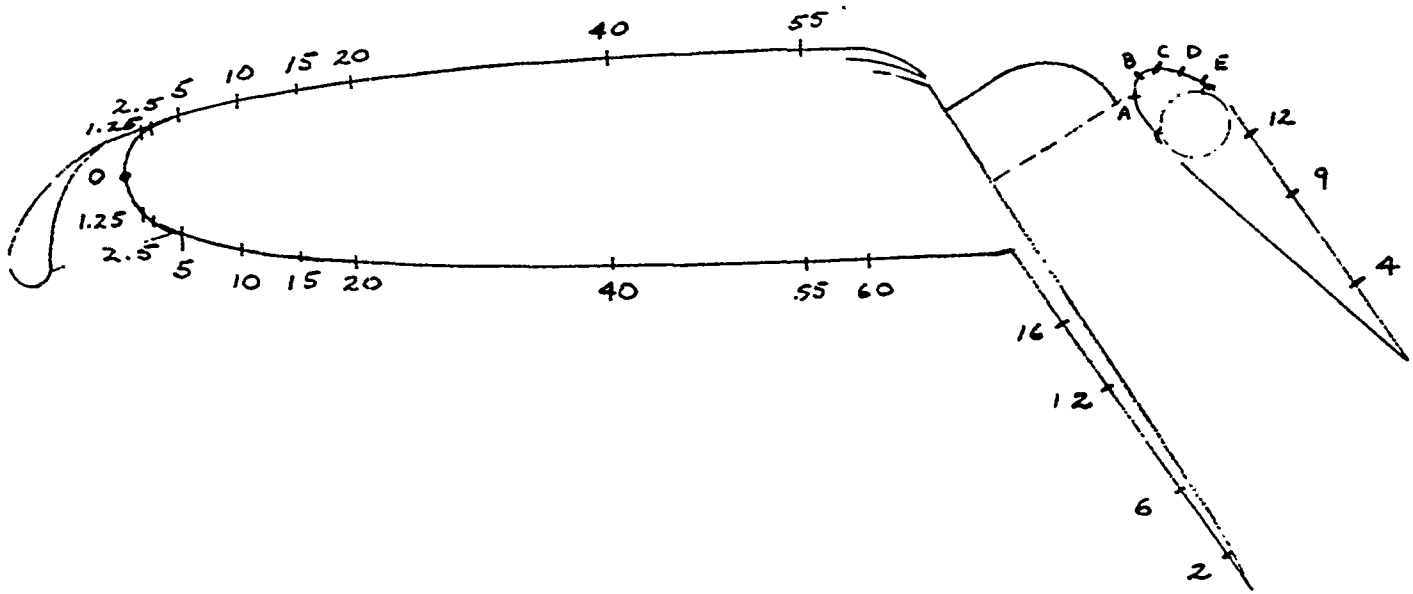

FIGURE 15. PRESSURE TAP LOCATIONS

TABLE VI

PRESSURE TAP LOCATIONS

Program Designation	X/C	Program Designation	X/C
0	0	A	.726
		B	.724
1.25	.0125	C	.730
2.5	.025	D	.746
5.0	.05	E	.764
10.0	.10	16	.734
15.0	.15	12	.80
20.0	.20	9	.85
40.0	.40	6	.90
55.0	.55	4	.934
60.0	.60	2	.966

$$WE = \sum_{I=1}^{12} \sum_{J=1}^{7} W(I,J)$$

$$FG = \frac{1}{32.2} \sum_{I=1}^{12} \sum_{J=1}^{7} (W(I,J))\,(VE(I,J))$$

The isentropic thrust (FI(K)) of each primary nozzle is computed using the isentropic velocity.

$$VIS(K) = \left((2)\,(Cp)\,(g)\,(J)\,T_2\left(1-\left(\frac{PO}{PT(K)}\right)^{\frac{\gamma-1}{\gamma}}\right)\right)^{\frac{1}{2}}$$

where, PT(K) is the plenum pressure for each primary nozzle. The subscript (K) denotes each of the three primary nozzles, inlet slot, hypermixing, diffuser slot.

$$FI = \sum_{K=1}^{3} \left(W(K)\right)\left(VI(K)\right)$$

The ram drag of the secondary air stream (FR) is determined as follows:

$$FR = \frac{(WE-WP)VO}{g}$$

where WP is the total primary flowrate and is the sum of the metered quantities passing the left and right main metering orifices.

The equivalent ram drag of the primary air is defined as

$$FRP = \frac{(WP)\,(VO)}{g}$$

All values labeled as drag (CD) or jet momentun (CMU) coefficients are printed as actual values of drag or thrust if QO is less than 3.0 (VO< 52.5 FPS).

The estimated flap thrust is that thrust which is produced by the BLC jet on the top surface of the flap. This value is always zero as this slot was not used in the current test program.

The values presented as 'Static Thrust Augmentation - Force Balance' is the resultant wing section thrust divided by the isentropic primary thrust. This value is only computed when QO is less than 2.0 but is not a true static thrust augmentation ratio to the extent that the model itself drives the tunnel to some value of QO other than zero.

Lines 38 to 41 on page 3 are a configuration summary, but includes the tunnel free stream velocity and the hypermixing nozzle plenum centerline pressure ratio (PRN).

Lines 43 through 52 present the aerodynamic data with blockage and curvature corrections applied. These corrections are discussed in section V A.

10. Miscellaneous Test Environmental Data (page 4)

This page contains the end-wall pressure tap, tunnel floor static pressure tap, and the floor boundary layer rake readings. The position of these readings is described on the output sheet itself.

The floor boundary layer rake is under the model, on the balance center, which is the model 40% chord point. The rake probe heights (HT) above the tunnel floor are given in inches.

VI TEST PLAN AND RESULTS

The model was tested at flap angles of 20 and 30 degrees. The primary test variables were diffuser area ratio, primary nozzle pressure ratio, freestream velocity and angle of attack. Table VII is a summary of the test schedule presenting the test conditions and range of variability of the primary test variable for each individual run. The runs are numbered in the sequence that they were made during the test program and are coincident with the run numbers presented in the plotted and tabulated data.

The test results were plotted according to the plotting schedule of Table VIII. Presented in the table are the figure number and its title, the pertinent configuration data, the plotted parameters and the runs used to make up each plot. The figures as defined by the plot schedule are presented in Appendix A.

The tabulated data compiled according to the format defined in Sec. V for each of the Table VII runs is available at the FDL of WPAFB.

In evaluating the data of Appendix A the anomalies and failures noted in Table IX should be taken into consideration. The data of these various runs and points within a given run were not voided because in all cases either the aerodynamic or pressure data would provide good results although one or the other could be in question. In all cases the data was repeated to insure that the points would be covered. The data that can be salvaged from these specific data points can be used for checks on the repeated data.

TABLE VII. 2D-CTA WIND TUNNEL TEST SCHEDULE $A_1/A_o \approx 15$

Run	δ_F	V_o	P_T/P	α	Slot	A_3/A_2	
1	Trapeze Tare						
2	End Plate Blowing Tare						
3	30	0	1.87	0	ON	1.4 to 2.0	
4			1.3 to 2.25	0		1.8	
5			1.87	-10 to +32		1.8	Leakage out of BLC supply line
6			1.87	-10 to +24		1.8	Repeat Run 5
7		80	1.87	-10 to α_R		1.4	
8		0"	1.3 to 1.87	0		1.8	
9		100	1.87	-10 to α_S		1.4	End plate seal failure at high
10		130		-10 to α_S		1.4	Stiffened end walls - solved seal problem
11		165		-4, 0, +4		1.4	
12		80		-10 to α_S		1.6	
13		100					
14		130					
15		165		-4, 0, +4			Nozzle chips failed previous to this run
16		130	1.0	-10 to α_S		1.4	Nozzle failure repaired
17		130	1.0			2.0	
18		0.80	1.87			1.8	
19		100					
20		130					
21		165.0		-4, 0 +4			
22		130		-10 to α_S		1.6	Repeat Run 14 - Nozzles Repaired
23		80				1.6	
24		0		0		1.6 to 2.0	" " 12 - " "
25		80		-10 to α_S		2.0	
26		100					
27		130					
28		165		-4, 0, +4			
29		80		9, 8, 16, 20			Floor blowing on - data doesn't appear correct
30	20	0		0		1.3 to 2.0	
31			1.3 to 1.87	0		1.8	
32			1.87	-10 to 32		1.8	
33		130		-10 to α_S		1.4	
34		0, 130				1.6	
35						1.8	
36						2.0	
37						1.7	
38		80				1.6	
39		100					
40		130					
41		165		-4, 0, +4			
42		0	2.1	0		1.4 to 2.0	
43		80		-10 to α_S		1.4	
44		130				1.4	
45		130				1.5	
46		130				1.3	
47		0	2.25	0		1.4 to 2.0	
48		0	2.1	0		1.4 to 2.0	
102	30	0	1.87	0	ON	1.3 to 2.0	
103		0	2.1	0		1.3 to 2.0	
104		130		- 0 to α_S		1.68	
105						1.46	
106						1.95	
107		80				1.75	
108		100					
109		130					
110		165		-4, 0, 4			
111		130	1.87	-10,0,4,12, 20		1.8	
112		0	2.25	0		1.3 to 2.0	
113		0	1.4	7.5		1.8	Model fed from right side only - left side valve closed

TABLE VIII
PLOTTING SCHEDULE

FIGURE No.	TITLE	PLOTTED PARAMETERS	δ_F	A_3/A_2	P/p	α	V	RUN NOS.
16	STATIC THRUST ADJUSTMENT AS AFFECTED BY P/p & A_3/A_2	ϕ_{GROSS} VS A_3/A_2	30°	VARY	1.87 2.1, 2.25	0	≈0	3, 102, 103, 112
17	VARIATION OF STATIC ϕ_{GROSS} WITH P/p	" " P/p	"	1.8	VARY	"	"	8
18, 19	" " ϕ_{GROSS} & ϕ_{NET} WITH V_0 AND α	ϕ_{GROSS} & ϕ_{NET} VS V_0	"	1.4	1.87	VARY	VARY	7, 9, 10, 11
20, 21	" " " " " " " "	" " " "	"	1.6	"		"	12, 13, 14, 15
22, 23	" " " " " " " "	" " " "	"	1.8	"		"	18, 19, 20, 21
24, 25	" " " " " " " "	" " " "	"	2.0	"		"	25, 26, 27, 28
26, 27	" " " " " " " "	" " " "	"	VARY	"	0	"	CROSS PLOT 7 THRU 28
28, 29	" " " " " " " "	" " " "	"	1.75	2.1	VARY	"	107, 108, 109, 110
30	" " STATIC ϕ_{GROSS} WITH A_3/A_2	ϕ_{GROSS} VS A_3/A_2	20°	VARY	1.87 2.1, 2.25	0	≈0	30, 42, 47, 48
31	" " " " " P/p	" " P/p	"	"	VARY	"	"	31
32, 33	" " ϕ_{GROSS} & ϕ_{NET} " V_0 & α	ϕ_{GROSS} & ϕ_{NET} VS V_0	"	1.6	1.87	VARY	"	38, 39, 40, 41
34, 35	" " " " " " A_3/A_2	" " " A_3/A_2	"	VARY	"	0	130	33, 34, 35, 36, 37
36	TYPICAL VARIATION OF $\dot{W}_{PRIMARY}$ WITH P/p	$\dot{W}_{PRIMARY}$ VS P/p	20°, 30°	1.8	VARY	"	≈0	8, 31
37	" " " FISENTROPIC " "	FISENTROPIC " "	"	"	"	"	"	"
38	VARIATION OF ϕ_{GROSS} WITH P/p	ϕ_{GROSS} " "	"	"	"	"	"	"
39, 40	" " ϕ_{MASS} & $\dot{W}_{SECONDARY}$ WITH P/p	ϕ_{MASS} & $\dot{W}_{SECONDARY}$ VS P/p	"	"	"	"	"	"
41, 42, 43	POWER OFF AERODYNAMIC CHARACTERISTICS	C_L VS α, C_L VS C_D, C_L VS C_M	30°	1.4, 2.0	1.0	VARY	130	16, 17
44, 45, 46	EFFECT OF C_μ ON AERODYNAMIC CHARACTERISTICS	" " "	"	1.4	1.87	"	VARY	7, 9, 10, 11
47, 48, 49	" " " " " "	" " "	"	1.6	"	"		12, 13, 14, 15
50, 51, 52	" " " " " "	" " "	"	1.8	"	"		18, 19, 20, 21
53, 54, 65	" " " " " "	" " "	"	2.0	"	"		25, 26, 27, 28
56, 57, 58	" " " " " "	" " "	"	1.75	2.1	"		107, 108, 109, 110
59, 60, 61	" " A_3/A_2 AT V_0 = 80 FPS ON AERO. CHAR.	" " "	"	VARY	1.87	"	80	7, 12, 18, 25
62, 63, 64	" " " " " 100 " " "	" " "	"	"	"	"	100	9, 13, 19, 26
65, 66, 67	" " " " " 130 " " "	" " "	"	"	"	"	130	10, 14, 20, 27
68, 69, 70	" " " " " 165 " " "	" " "	"	"	"	"	165	11, 15, 21, 28
71, 72, 73	" " " " " 130 " " "	" " "	20°	"	"	"	130	33, 34, 35, 36
74, 75, 76	" " C_μ ON AERO. CHAR.	" " "	"	1.6	"	"	VARY	38, 39, 40, 41
77, 78, 79	" " A_3/A_2 " " "	" " "	"	VARY	2.1	"	130	44, 45, 46
80, 81, 82	POWER OFF CHARACTERISTICS SLAT ON	" " "	"	1.7	1.0	"	"	57
83, 84, 85	" " " " " OFF	" " "	"	"	"	"	"	64
86, 87, 88	" " " " "	" " "	"	0	"	"	"	PREVIOUS TEST PROGRAM

TABLE IX

ANOMALIES AND FAILURES ENCOUNTERED DURING SPECIFIC TEST POINTS

DATE	RUN	PTS	REMARKS
7/24	3	1-6	Progressive Leak at blanked flap slot (Approx. 1.2% of Primary flow).
7/25	4 5	4-5 1-7	Inlet plenum hose starts slipping and at Pt 5-7 blows completely off.
	4 5	5 1-7	Right side hose from manifold to hyper-mixing nozzle plenum leaking.
	8	3	Approx. 2% primary flow leaking through blanked flap slot.
7/26 7/27	9 10 11 12 13 14 15	1-15 1-12 1-3 1-12 1-13 1-13 1-4	Hypermixing nozzle exit clip failures
7/26	9	9 12-15	Tunnel q changed abrubtly, point repeated. end seal, left side failed
7/30	19	4-8	Side force & yawing moment problem, points re-run
	20	8	Leading edge slat came loose from center support at or before Pt. 8
7/31			After Run 29 the flap plenum is noted to have rotated by 0.18 inches along its circumference. The flap leading edge rotated forward.
8/9	103	2-3	Inlet plenum hose blew loose.
	102 thru113		Suspect partially blocked flap BLC nozzle

The discrepancy, (line 32 column 5 Table IV) between the total air flowrate to the model as measured by the Lockheed main metering orifice and the total flowrate arrived at by summing the values from the two primary orifices and the end and floor blowing orifices consistently ran between 5 and 20 percent. It was originally hoped that these totals would agree to within $\pm$ 2%.

The main orifice, except at very low flowrate, consistently indicated a lower air flow than the run of the remaining orifices.

The orifice instrumentation and pressure fittings were checked for leaks and these checks failed to uncover the cause of the discrepancy. Other explanations were logically ruled out. For example;

(a) If a leak occurred between the main orifice and the remaining orifices the main orifice would have given the higher reading.

(b) If the air had cooled before it reached the downstream orifices the main orifice again would be expected to give the higher reading.

In the absence of any direct evidence as to the cause of the discrepancy it was decided that the main orifice readings would be disregarded and the values recorded by the remaining orifices would be used to compute the CTA performance. This was done for the following reasons.

(a) The magnitude of the pressure differentials across the downstream orifices were much greater than across the main orifice and thought to be less sensitive to instrumentation error.

(b) The computed effective area of the hypermixing nozzles were nearer the values obtained by independent (ARL) calibrations if the remaining orifices and not the main orifice readings were used to make the computation.

APPENDIX A

PLOTTED DATA RESULTS

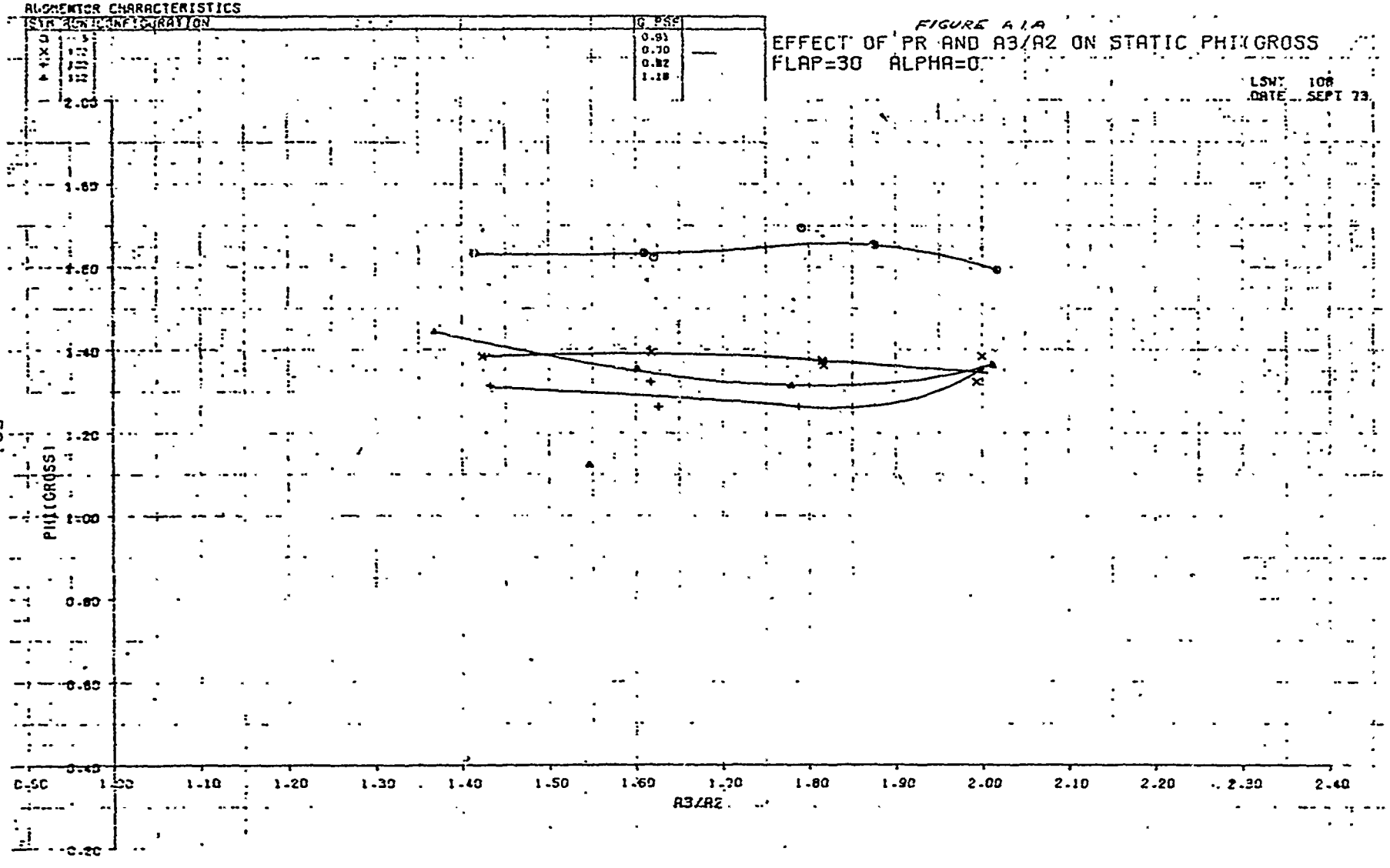
AEROMETER CHARACTERISTICS
STATIC CONFIGURATION
G PSS
0.93
0.70
0.82
1.18
FIGURE A.1.A
EFFECT OF PR AND A3/A2 ON STATIC PHI(GROSS
FLAP=30 ALPHA=0.
LSWT 108
DATE SEPT 73
PHI(GROSS)
A3/A2
2.00
1.80
1.60
1.40
1.20
1.00
0.80
0.60
0.40
0.20
0.50
1.00
1.10
1.20
1.30
1.40
1.50
1.60
1.70
1.80
1.90
2.00
2.10
2.20
2.30
2.40

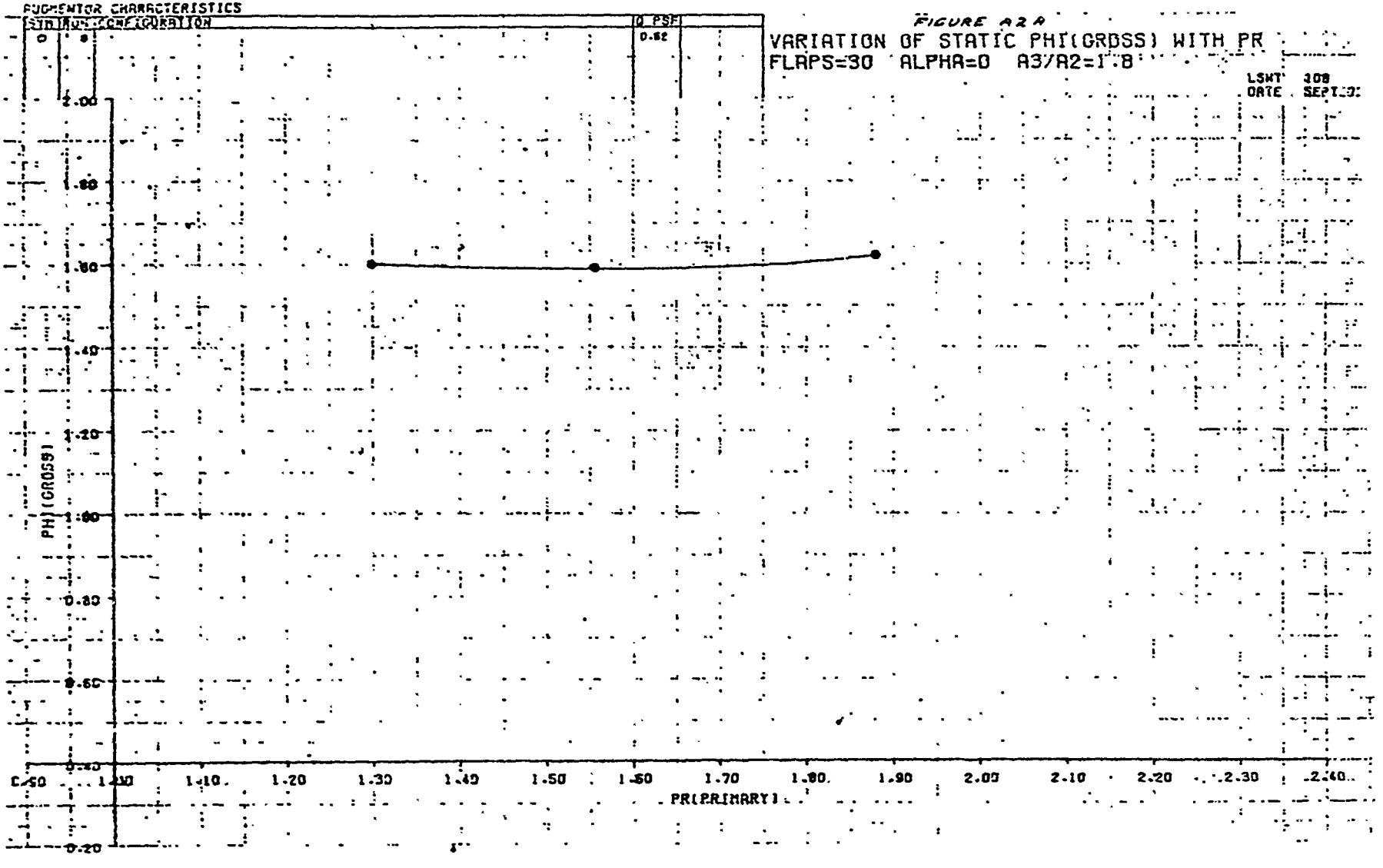
AUGMENTOR CHARACTERISTICS
SUBSONIC CONFIGURATION
0 PSF
0.82
FIGURE A2A
VARIATION OF STATIC PHI(GROSS) WITH PR
FLAPS=30 ALPHA=0 A3/A2=1.8
LSNT 308
DATE SEPT.0
PHI(GROSS)
PR(PRIMARY)
2.00
1.80
1.60
1.40
1.20
1.00
0.80
0.60
0.40
0.20
1.50
1.60
1.70
1.80
1.90
2.00
2.10
2.20
2.30
2.40

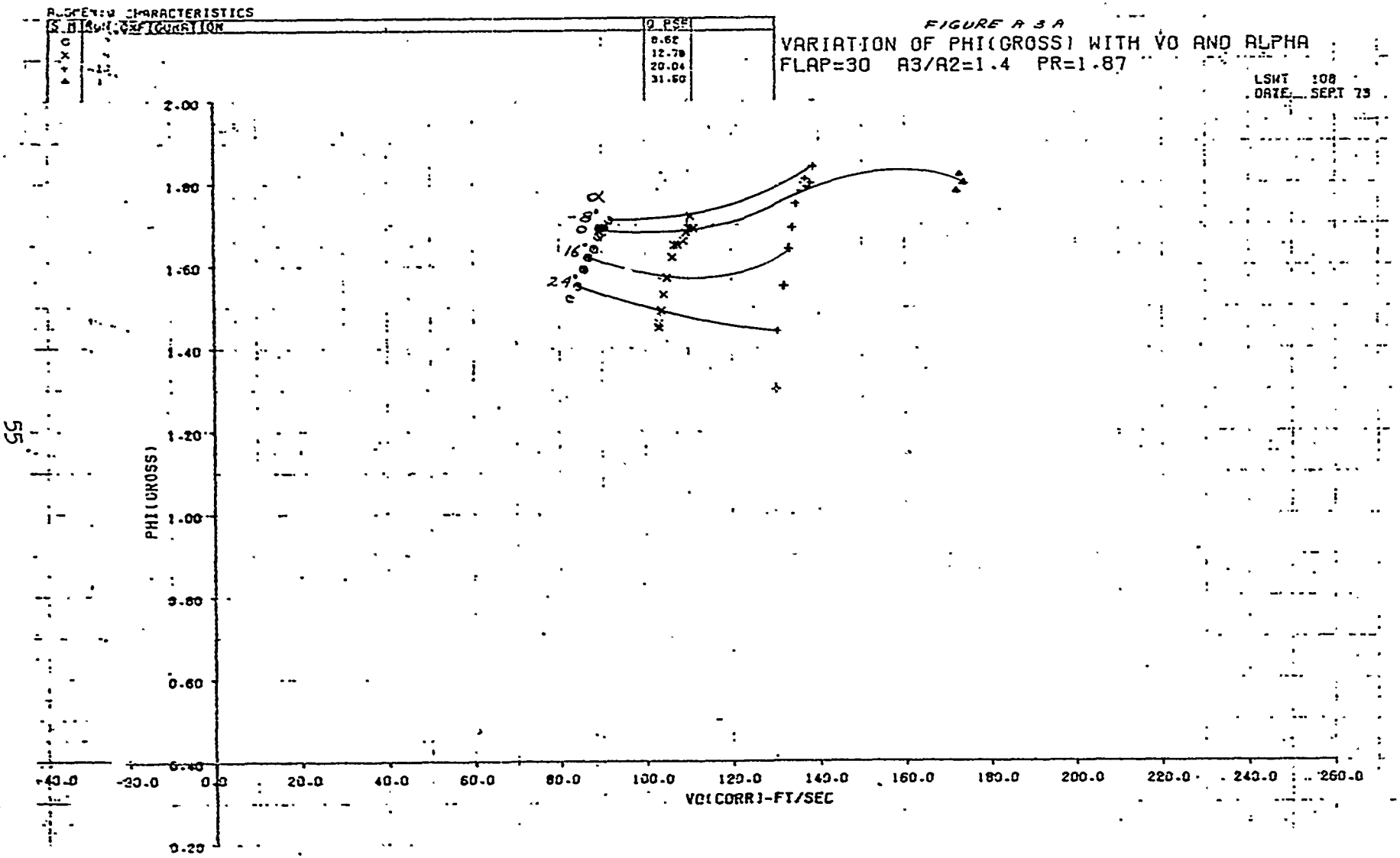

FIGURE A 3 A

VARIATION OF PHI(GROSS) WITH VO AND ALPHA

FLAP=30 A3/A2=1.4 PR=1.87

LSWT 108

DATE SEPT 73

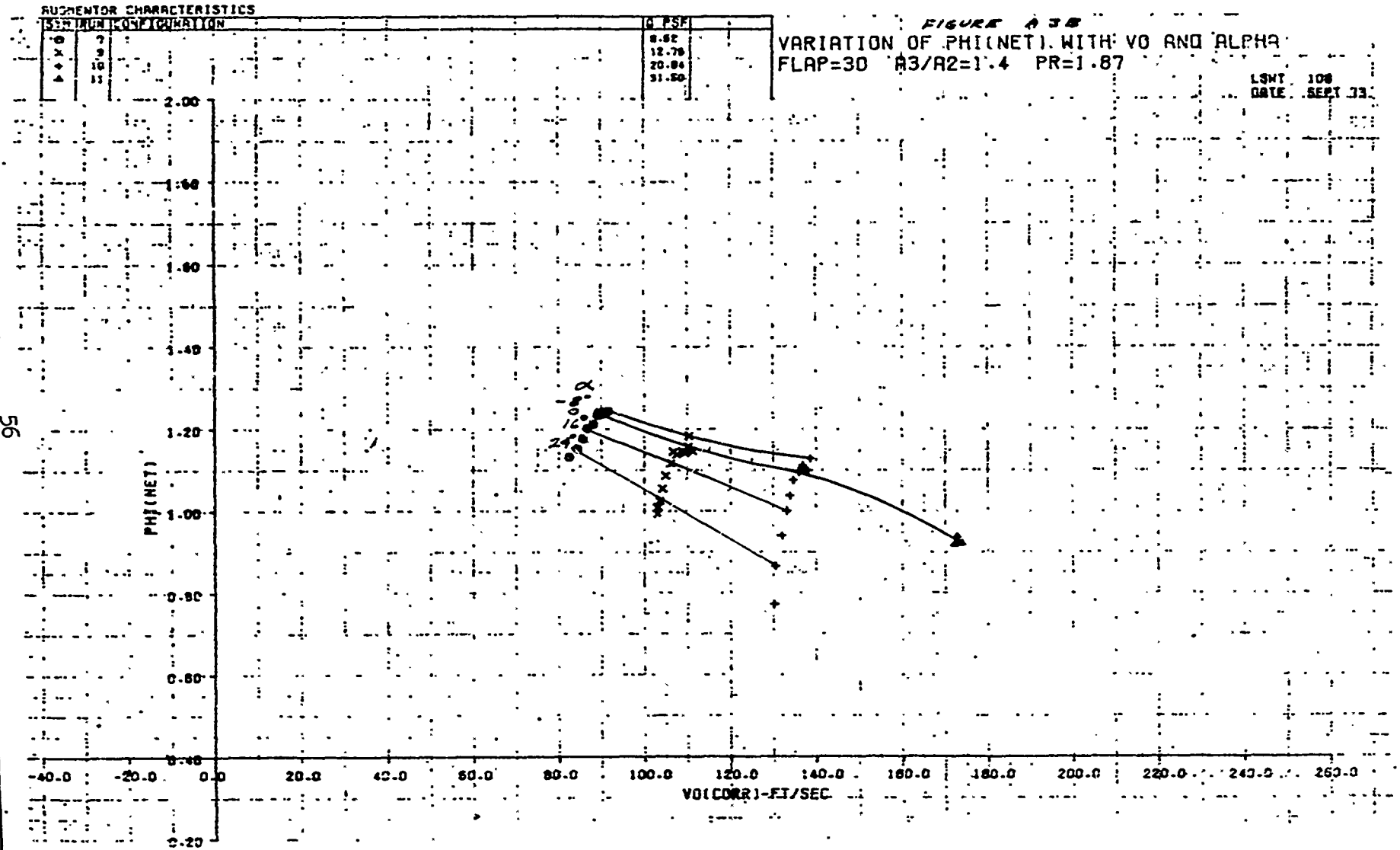
AUGMENTOR CHARACTERISTICS
SSN RUN CONFIGURATION
Q PSF
8.62
12.76
20.84
31.50
FIGURE A 38
VARIATION OF PHI(NET) WITH V0 AND ALPHA
FLAP=30 A3/A2=1.4 PR=1.87
LSWT 108
DATE SEPT 33
PHI(NET)
2.00
1.80
1.60
1.40
1.20
1.00
0.80
0.60
0.40
0.20
-40.0
-20.0
0.0
20.0
40.0
60.0
80.0
100.0
120.0
140.0
160.0
180.0
200.0
220.0
240.0
260.0
V0(CORR)-FT/SEC
α
8°
10°
12°
24°

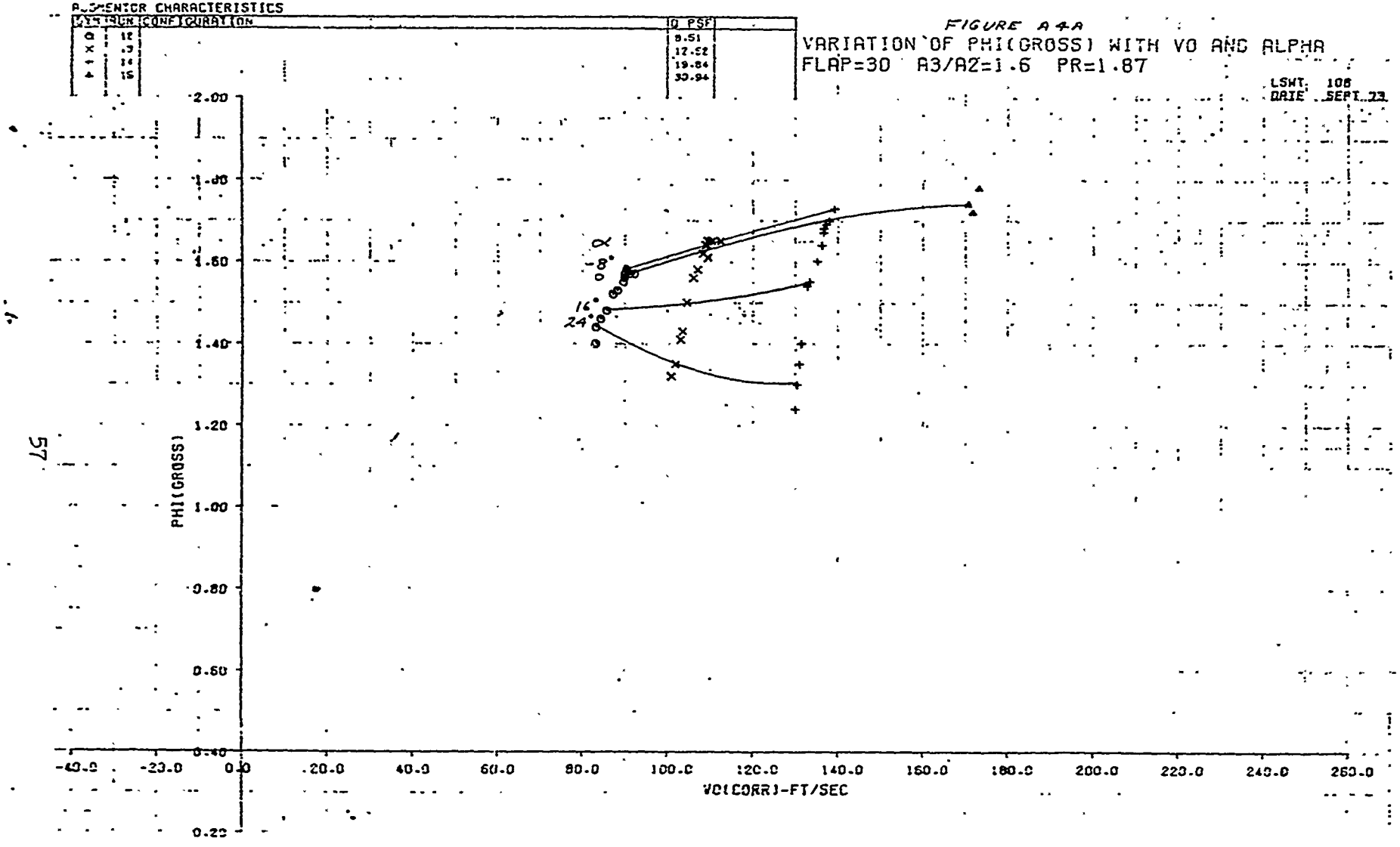

FIGURE A4A

VARIATION OF PHI(GROSS) WITH VO AND ALPHA

FLAP=30 A3/A2=1.6 PR=1.87

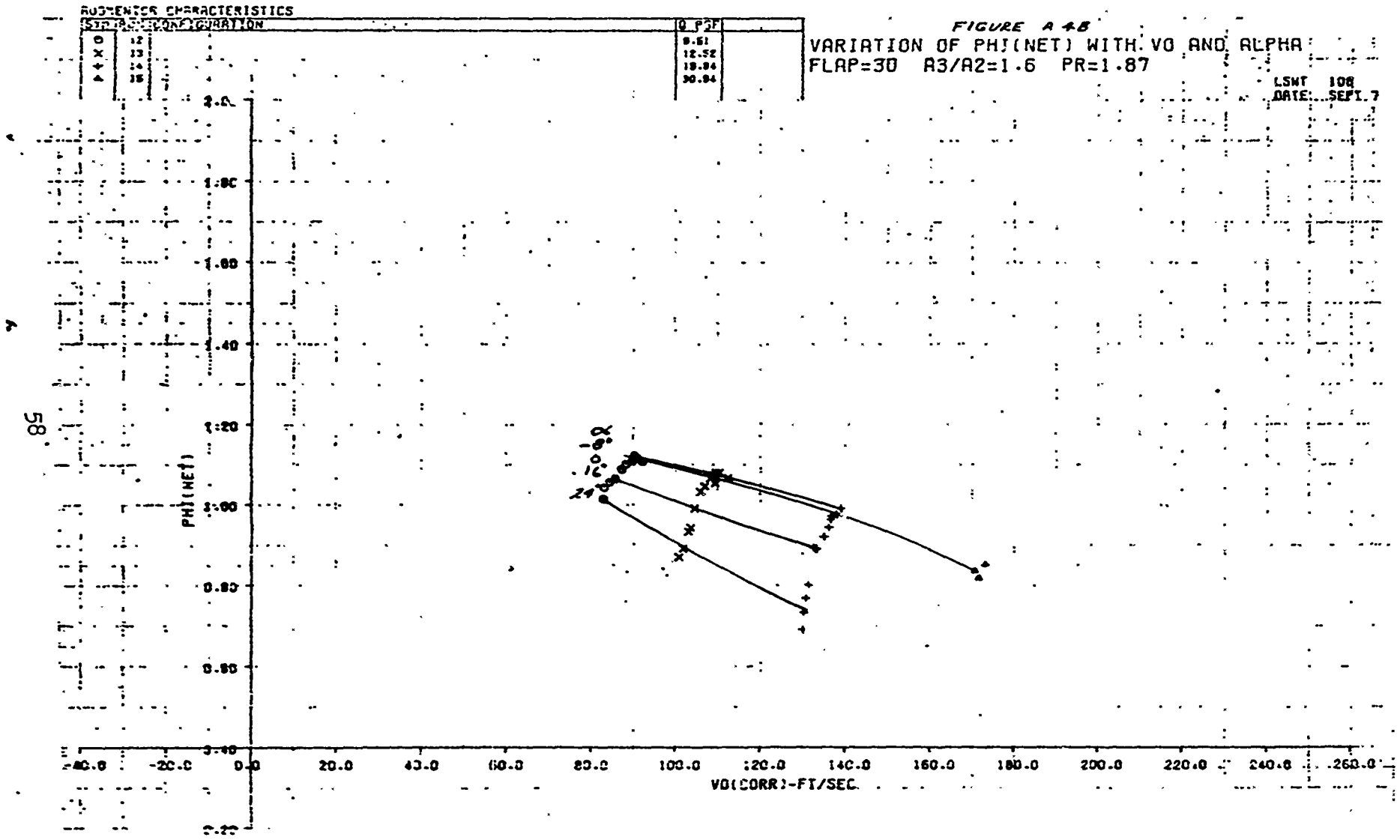
AUSTENITOR CHARACTERISTICS
STRAIGHT CONFIGURATION
Q PSF
9.51
12.52
19.84
30.94
FIGURE A 48
VARIATION OF PHI(NET) WITH VO AND ALPHA
FLAP=30 A3/A2=1.6 PR=1.87
LSWT 108
DATE SEPT.7
PHI(NET)
VO(CORR)-FT/SEC
-8°
12°
24°
2.00
1.80
1.60
1.40
1.20
1.00
0.80
0.60
0.40
0.20
-40.0
-20.0
0.0
20.0
40.0
60.0
80.0
100.0
120.0
140.0
160.0
180.0
200.0
220.0
240.0
260.0

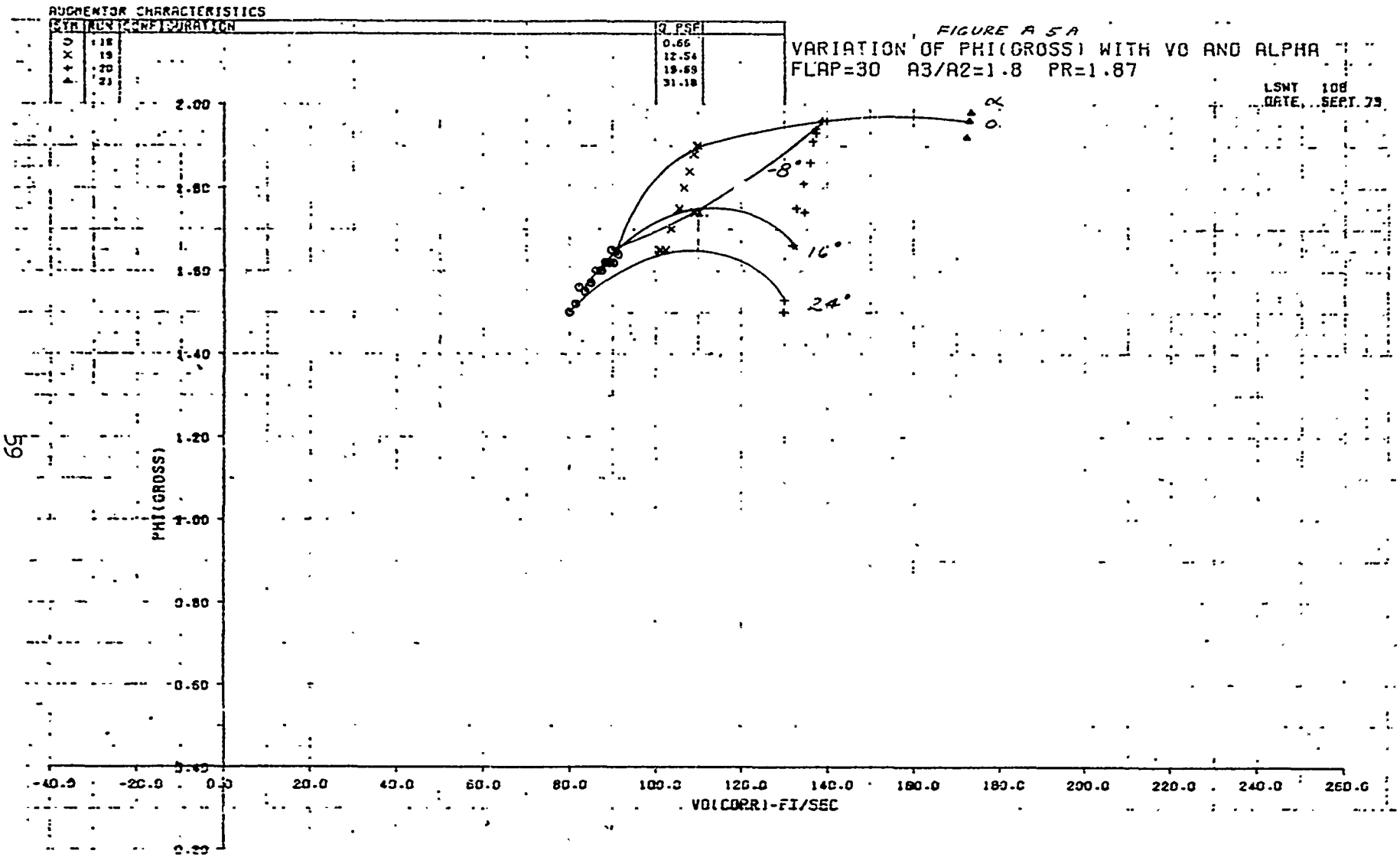
AUGMENTOR CHARACTERISTICS
CONFIGURATION
Q, PSF
0.66
12.54
19.69
31.18
FIGURE A 5A
VARIATION OF PHI(GROSS) WITH V0 AND ALPHA
FLAP=30 A3/A2=1.8 PR=1.87
LSNT 108
DATE, SEPT. 73
α
0.
-8°
16°
24°
PHI(GROSS)
V0(CORR)-FT/SEC
2.00
1.80
1.60
1.40
1.20
1.00
0.80
0.60
-40.0
-20.0
0.0
20.0
40.0
60.0
80.0
100.0
120.0
140.0
160.0
180.0
200.0
220.0
240.0
260.0

FIGURE A 5B

VARIATION OF PHI(NET) WITH VO AND ALPHA

FLAP=30 A3/A2=1.8 PR=1.87

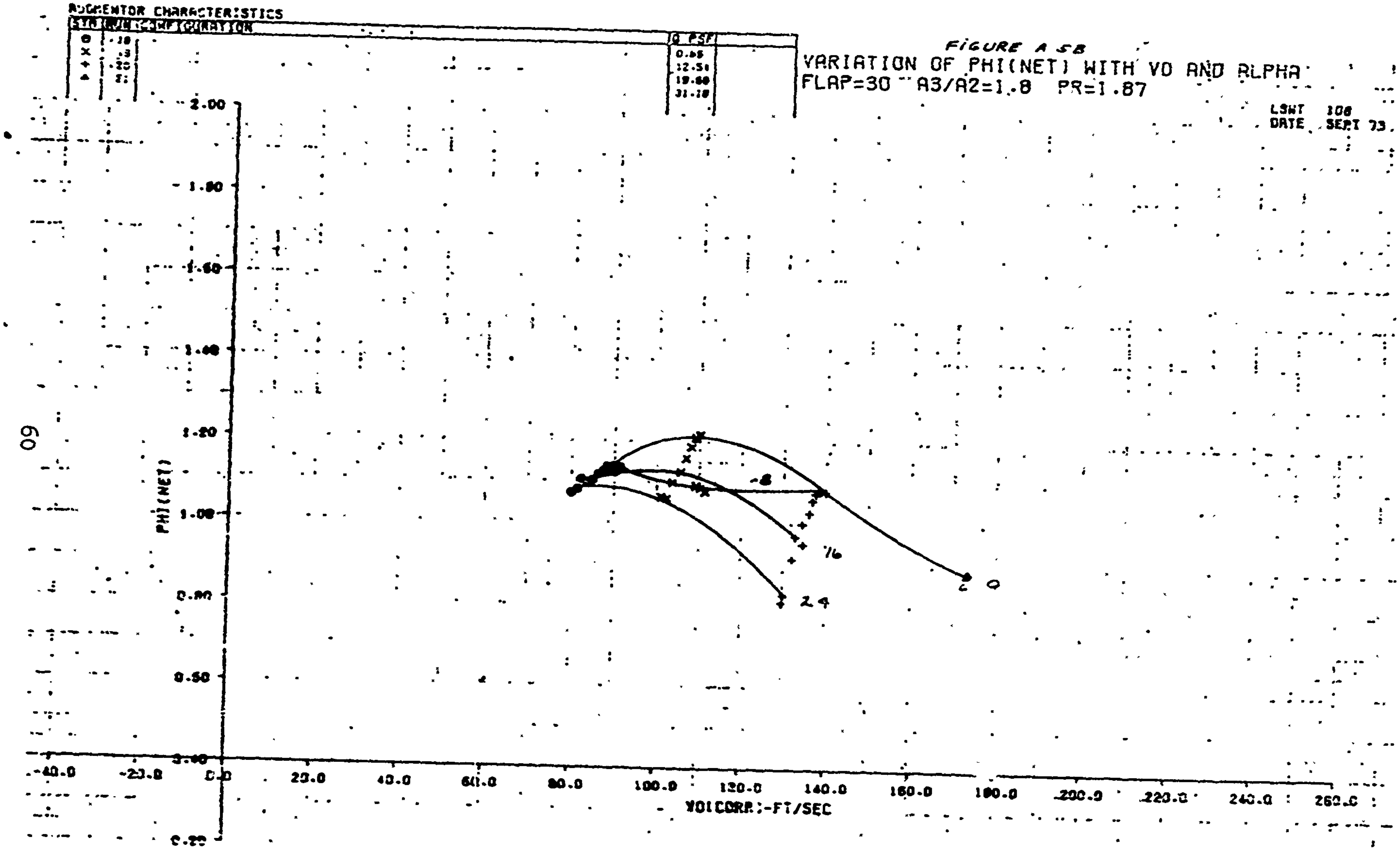

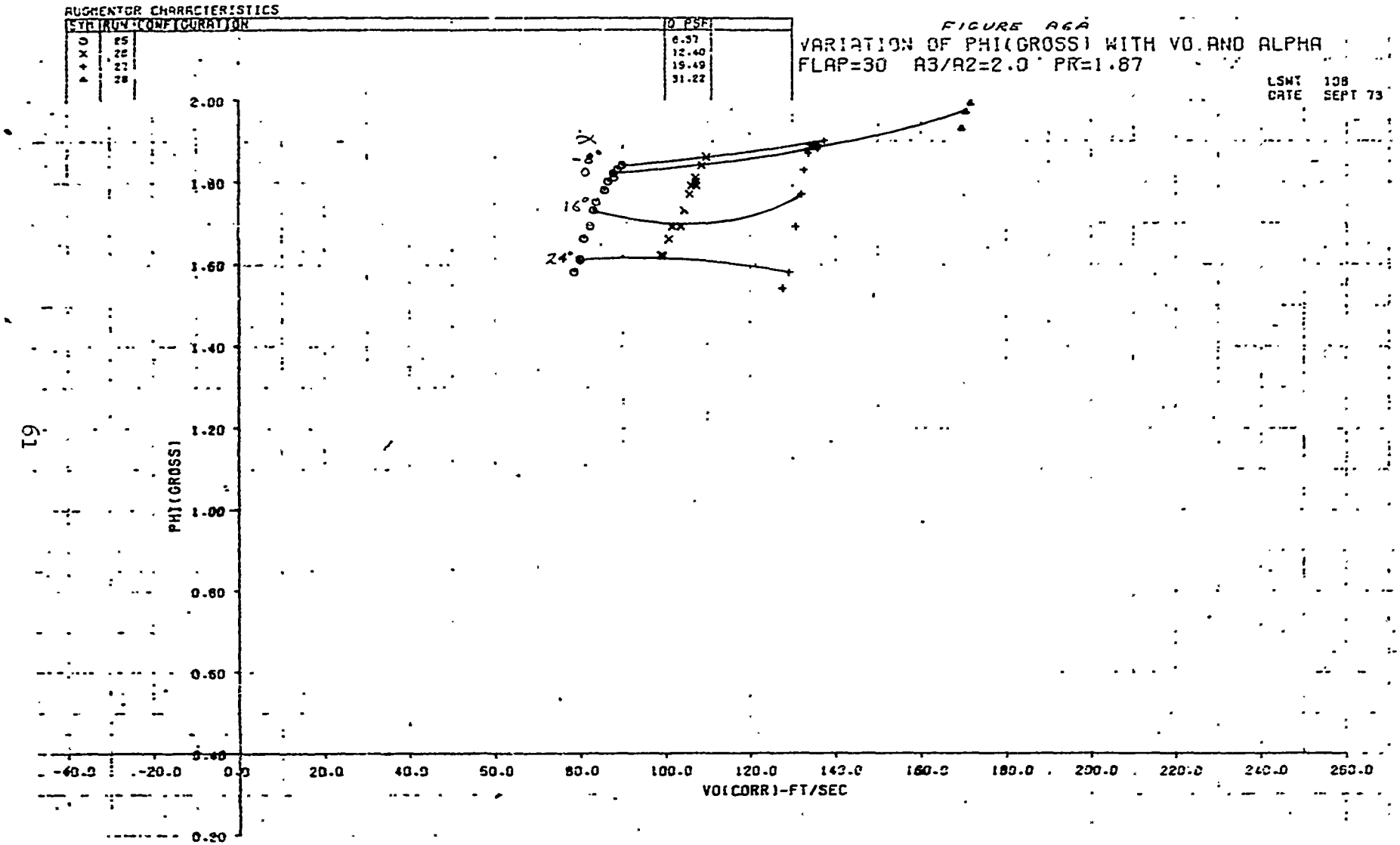
AUGMENTOR CHARACTERISTICS
SYM RUN CONFIGURATION
Q PSF
6.37
12.40
19.49
31.22
FIGURE A6A
VARIATION OF PHI(GROSS) WITH VO AND ALPHA
FLAP=30 A3/A2=2.0 PR=1.87
LSWT 108
DATE SEPT 73
-8°
16°
24°
PHI(GROSS)
VO(CORR)-FT/SEC
2.00
1.80
1.60
1.40
1.20
1.00
0.80
0.60
0.40
0.20
-40.0
-20.0
0.0
20.0
40.0
60.0
80.0
100.0
120.0
140.0
160.0
180.0
200.0
220.0
240.0
260.0

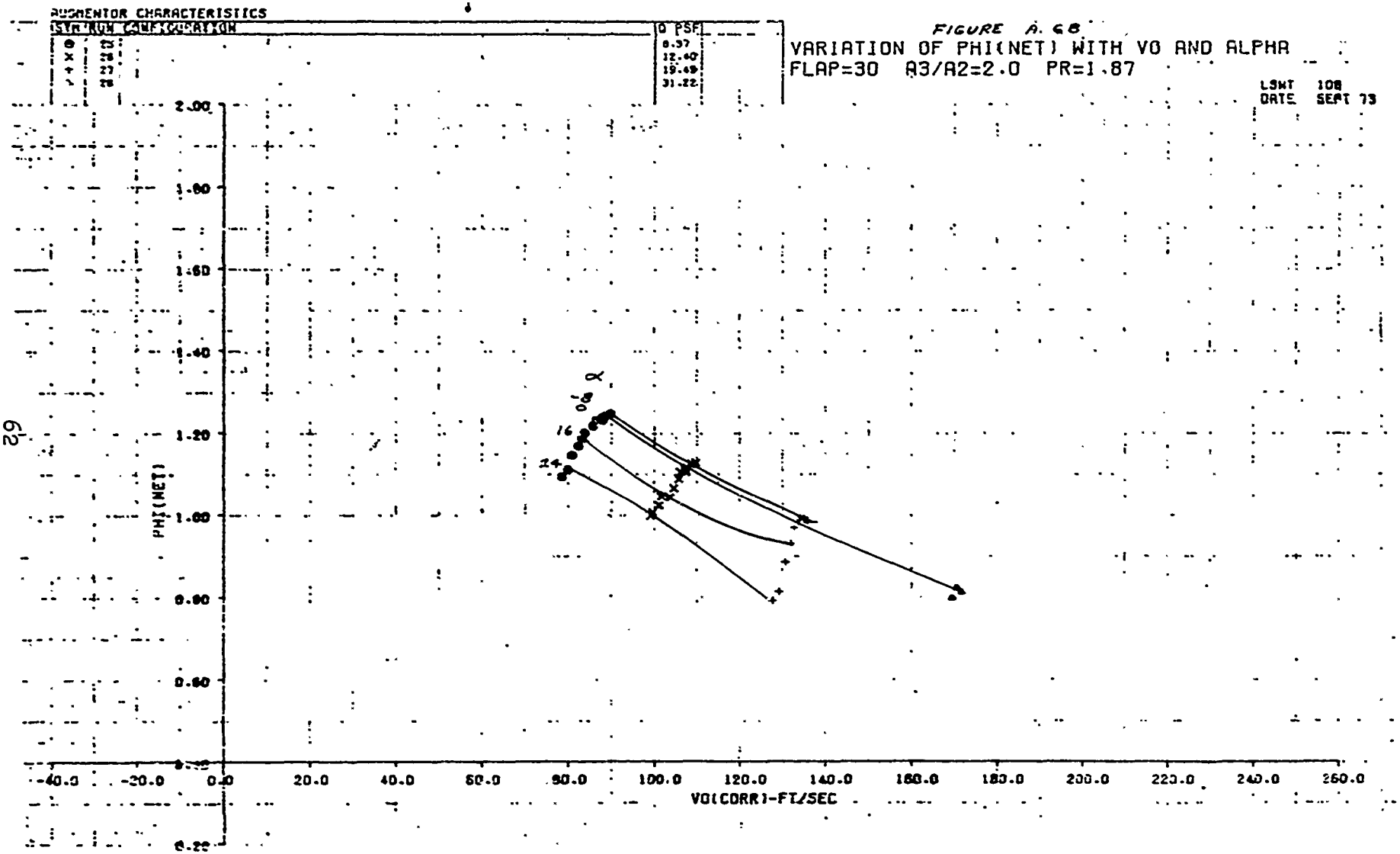

FIGURE A.68
VARIATION OF PHI(NET) WITH VO AND ALPHA
FLAP=30 A3/A2=2.0 PR=1.87

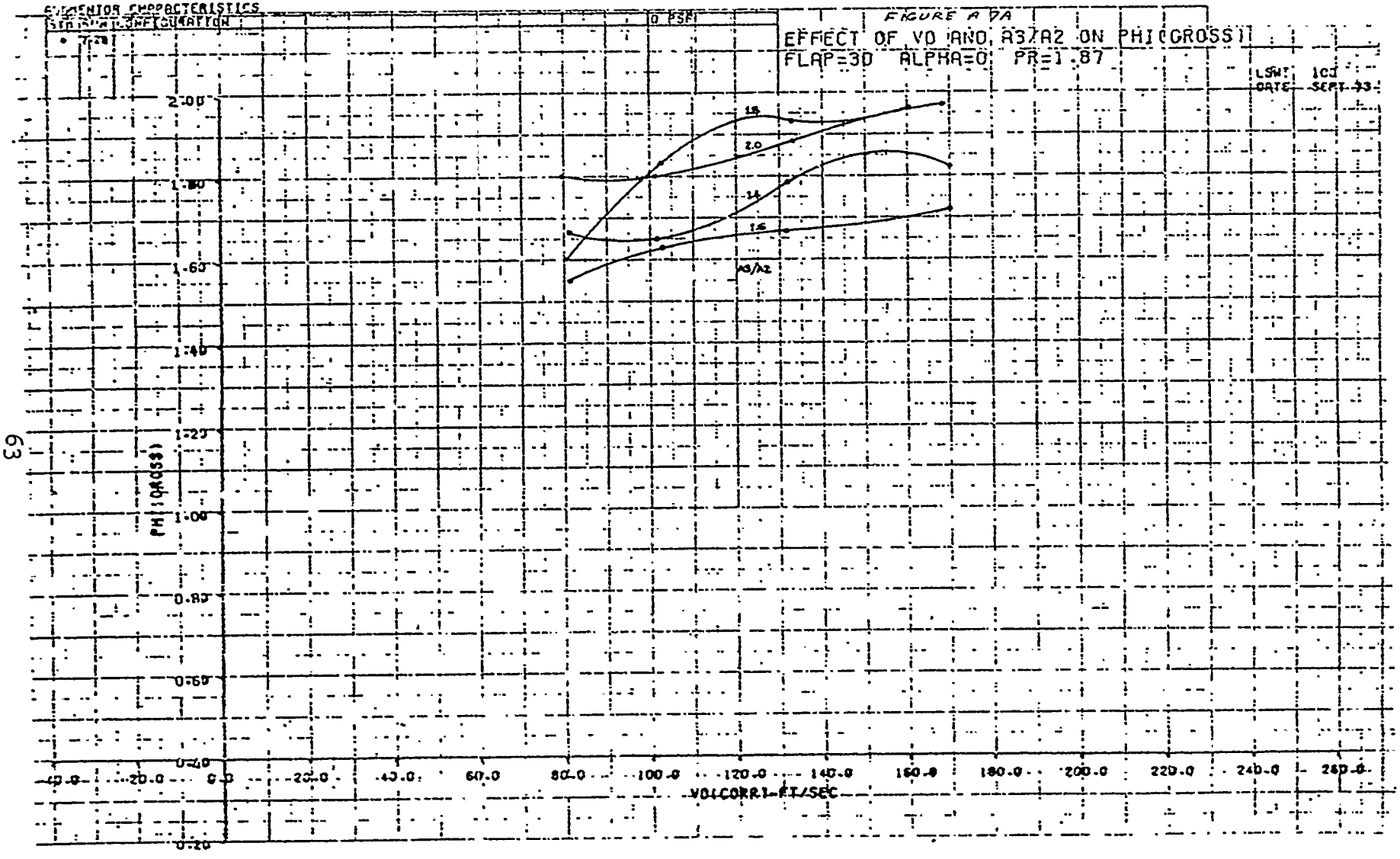
FIGURE A 9A
EFFECT OF V0 AND A3/A2 ON PHI(GROSS)
FLAP=30 ALPHA=0 PR=1.87
0 PSF
PHI(GROSS)
V0(CORR)-FT/SEC
A3/A2
1.8
2.0
1.4
1.6
2.00
1.80
1.60
1.40
1.20
1.00
0.80
0.60
0.40
0.20
-40.0
-20.0
0.0
20.0
40.0
60.0
80.0
100.0
120.0
140.0
160.0
180.0
200.0
220.0
240.0
260.0

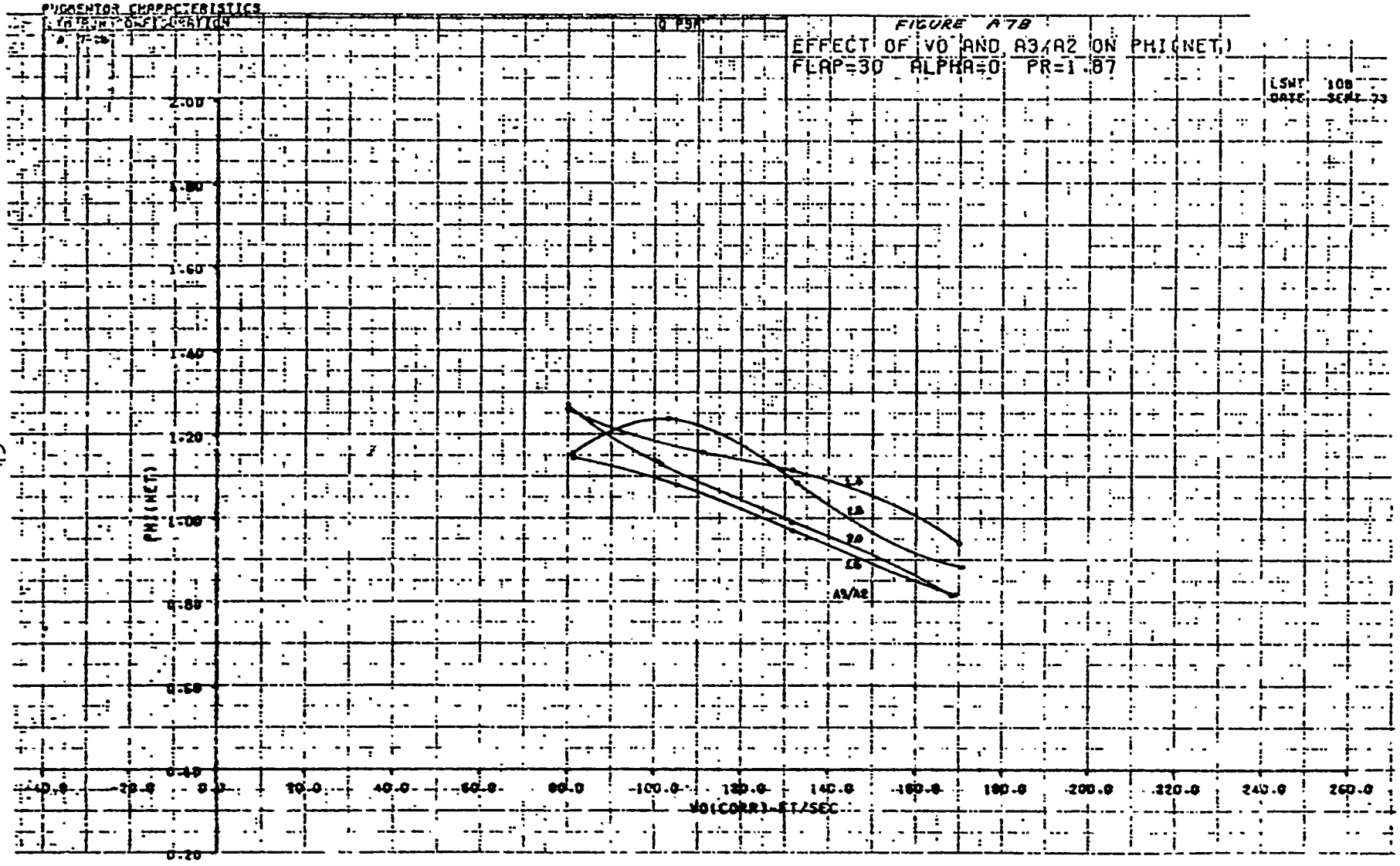

FIGURE A7B

EFFECT OF VO AND A3/A2 ON PHI(NET)

FLAP=30 ALPHA=0 PR=1.87

LSWT 10B
DATE SCRN 23

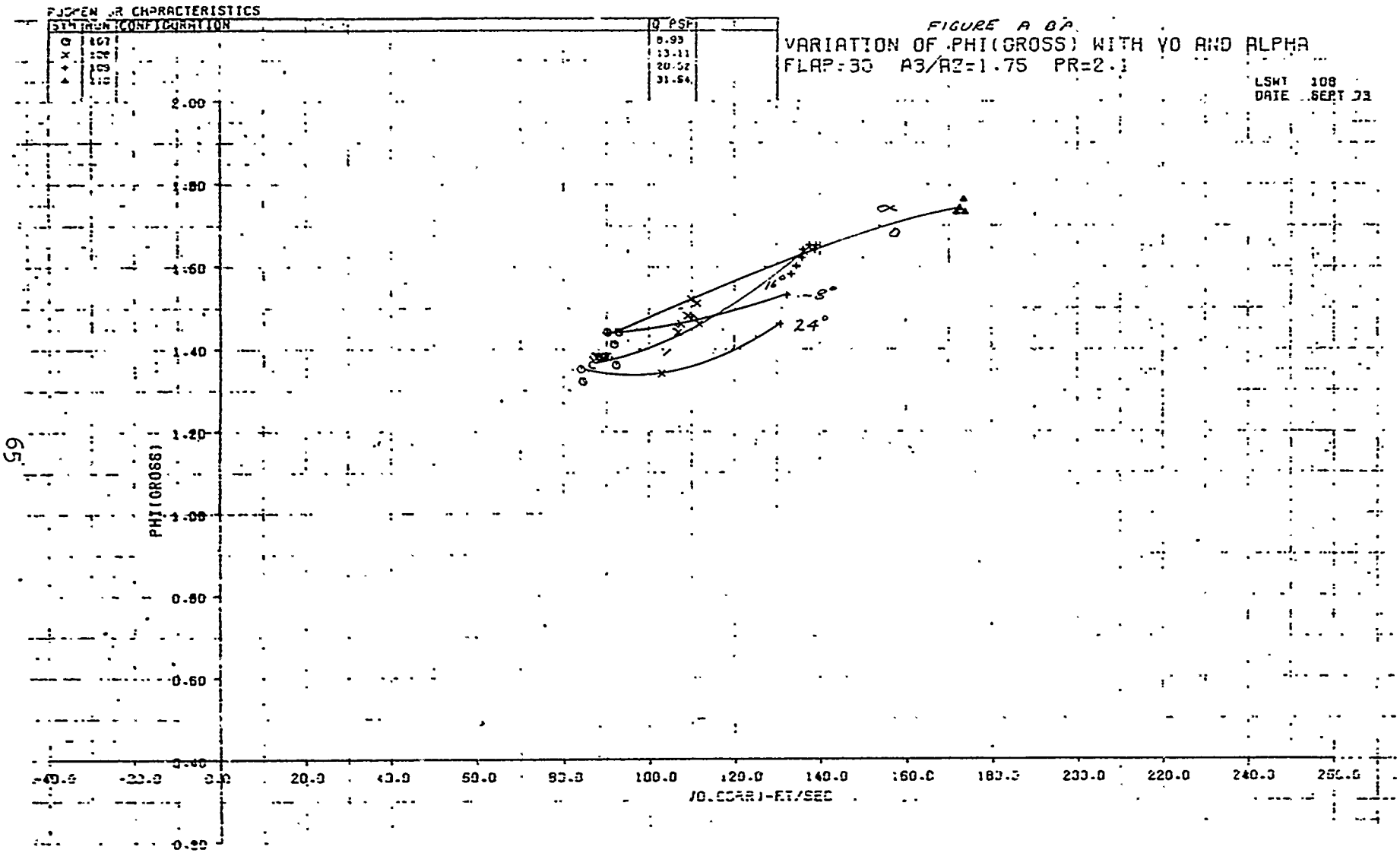

FIGURE A 6P.
VARIATION OF PHI(GROSS) WITH VO AND ALPHA
FLAP=30 A3/A2=1.75 PR=2.1

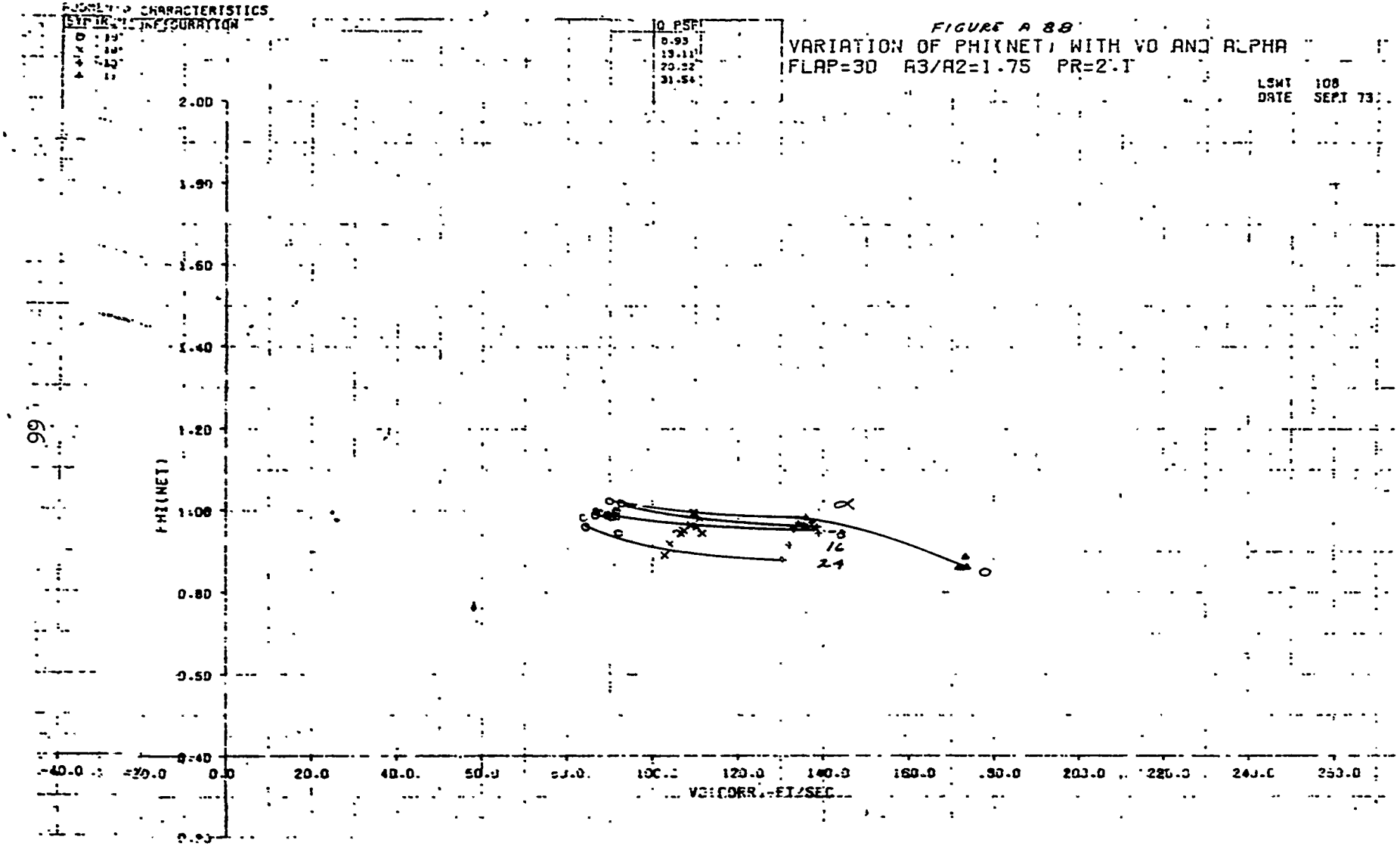

FIGURE A 88
VARIATION OF PHI(NET) WITH VO AND ALPHA
FLAP=30 A3/A2=1.75 PR=2.1

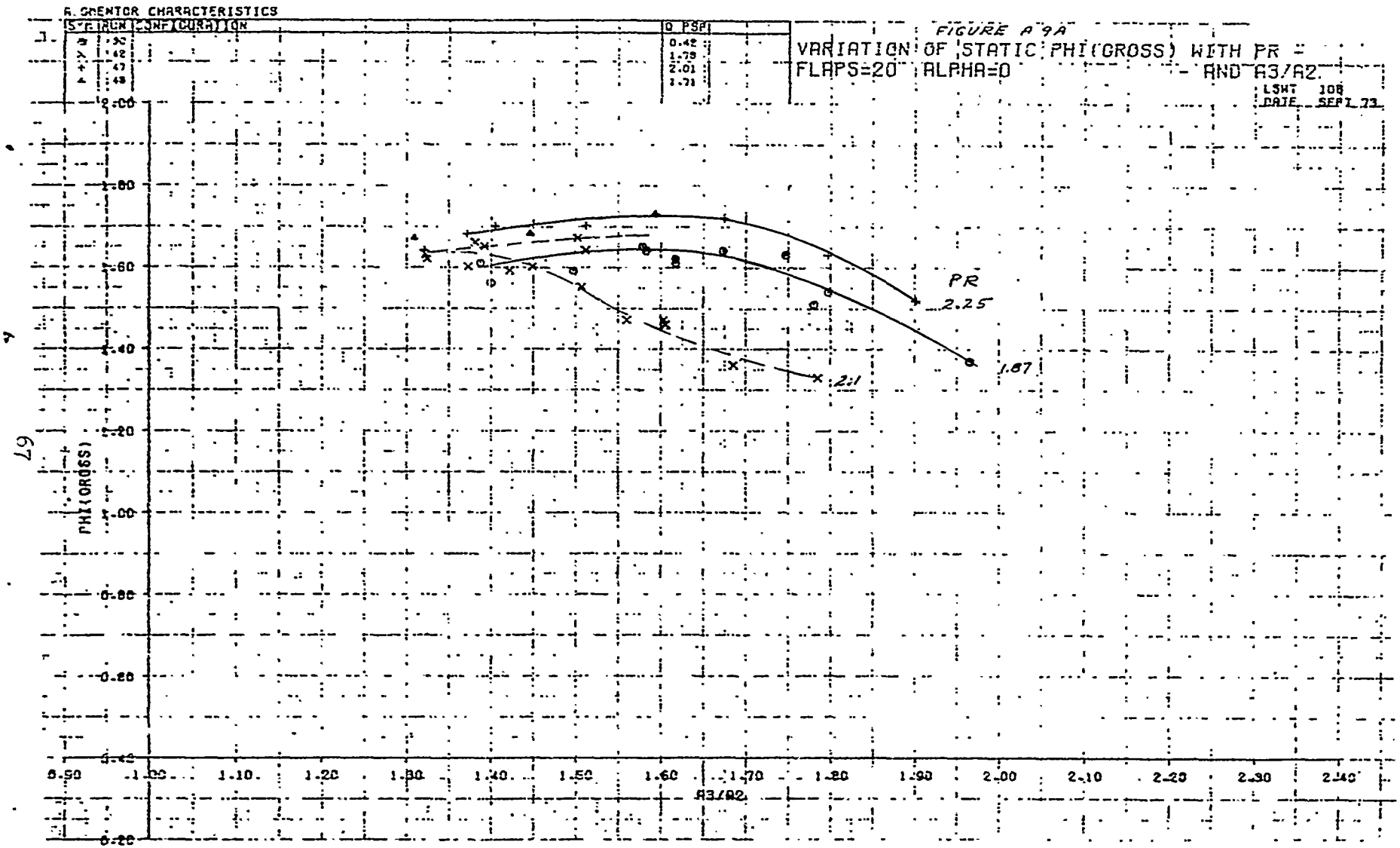
A. GREENTOR CHARACTERISTICS
SYMBOL CONFIGURATION
Q PSF
0.42
1.79
2.01
1.71
FIGURE A 9A
VARIATION OF STATIC PHI(GROSS) WITH PR =
FLAPS=20 ALPHA=0 - AND A3/A2.
LSHT 108
DATE SEPT 73
PR
2.25
1.87
2:1
PHI(GROSS)
A3/A2
1.00
1.10
1.20
1.30
1.40
1.50
1.60
1.70
1.80
1.90
2.00
2.10
2.20
2.30
2.40

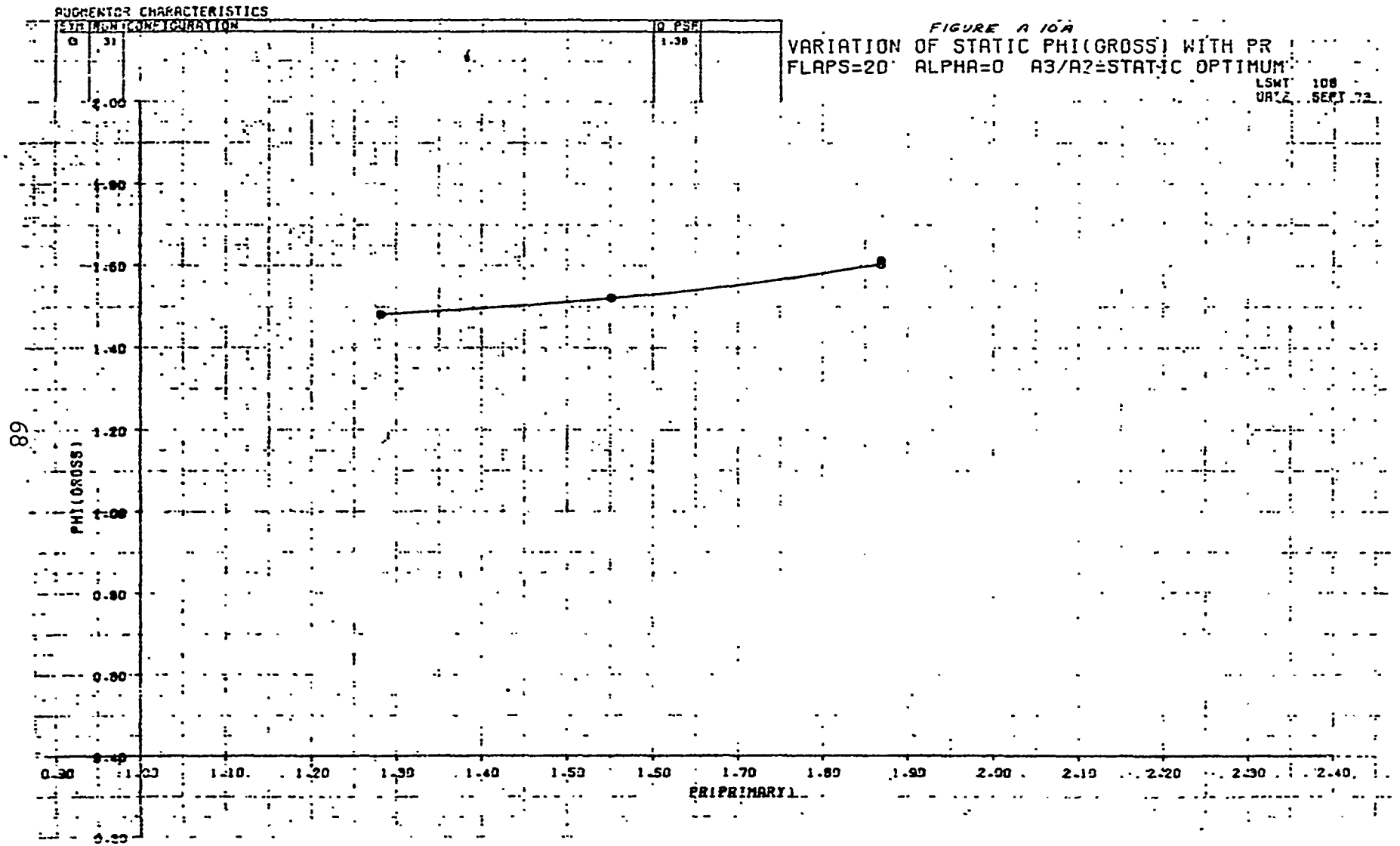

FIGURE A 10A

VARIATION OF STATIC PHI(GROSS) WITH PR

FLAPS=20° ALPHA=0 A3/A2=STATIC OPTIMUM

LSWT 108
UAIC SEPT 72

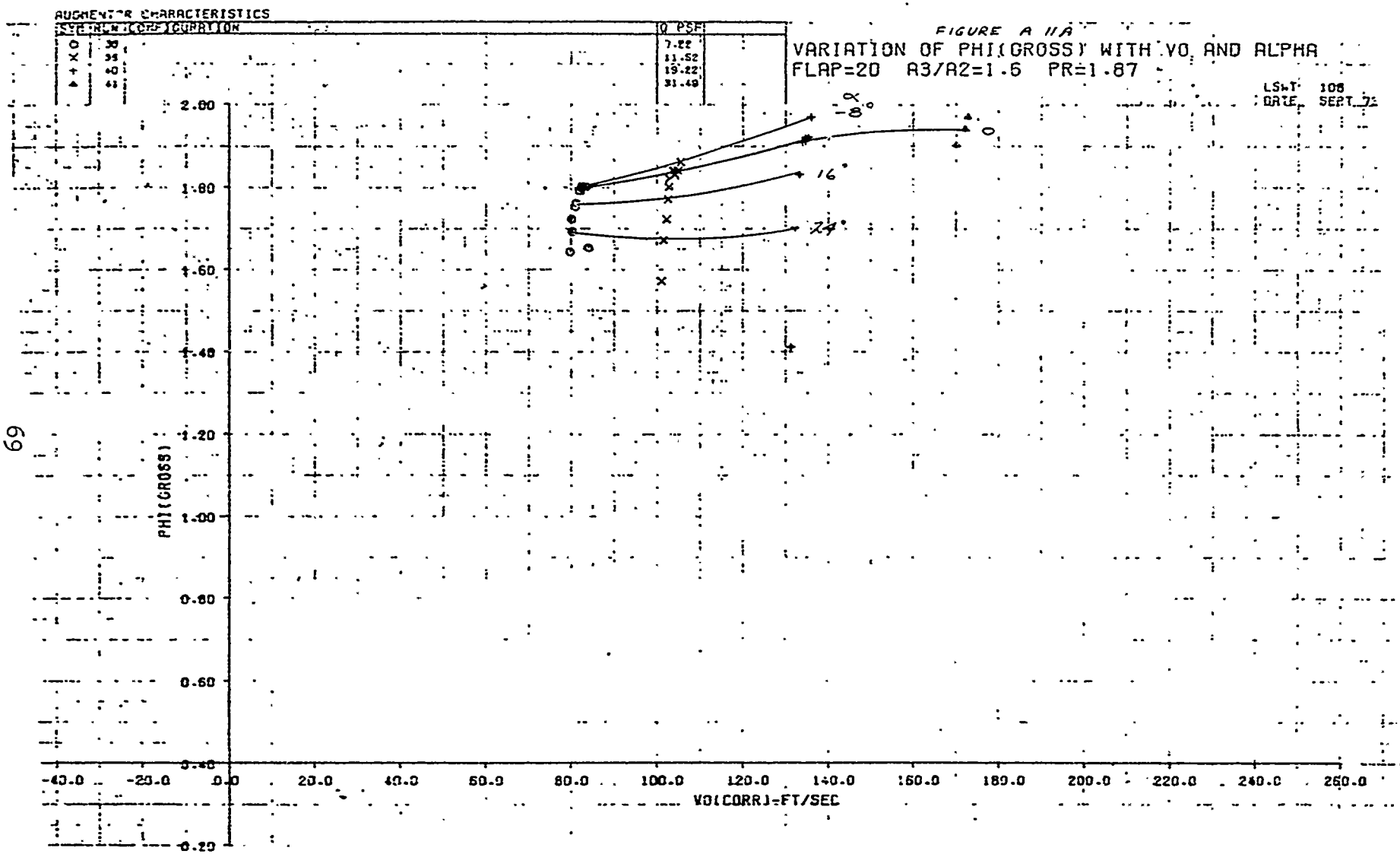
AUGMENTOR CHARACTERISTICS
SYSTEM CONFIGURATION
Q PSF
7.22
11.52
19.22
31.49
30
35
40
45
FIGURE A IIA
VARIATION OF PHI(GROSS) WITH VO AND ALPHA
FLAP=20 A3/A2=1.6 PR=1.87
LSWT 108
DATE SEPT 7
α
-8°
0
16°
24°
PHI(GROSS)
2.00
1.80
1.60
1.40
1.20
1.00
0.80
0.60
0.40
0.20
-40.0
-20.0
0.0
20.0
40.0
60.0
80.0
100.0
120.0
140.0
160.0
180.0
200.0
220.0
240.0
260.0
VO(CORR)=FT/SEC

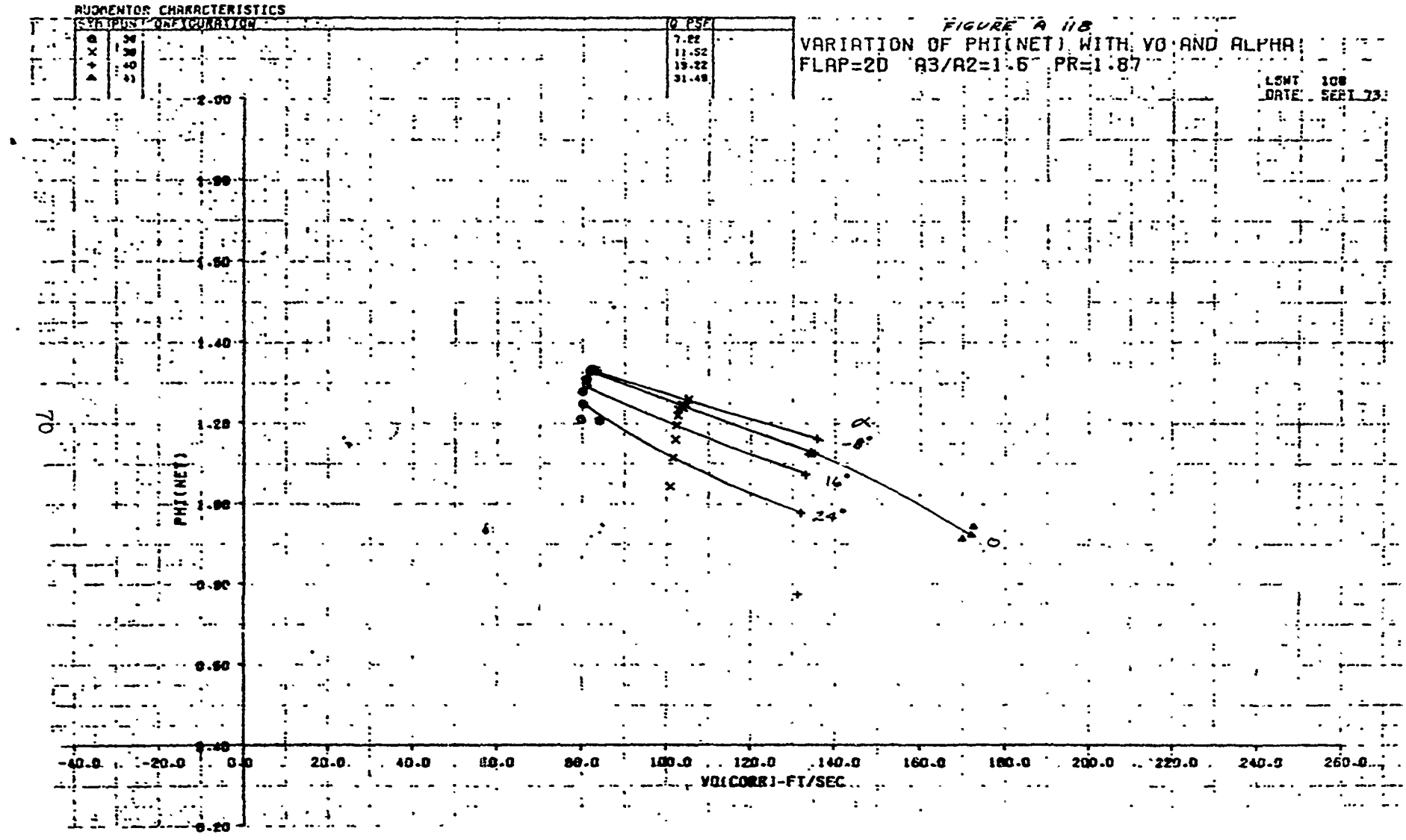
AUGMENTOR CHARACTERISTICS
SYMBOL CONFIGURATION
Q PSF
7.82
11.52
19.22
31.48
FIGURE A 118
VARIATION OF PHI(NET) WITH VO AND ALPHA
FLAP=20 A3/A2=1.6 PR=1.87
LSWT 108
DATE SEPT 73
PHI(NET)
VO(CORR)-FT/SEC
α
-8°
16°
24°
0
2.00
1.80
1.60
1.40
1.20
1.00
0.80
0.60
0.40
0.20
-40.0
-20.0
0.0
20.0
40.0
60.0
80.0
100.0
120.0
140.0
160.0
180.0
200.0
220.0
240.0
260.0

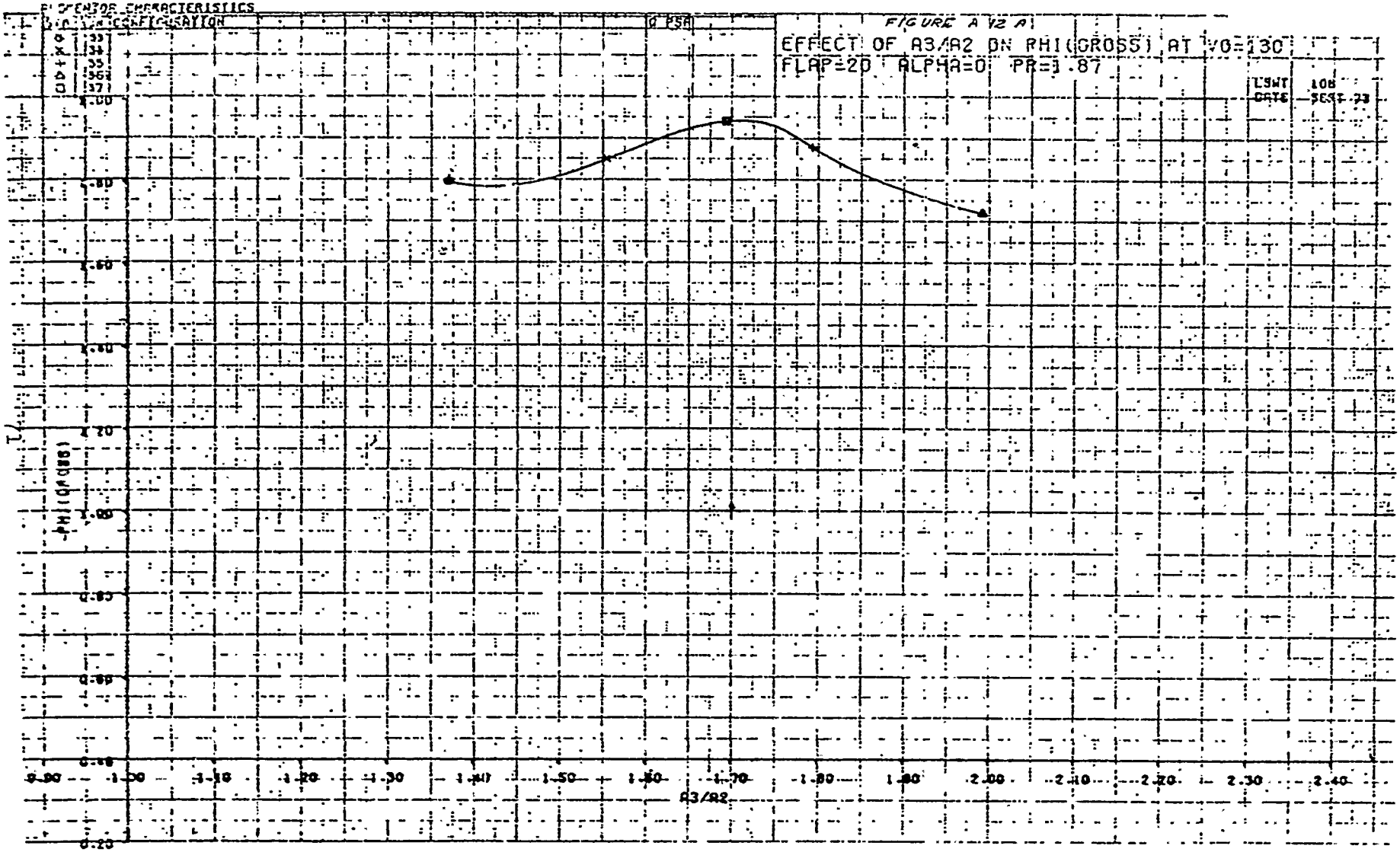
FIGURE A V2 A1
EFFECT OF A3/A2 ON RHI(CROSS) AT V0=130
FLAP=20 ALPHA=0 PR=1.87
LSWT
108
TEST 73
RHI(CROSS)
A3/A2
1.00
.80
.60
.40
.20
0.85
0.90
0.95
1.00
1.10
1.20
1.30
1.40
1.50
1.60
1.70
1.80
1.90
2.00
2.10
2.20
2.30
2.40

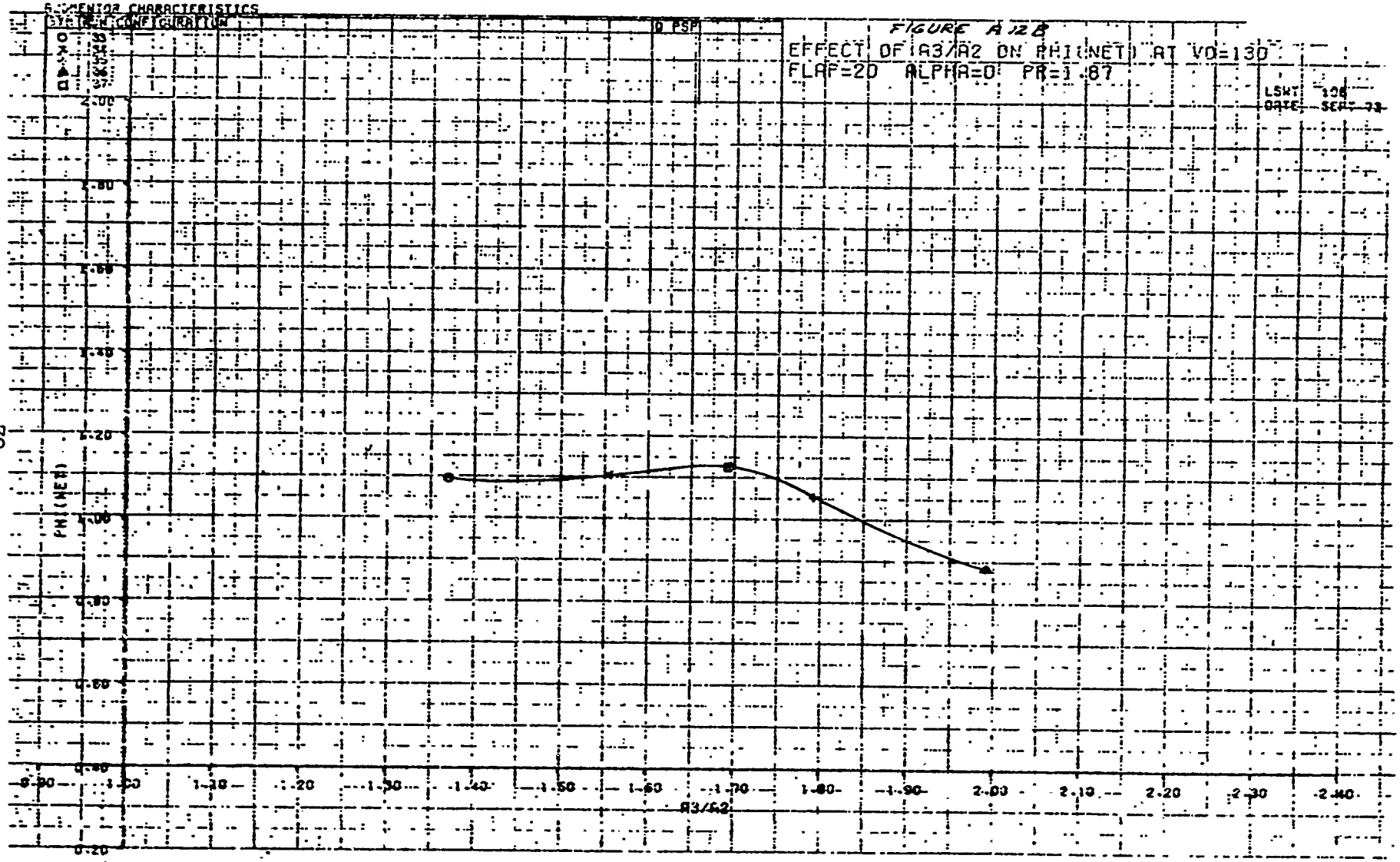
FIGURE A 12 B
EFFECT OF A3/A2 ON PHI(NET) AT VD=130
FLAP=20 ALPHA=0 PR=1.87
LSWT 10
DATE SEPT 73
PHI(NET)
A3/A2

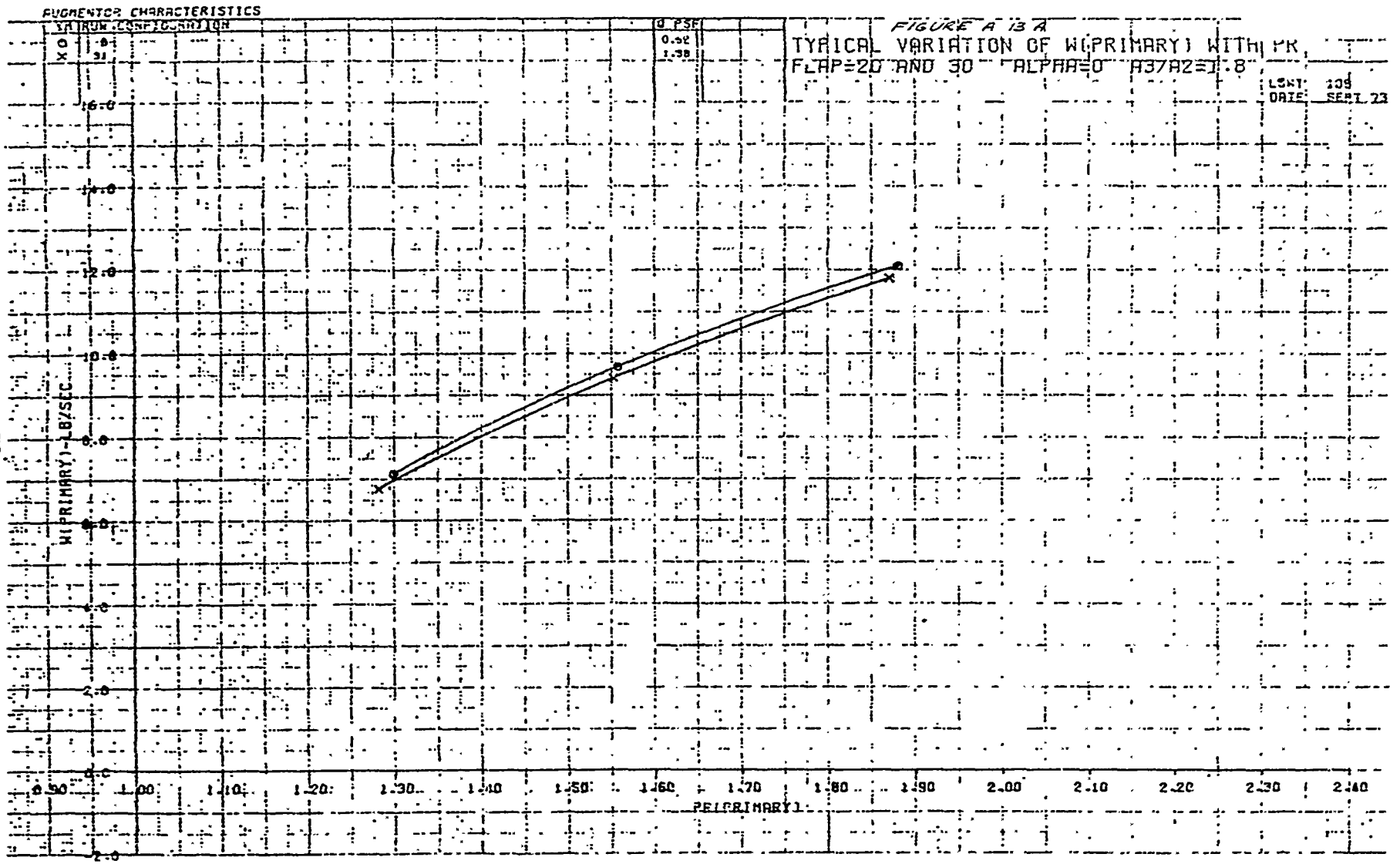
AUGMENTOR CHARACTERISTICS
VARIABLE CONFIGURATION
Q PSF
0.98
1.38
FIGURE A 13 A
TYPICAL VARIATION OF W(PRIMARY) WITH PR
FLAP=20 AND 30 ALPHA=0 A37A2=1.8
LENT 108
DATE SEPT 23
W(PRIMARY)-LB/SEC
PR(PRIMARY)
16.0
14.0
12.0
10.0
8.0
6.0
4.0
2.0
0.0
-2.0
0.90
1.00
1.10
1.20
1.30
1.40
1.50
1.60
1.70
1.80
1.90
2.00
2.10
2.20
2.30
2.40

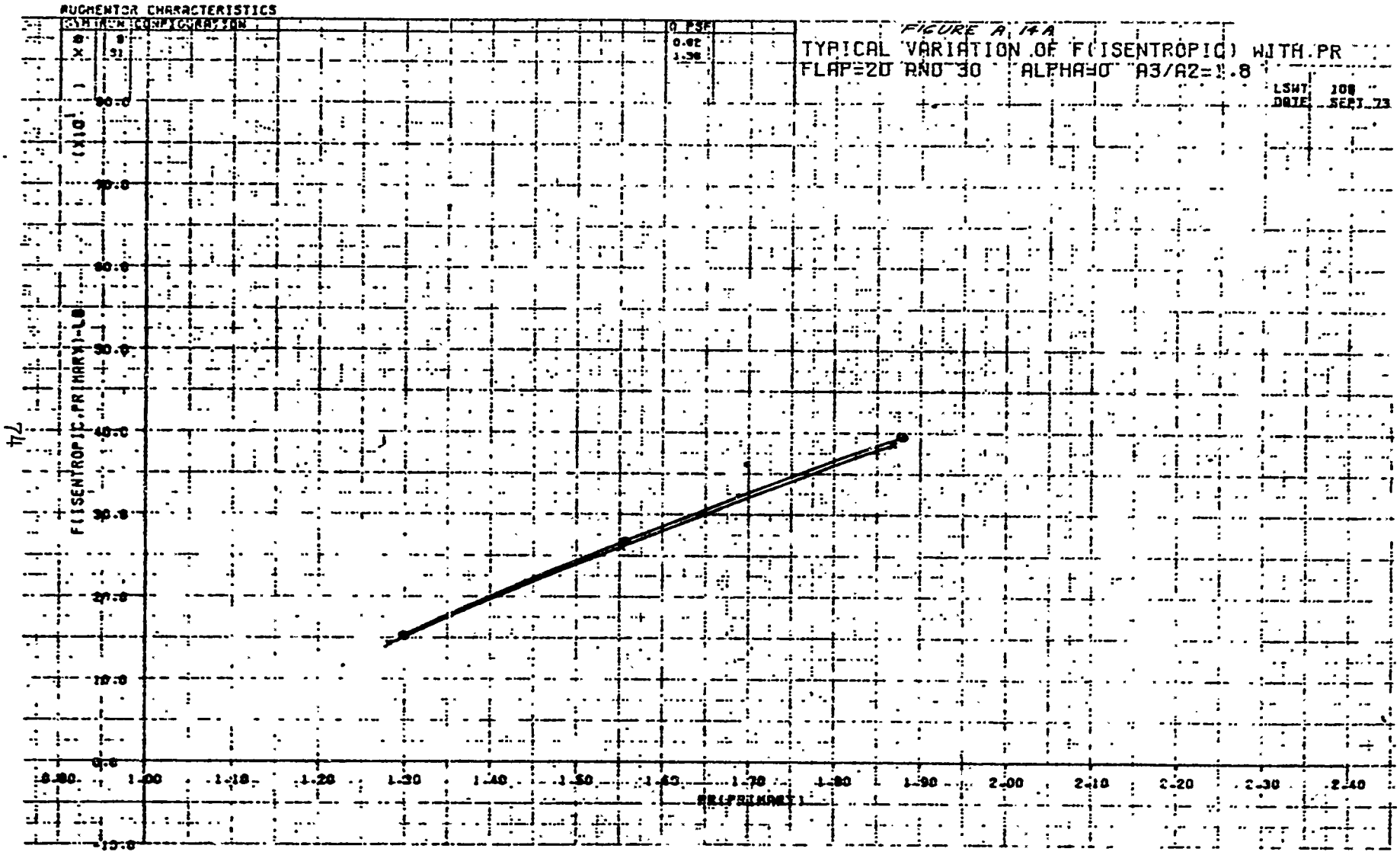
AUGMENTOR CHARACTERISTICS
CARTESIAN COMPUTER PLOT
Q PSF
0.02
1.36
FIGURE A.14A
TYPICAL VARIATION OF F(ISENTROPIC) WITH PR
FLAP=20 RND 30 ALPHA=0 A3/A2=1.8
LSWT 108
DATE SEPT 73
F(ISENTROPIC,PRIMARY)-LB
PR(PRIMARY)
74

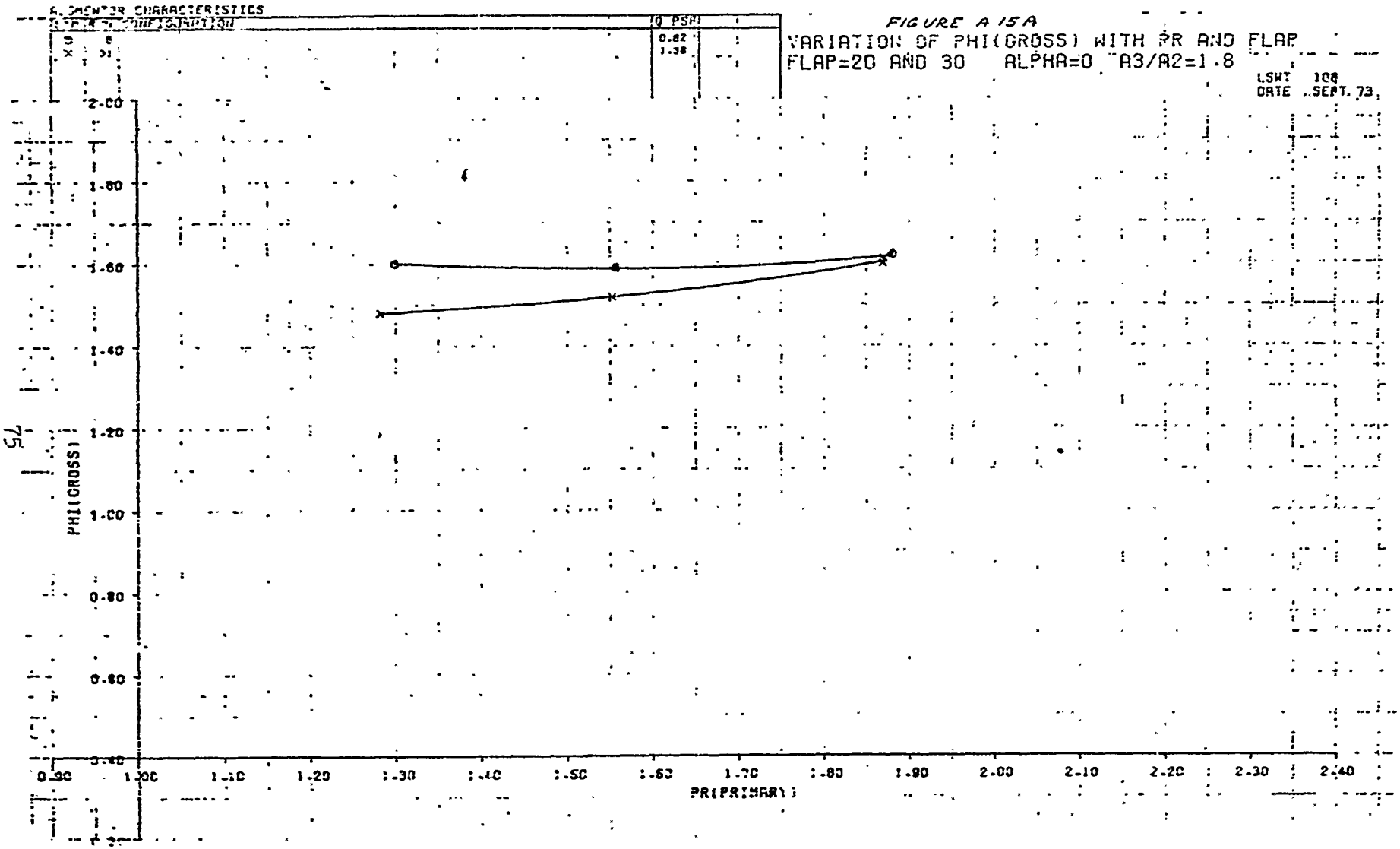

FIGURE A 15A

VARIATION OF PHI(GROSS) WITH PR AND FLAP

FLAP=20 AND 30 ALPHA=0 A3/A2=1.8

LSWT 108
DATE SEPT. 73

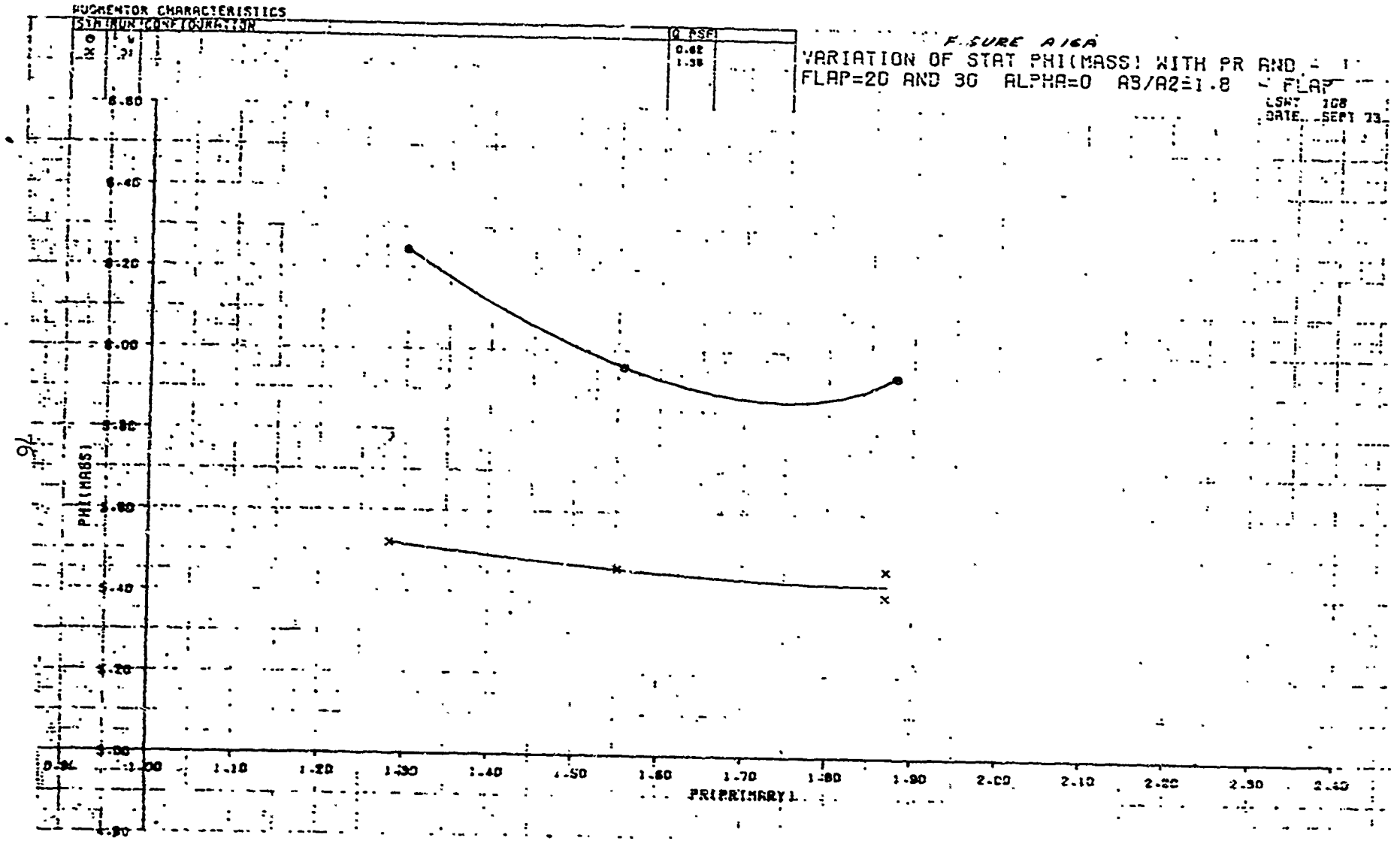
AUGMENTOR CHARACTERISTICS
SINGLE RUN CONFIGURATION
Q PSF
0.62
1.38
F-SURE A16A
VARIATION OF STAT PHI(MASS) WITH PR AND
FLAP=20 AND 30 ALPHA=0 A9/A2=1.8
FLAP
LSHT 108
DATE SEPT 73
PHI(MASS)
PR(PRIMARY)
1.00
1.10
1.20
1.30
1.40
1.50
1.60
1.70
1.80
1.90
2.00
2.10
2.20
2.30
2.40

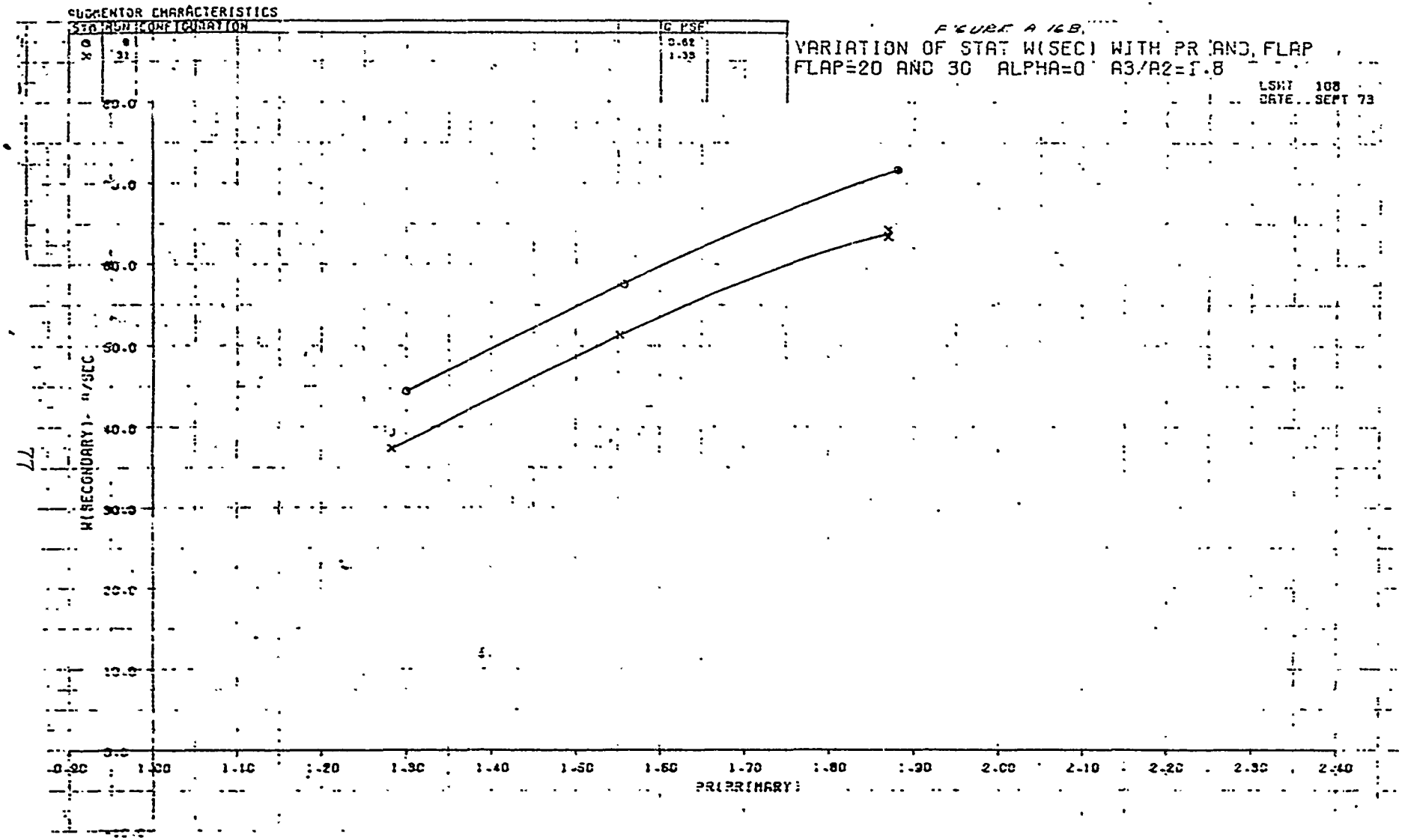
SUGMENTOR CHARACTERISTICS
STATIC CONFIGURATION
Q PSF
0.62
1.39
FIGURE A 16B.
VARIATION OF STAT W(SEC) WITH PR AND FLAP
FLAP=20 AND 30 ALPHA=0 A3/A2=1.8
LSNT 108
DATE..SEPT 73
W(SECONDARY)- FT/SEC
PR(PRIMARY)
77

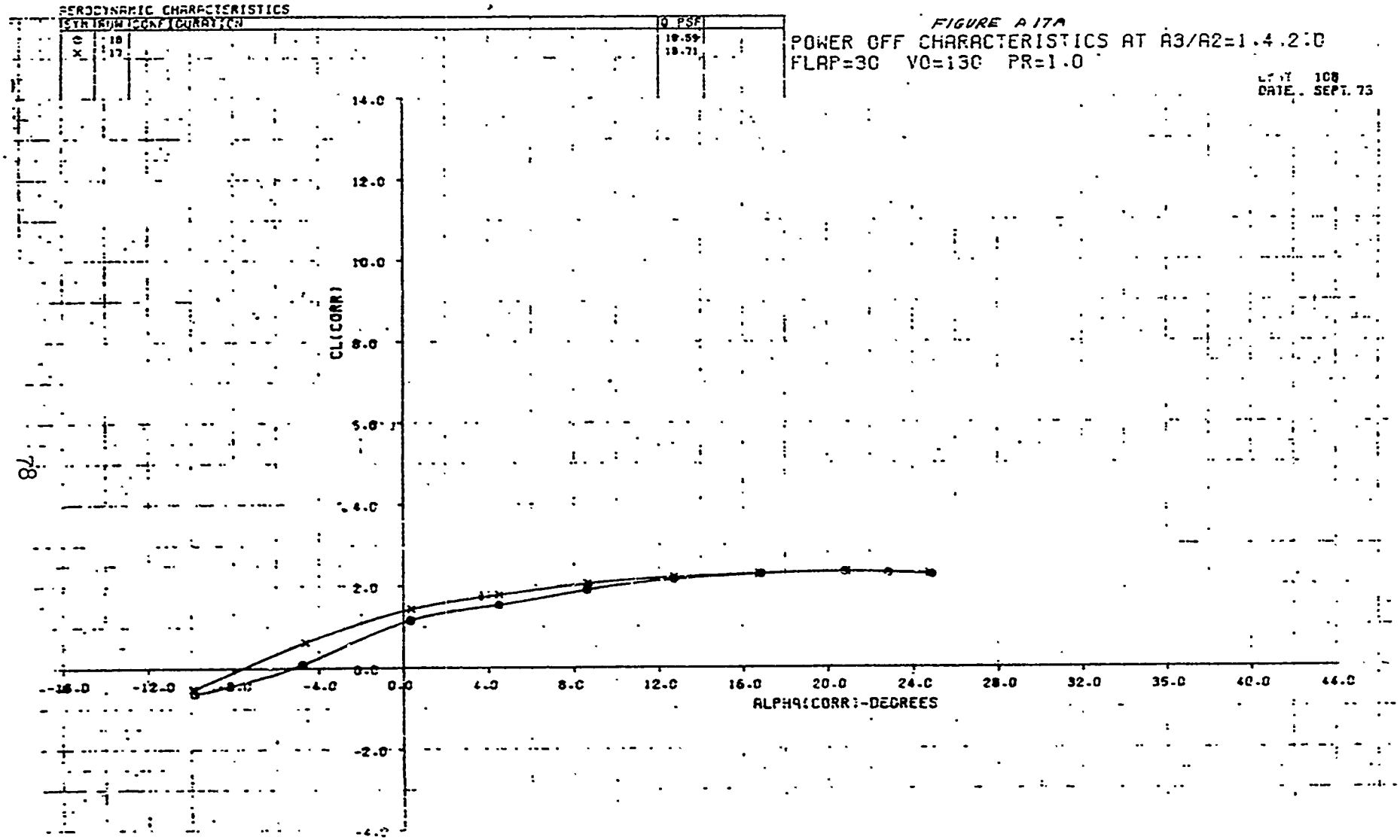

FIGURE A 17A

POWER OFF CHARACTERISTICS AT A3/A2=1.4.2.0
FLAP=30 V0=130 PR=1.0

DATE. SEPT. 75

V/

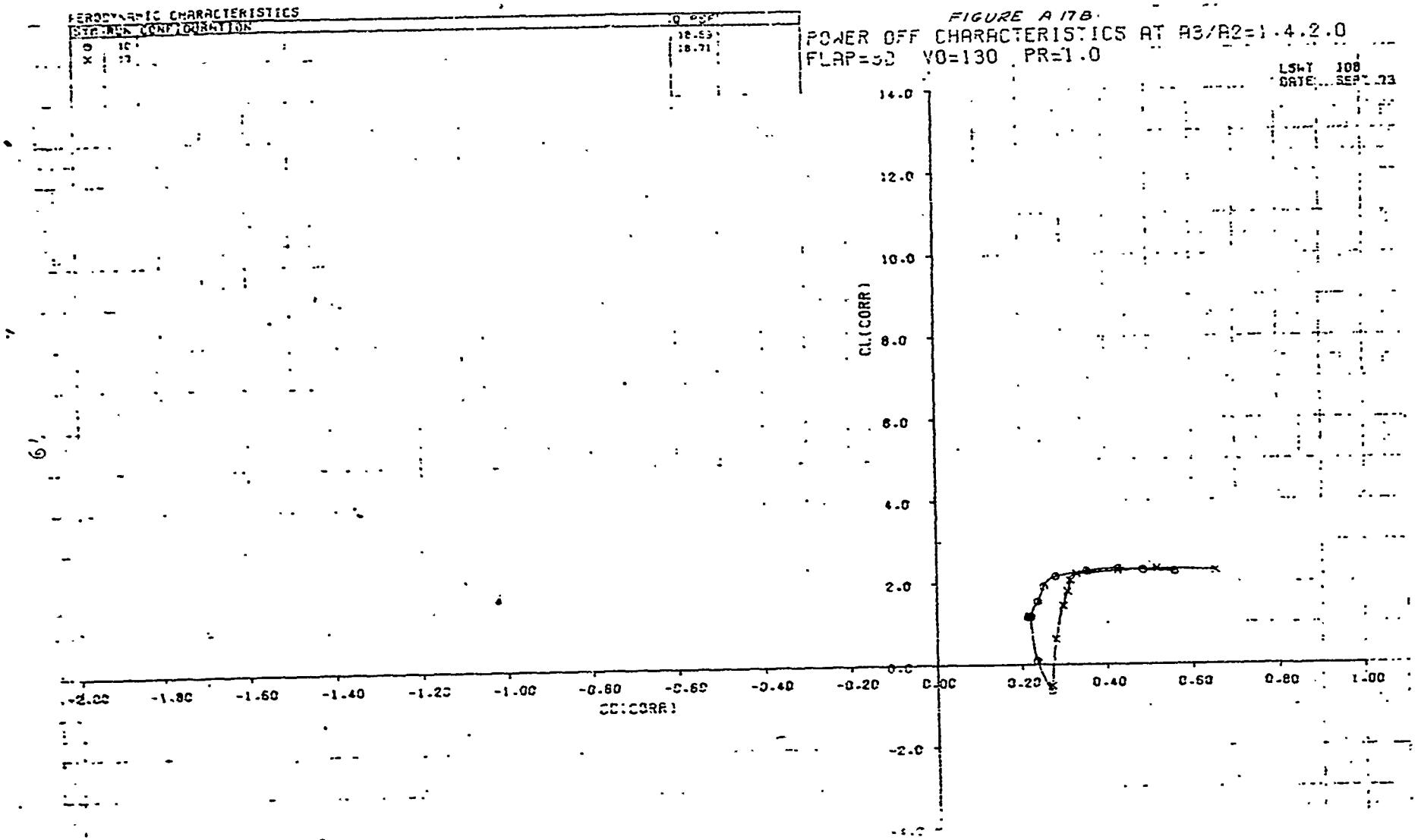

FIGURE A 17B

POWER OFF CHARACTERISTICS AT A3/A2=1.4.2.0
FLAP=30 V0=130 PR=1.0

LSWT 108
DATE SEPT 23

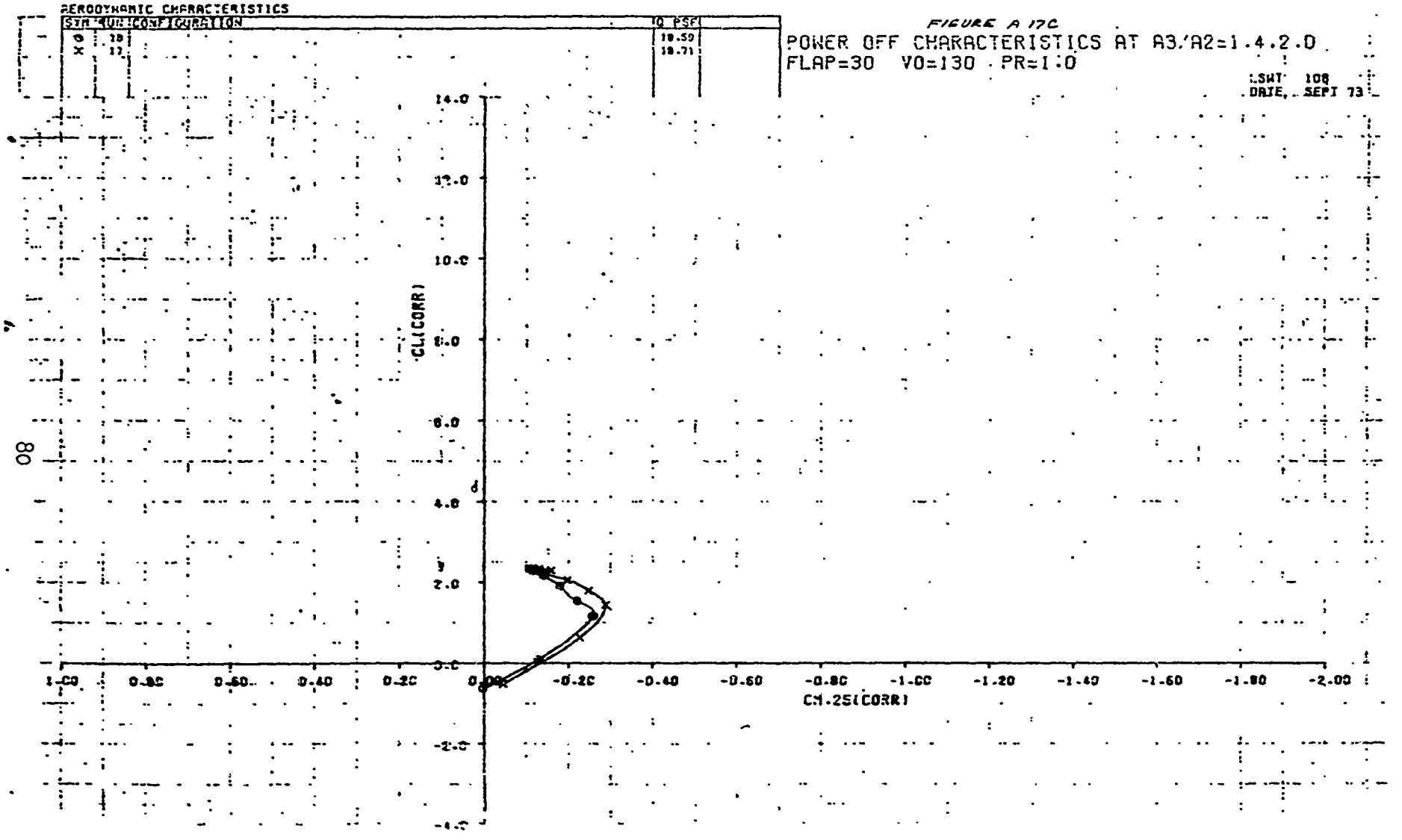

FIGURE A 17C

POWER OFF CHARACTERISTICS AT A3/A2=1.4.2.0
FLAP=30 V0=130 PR=1.0

LSHT 108
DATE, SEPT 73

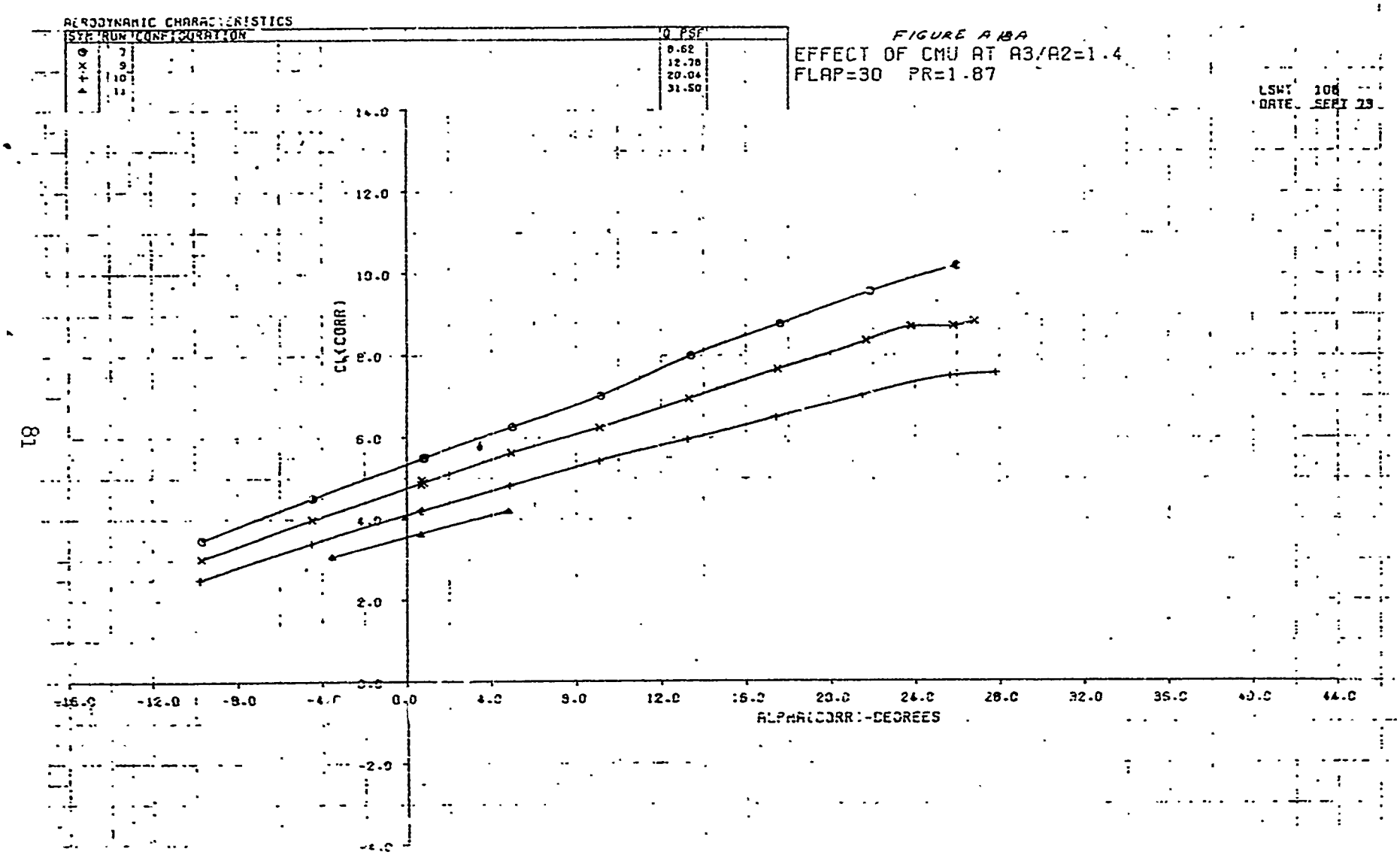

FIGURE A 18A

EFFECT OF CMU AT A3/A2=1.4
FLAP=30 PR=1.87

LSWT 108
DATE SEPT 23

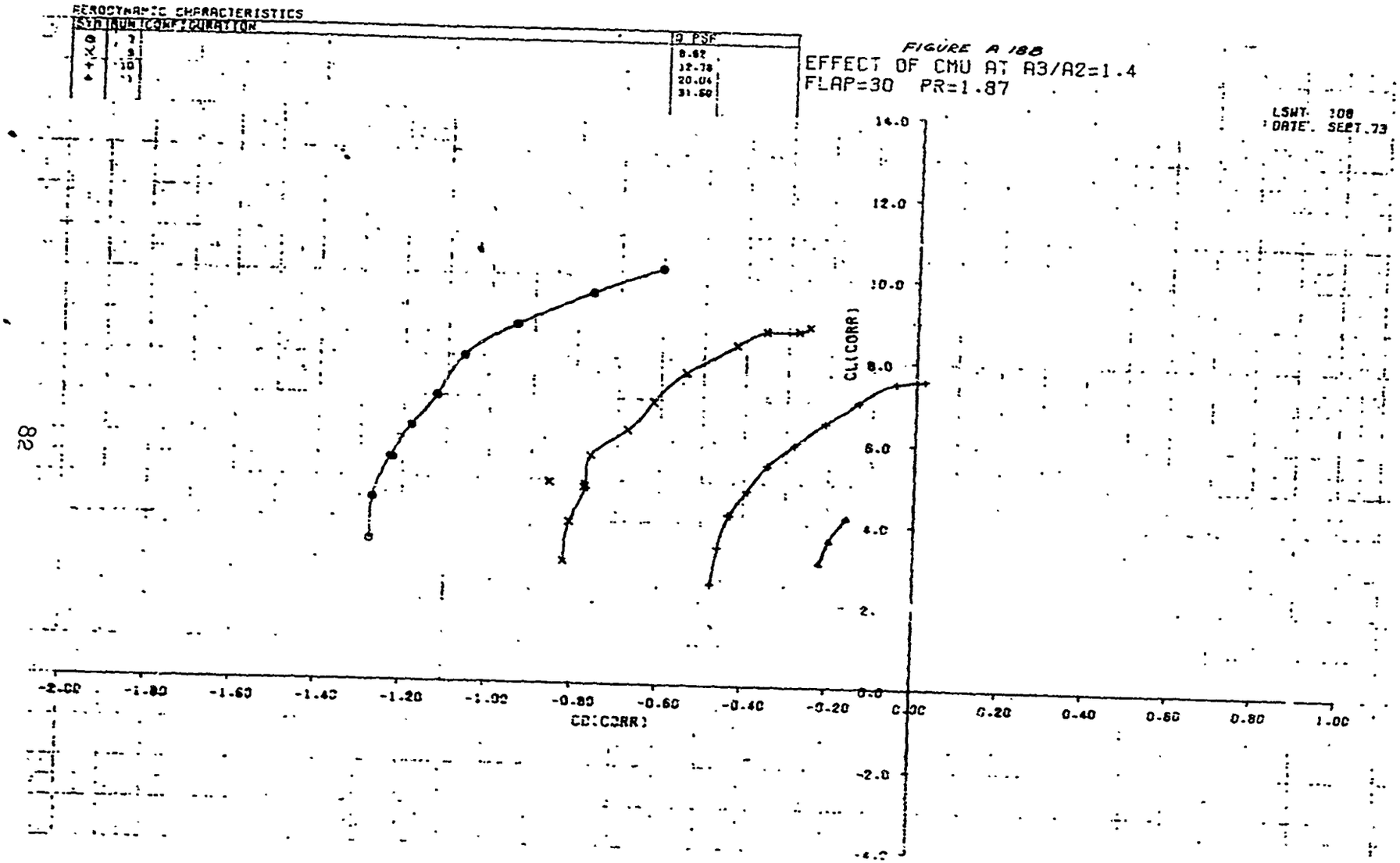

FIGURE A 188
EFFECT OF CMU AT A3/A2=1.4
FLAP=30 PR=1.87

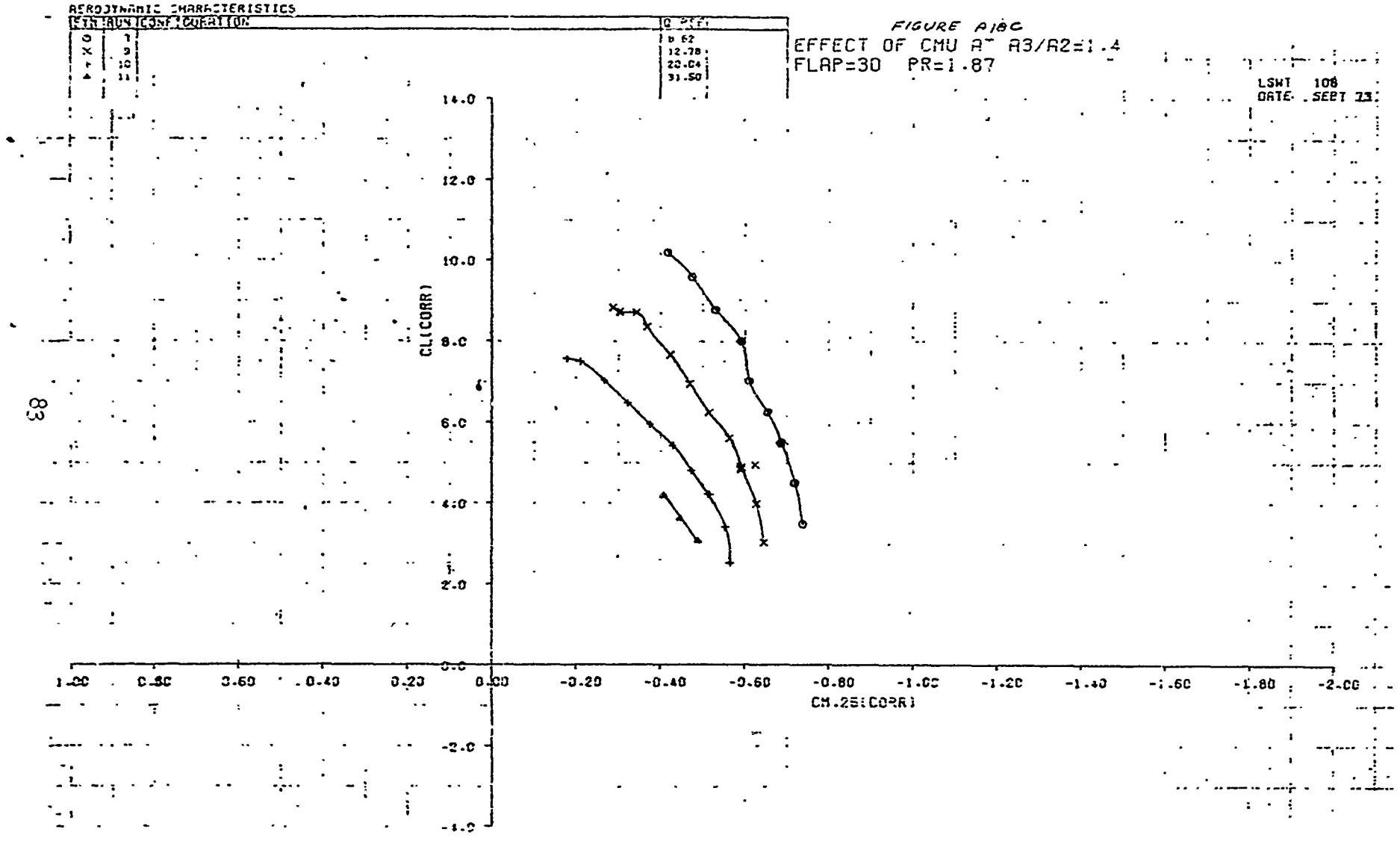
AERODYNAMIC CHARACTERISTICS
CONFIGURATION
FIGURE A18C
EFFECT OF CMU AT A3/A2=1.4
FLAP=30 PR=1.87
LSWT 108
DATE SEPT 73
CL(CORR)
CM.25(CORR)
14.0
12.0
10.0
8.0
6.0
4.0
2.0
0.0
-2.0
-4.0
1.00
0.80
0.60
0.40
0.20
0.00
-0.20
-0.40
-0.60
-0.80
-1.00
-1.20
-1.40
-1.60
-1.80
-2.00

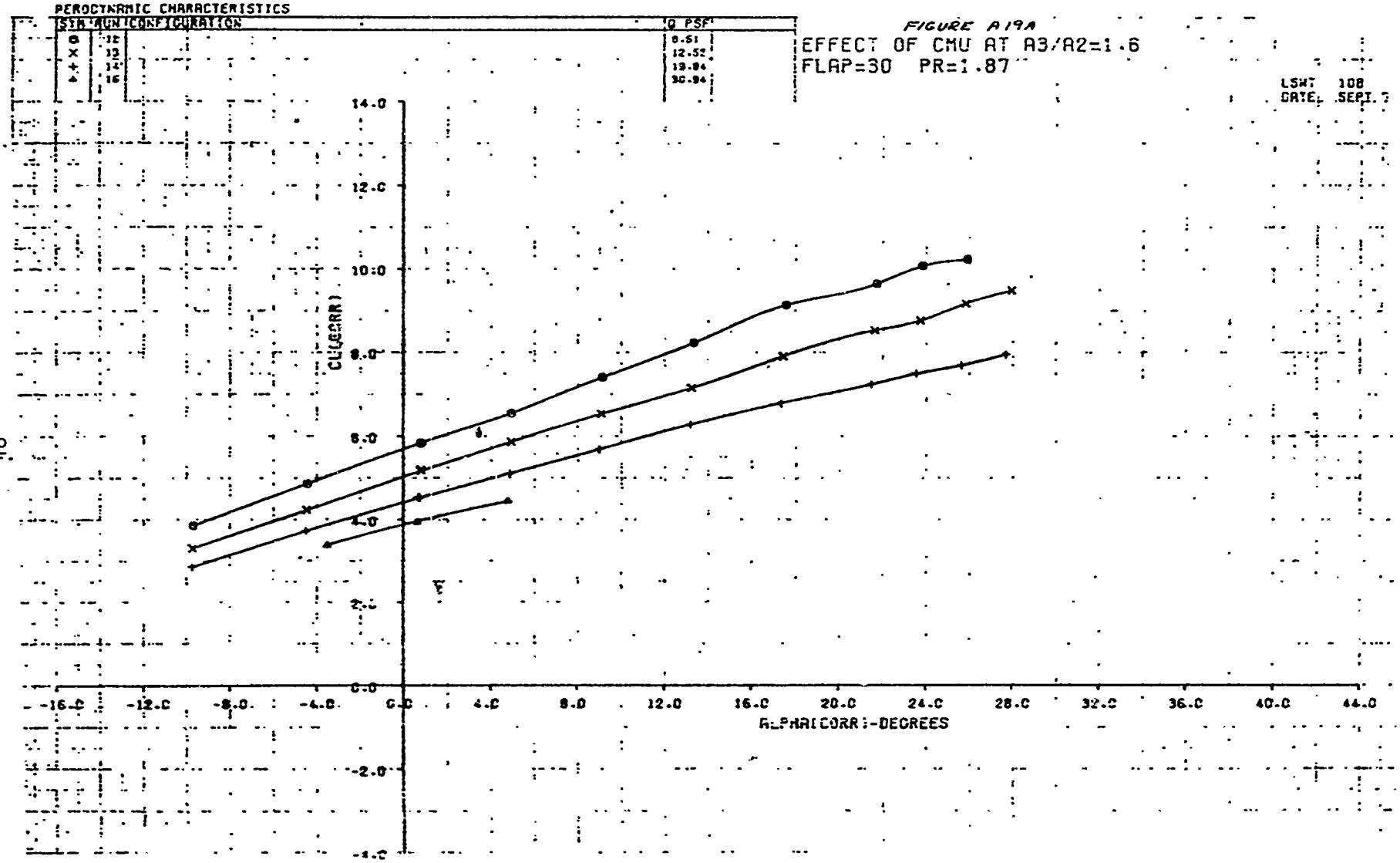
AERODYNAMIC CHARACTERISTICS
STR'AUN CONFIGURATION
Q PSF
0.51
12.52
19.84
30.94
FIGURE A19A
EFFECT OF CMU AT A3/A2=1.6
FLAP=30 PR=1.87
LSHT 108
DATE, SEPT.
CL(CORR)
14.0
12.0
10.0
8.0
6.0
4.0
2.0
0.0
-2.0
-16.0
-12.0
-8.0
-4.0
0.0
4.0
8.0
12.0
16.0
20.0
24.0
28.0
32.0
36.0
40.0
44.0
ALPHA(CORR):-DEGREES

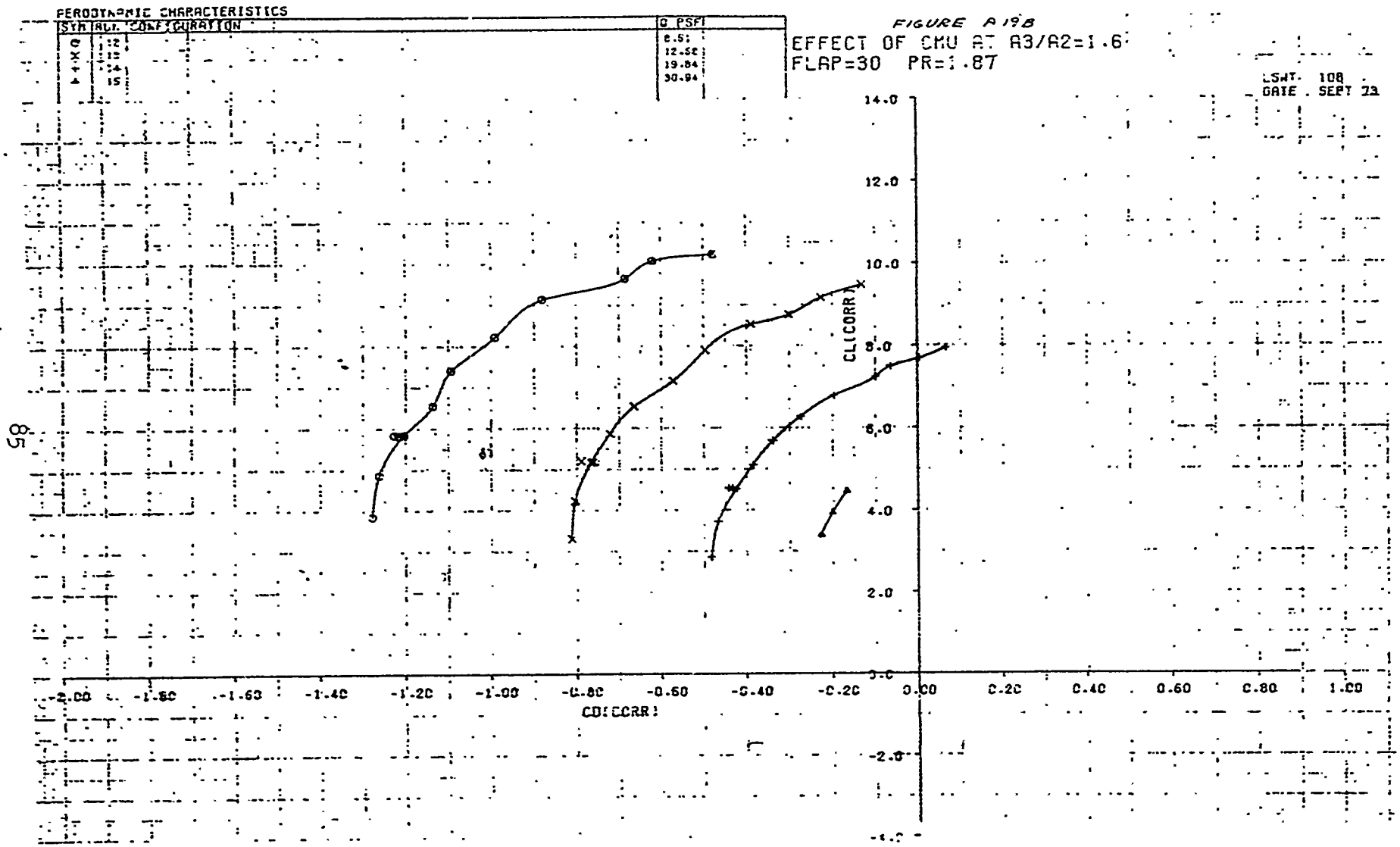
AERODYNAMIC CHARACTERISTICS
SYM ALT CONFIGURATION
Q PSF
6.51
12.52
19.84
30.94
FIGURE A19B
EFFECT OF CMU AT A3/A2=1.6
FLAP=30 PR=1.87
LSWT 108
GATE SEPT 23
CL(CORR)
CD(CORR)
14.0
12.0
10.0
8.0
6.0
4.0
2.0
0.0
-2.0
-2.00
-1.80
-1.60
-1.40
-1.20
-1.00
-0.80
-0.60
-0.40
-0.20
0.00
0.20
0.40
0.60
0.80
1.00

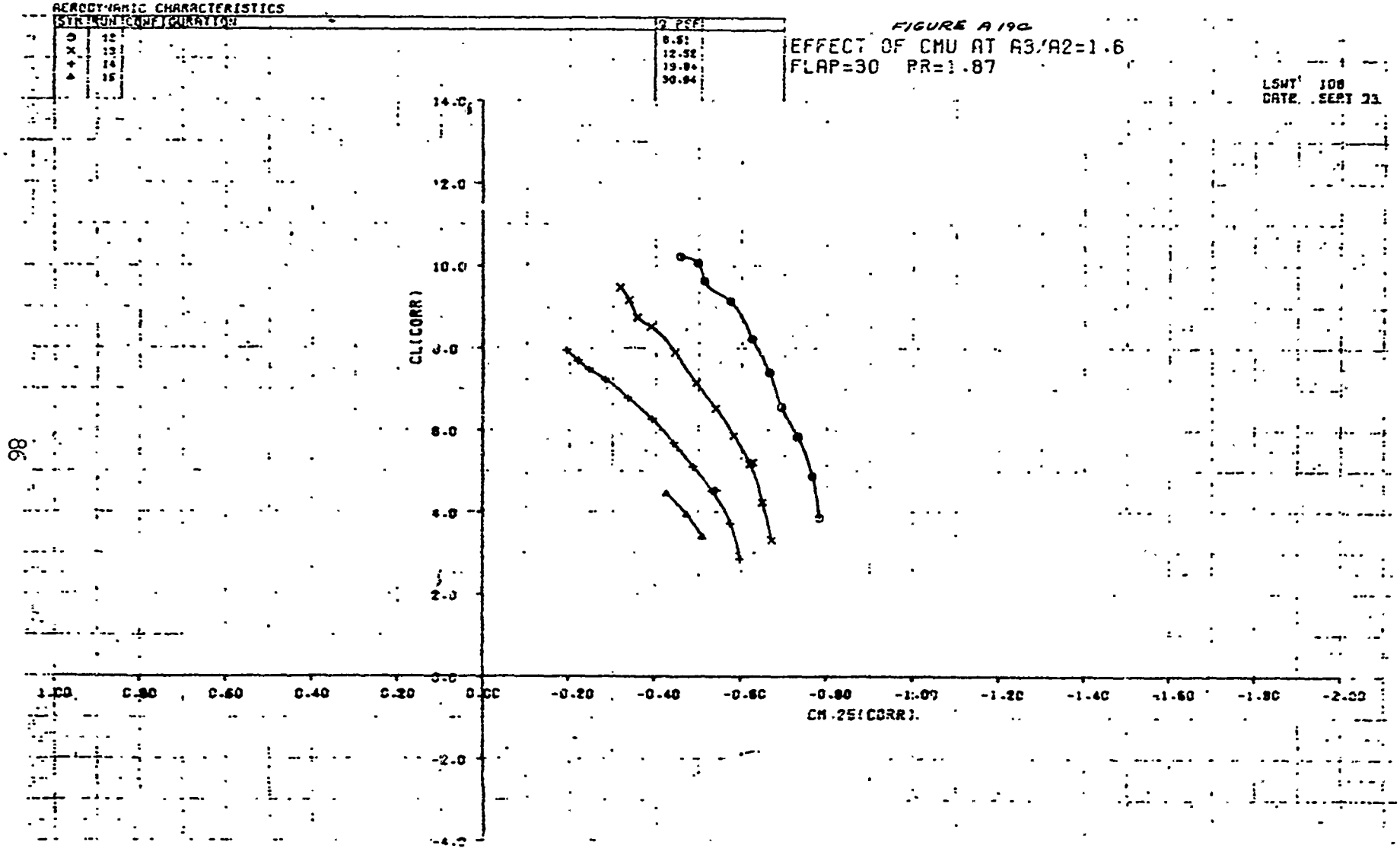
AERODYNAMIC CHARACTERISTICS
STATION CONFIGURATION
12
13
14
15
2 PSF
6.81
12.52
19.84
30.84
FIGURE A 19c
EFFECT OF CMU AT A3/A2=1.6
FLAP=30 PR=1.87
LSWT 108
DATE SEPT 21
CL(CORR)
14.0
12.0
10.0
8.0
6.0
4.0
2.0
0.0
-2.0
-4.0
1.00
0.80
0.60
0.40
0.20
0.00
-0.20
-0.40
-0.60
-0.80
-1.00
-1.20
-1.40
-1.60
-1.80
-2.00
CM.25(CORR).

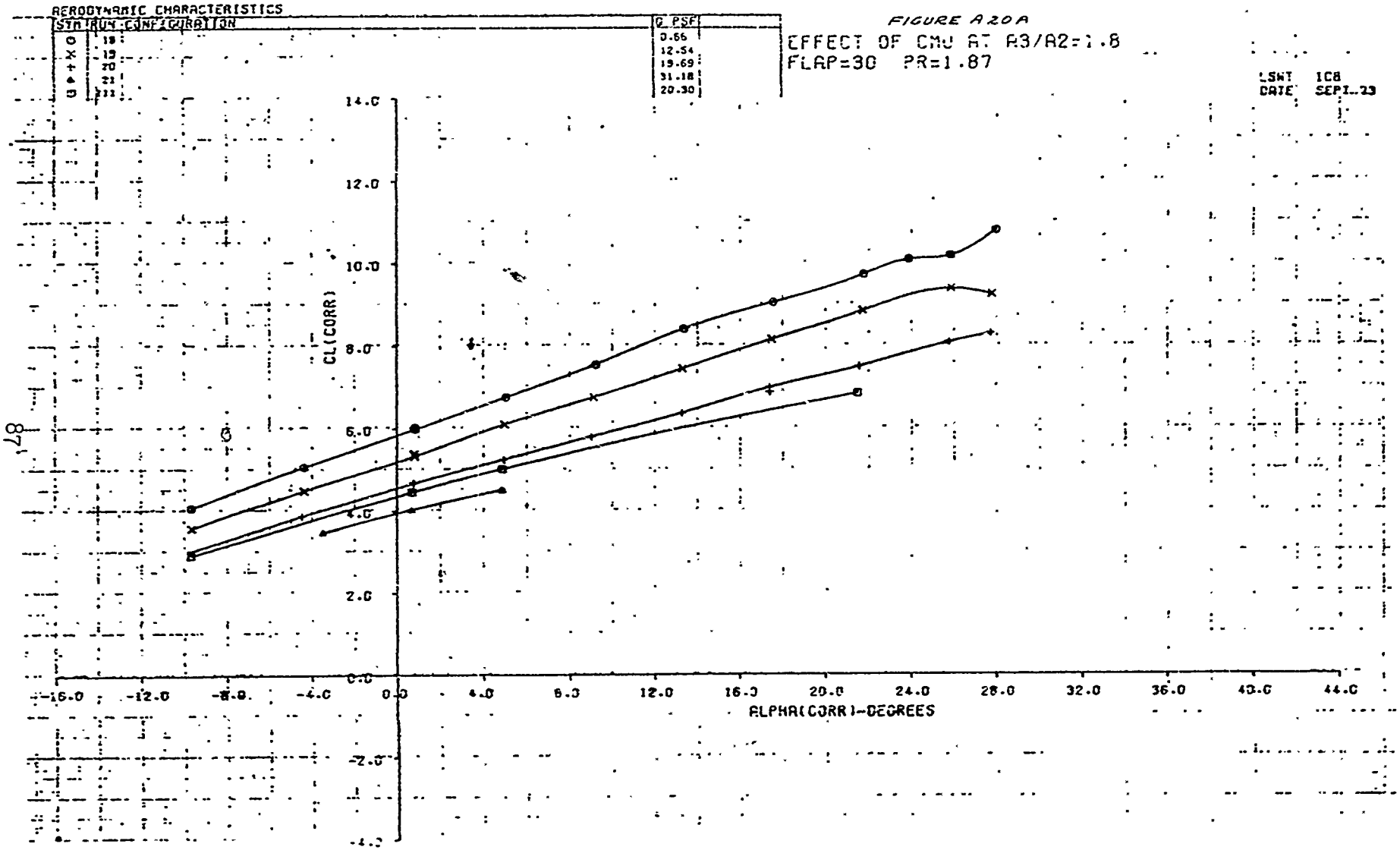
AERODYNAMIC CHARACTERISTICS
STN RUN CONFIGURATION
Q PSF
0.66
12.54
19.69
31.18
20.30
FIGURE A20A
EFFECT OF CMU AT A3/A2=1.8
FLAP=30 PR=1.87
LSWT IC8
DATE SEP1-23
CL(CORR)
ALPHA(CORR)-DEGREES
14.0
12.0
10.0
8.0
6.0
4.0
2.0
0.0
-2.0
-4.0
-16.0
-12.0
-8.0
-4.0
0.0
4.0
8.0
12.0
16.0
20.0
24.0
28.0
32.0
36.0
40.0
44.0

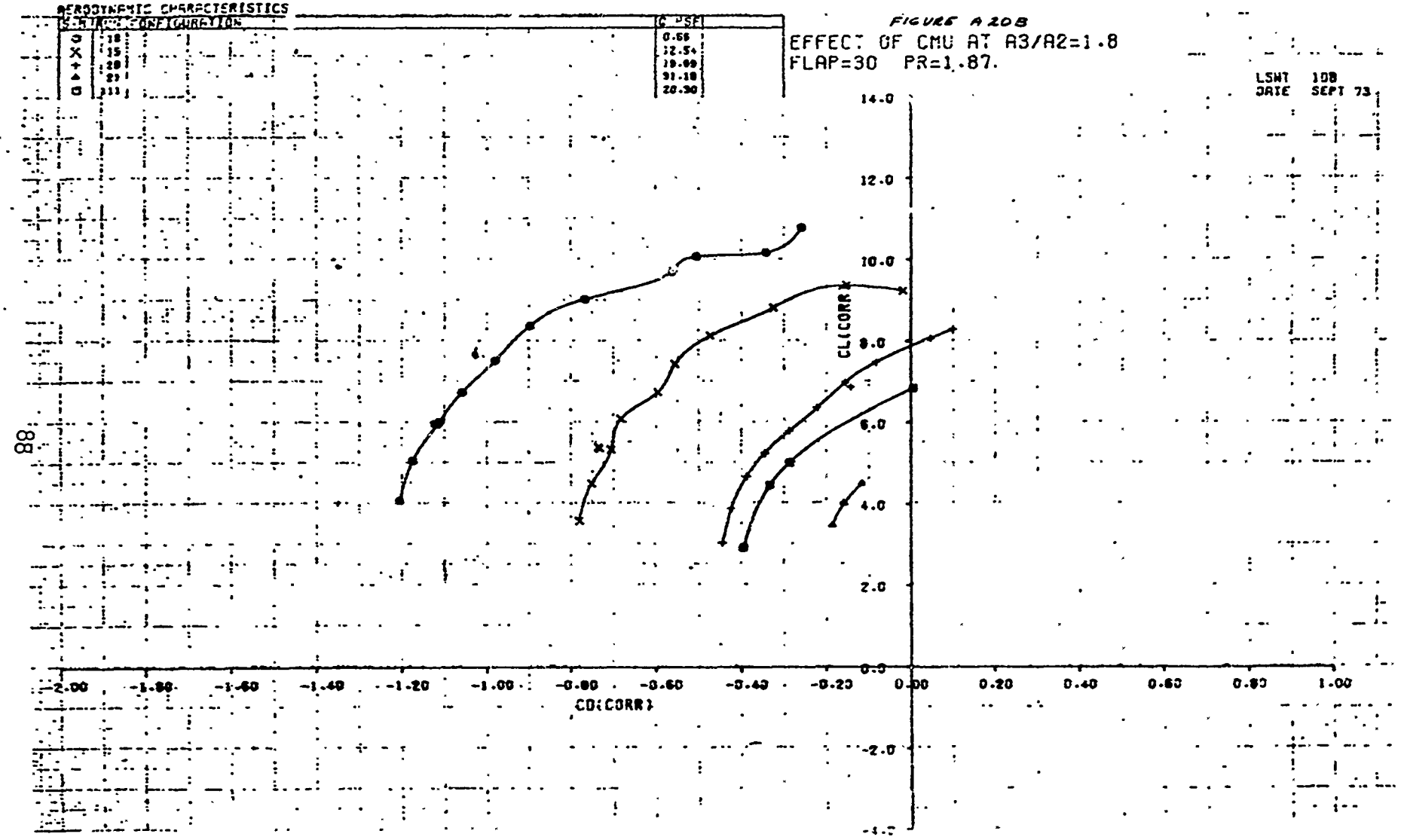

FIGURE A 20B

EFFECT OF CMU AT A3/A2=1.8
FLAP=30 PR=1.87.

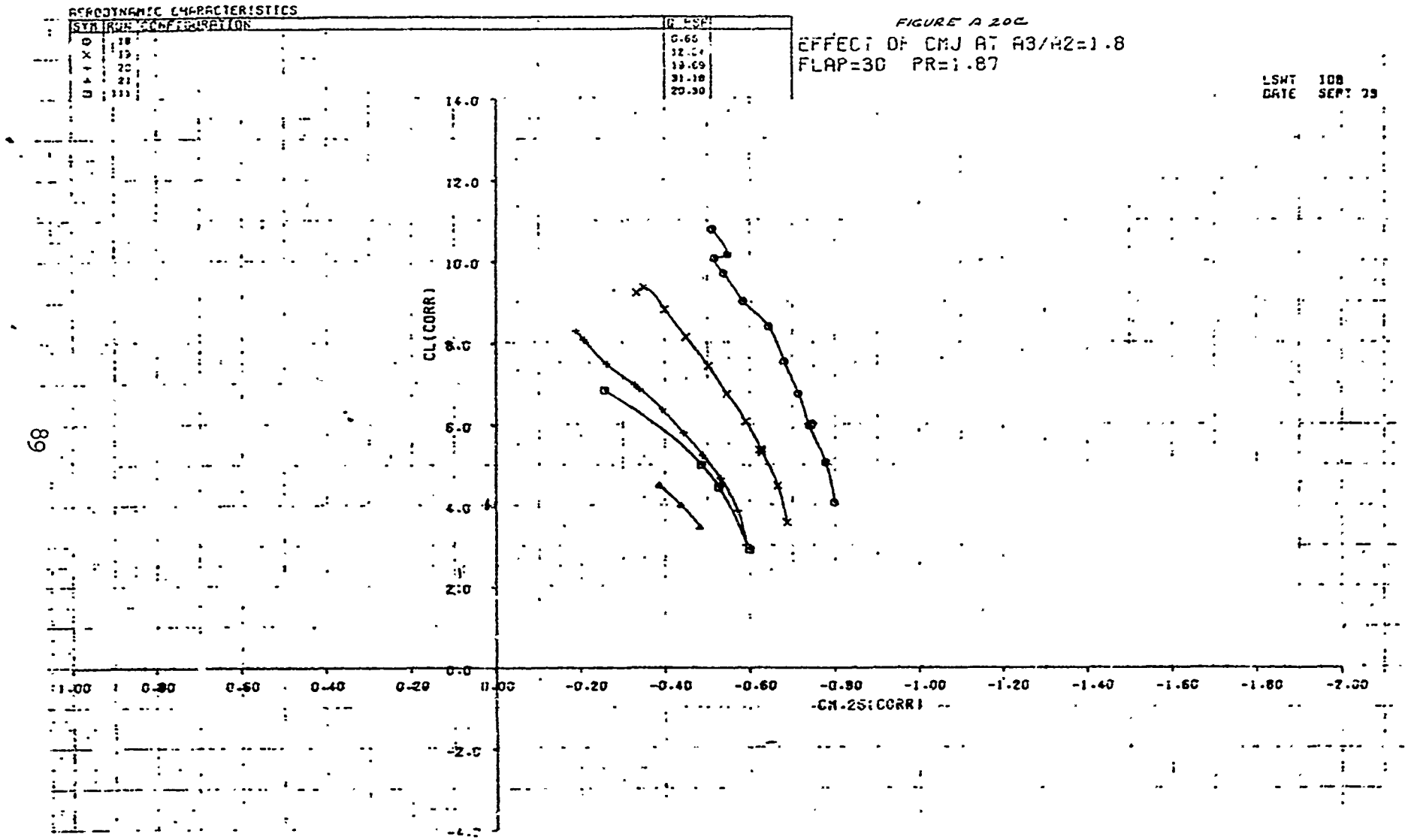
AERODYNAMIC CHARACTERISTICS
SYM RUN CONFIGURATION
FIGURE A 20C
EFFECT OF CMJ AT A3/A2=1.8
FLAP=30 PR=1.87
LSWT 108
DATE SEPT 79
CL(CORR)
-CM.25(CORR)
14.0
12.0
10.0
8.0
6.0
4.0
2.0
0.0
-2.0
1.00
0.80
0.60
0.40
0.20
0.00
-0.20
-0.40
-0.60
-0.80
-1.00
-1.20
-1.40
-1.60
-1.80
-2.00

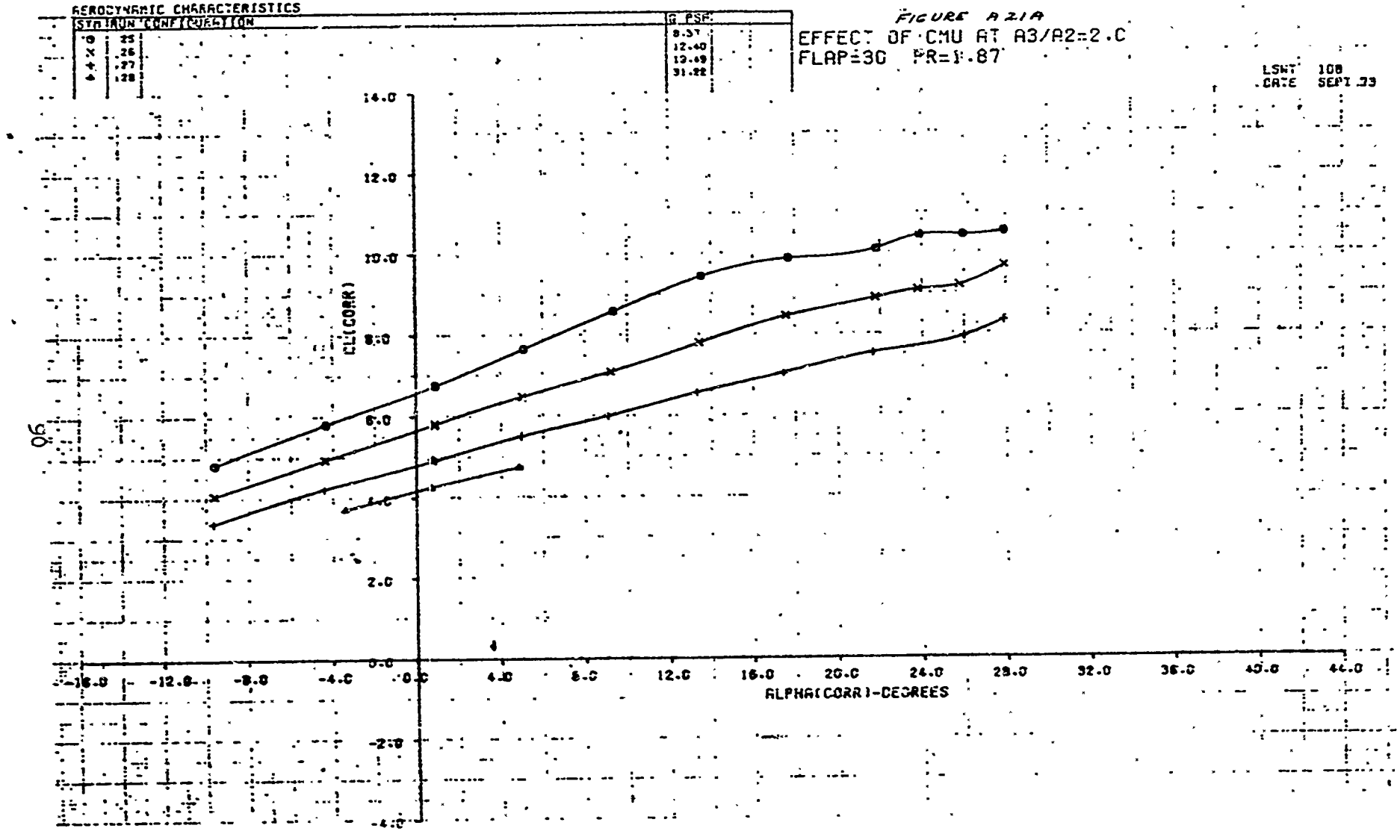
AERODYNAMIC CHARACTERISTICS
STD RUN CONFIGURATION
Q PSF
8.57
12.40
19.49
31.22
FIGURE A21A
EFFECT OF CMU AT A3/A2=2.C
FLAP=30 PR=1.87
LSWT 108
DATE SEPT 83
CL(CORR)
ALPHA(CORR)-DEGREES
14.0
12.0
10.0
8.0
6.0
4.0
2.0
0.0
-2.0
-4.0
-16.0
-12.0
-8.0
-4.0
0.0
4.0
8.0
12.0
16.0
20.0
24.0
28.0
32.0
36.0
40.0
44.0

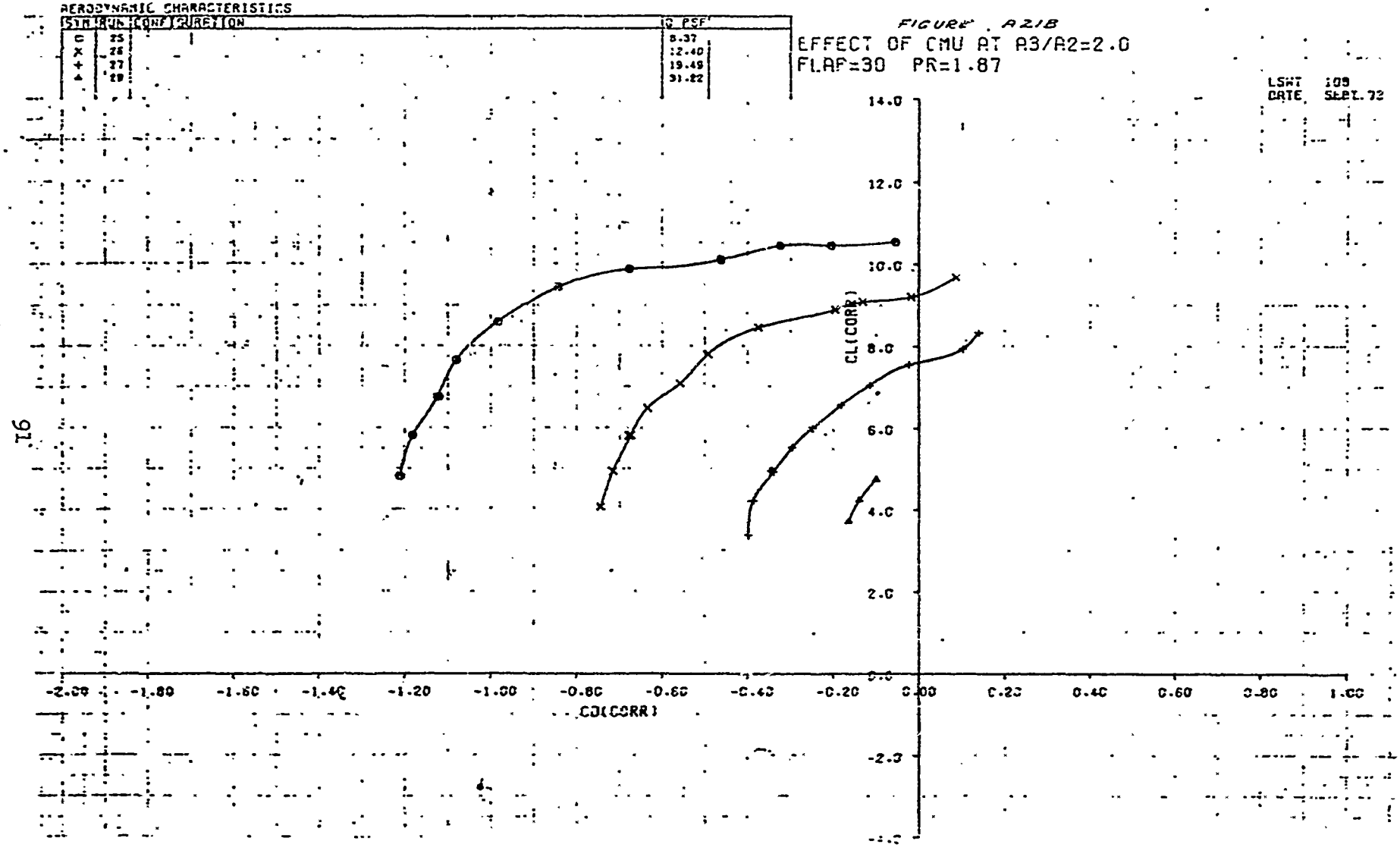
AERODYNAMIC CHARACTERISTICS
STN RUN CONFIGURATION
Q PSF
8.37
12.40
19.49
31.22
FIGURE A21B
EFFECT OF CMU AT A3/A2=2.0
FLAP=30 PR=1.87
LSHT 109
DATE SEPT. 72
CL(CORR)
CD(CORR)
14.0
12.0
10.0
8.0
6.0
4.0
2.0
-2.0
-2.00
-1.80
-1.60
-1.40
-1.20
-1.00
-0.80
-0.60
-0.40
-0.20
0.00
0.20
0.40
0.60
0.80
1.00

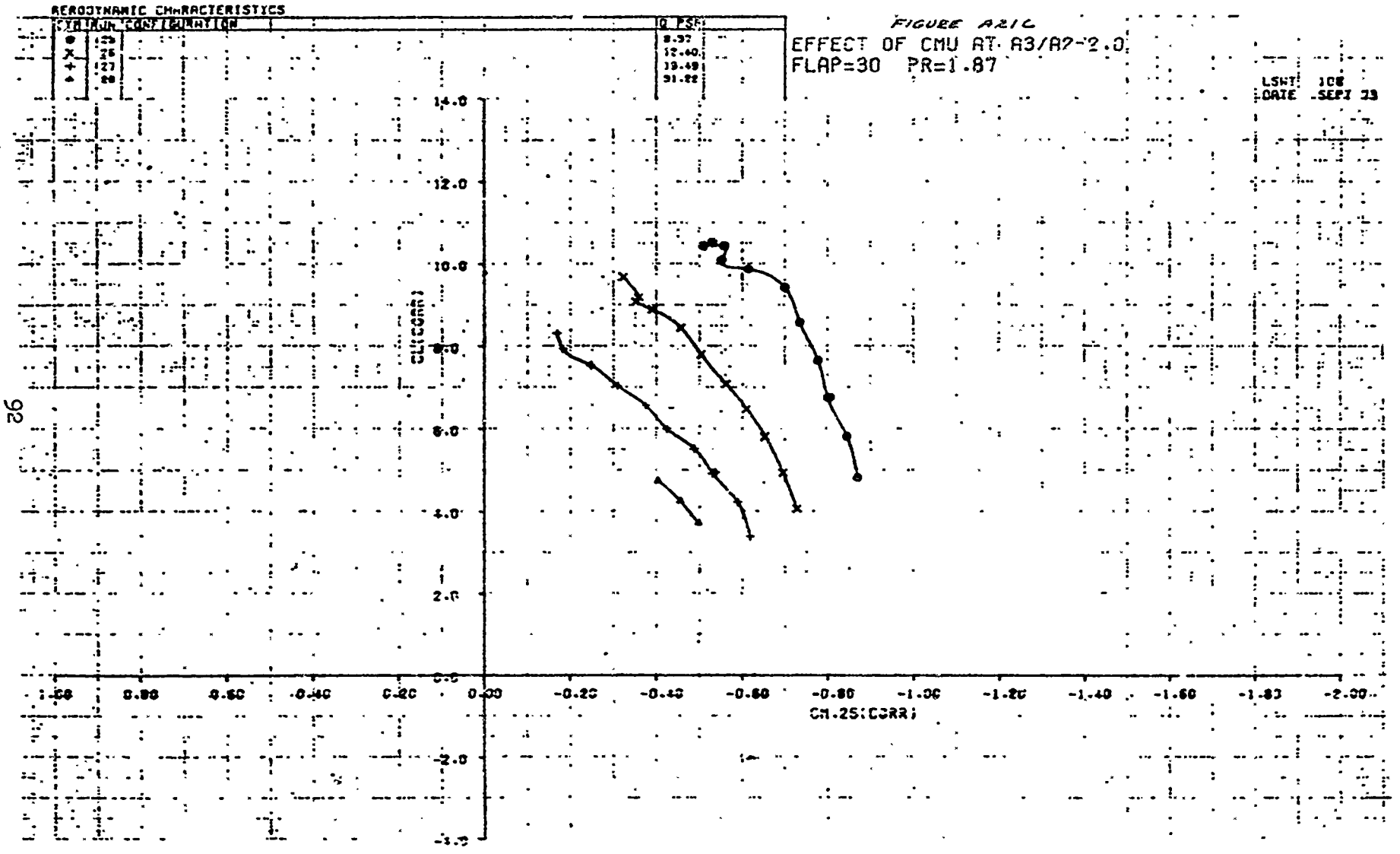
AERODYNAMIC CHARACTERISTICS
CYLINDER CONFIGURATION
Q PSF
8.37
12.40
19.49
31.82
FIGURE A21C
EFFECT OF CMU AT A3/A2=2.0
FLAP=30 PR=1.87
LSHT ICE
DATE SEPT 23
CL(CORR)
CM.25(CORR)
14.0
12.0
10.0
8.0
6.0
4.0
2.0
0.0
-2.0
-0.20
-0.40
-0.60
-0.80
-1.00
-1.20
-1.40
-1.60
-1.80
-2.00

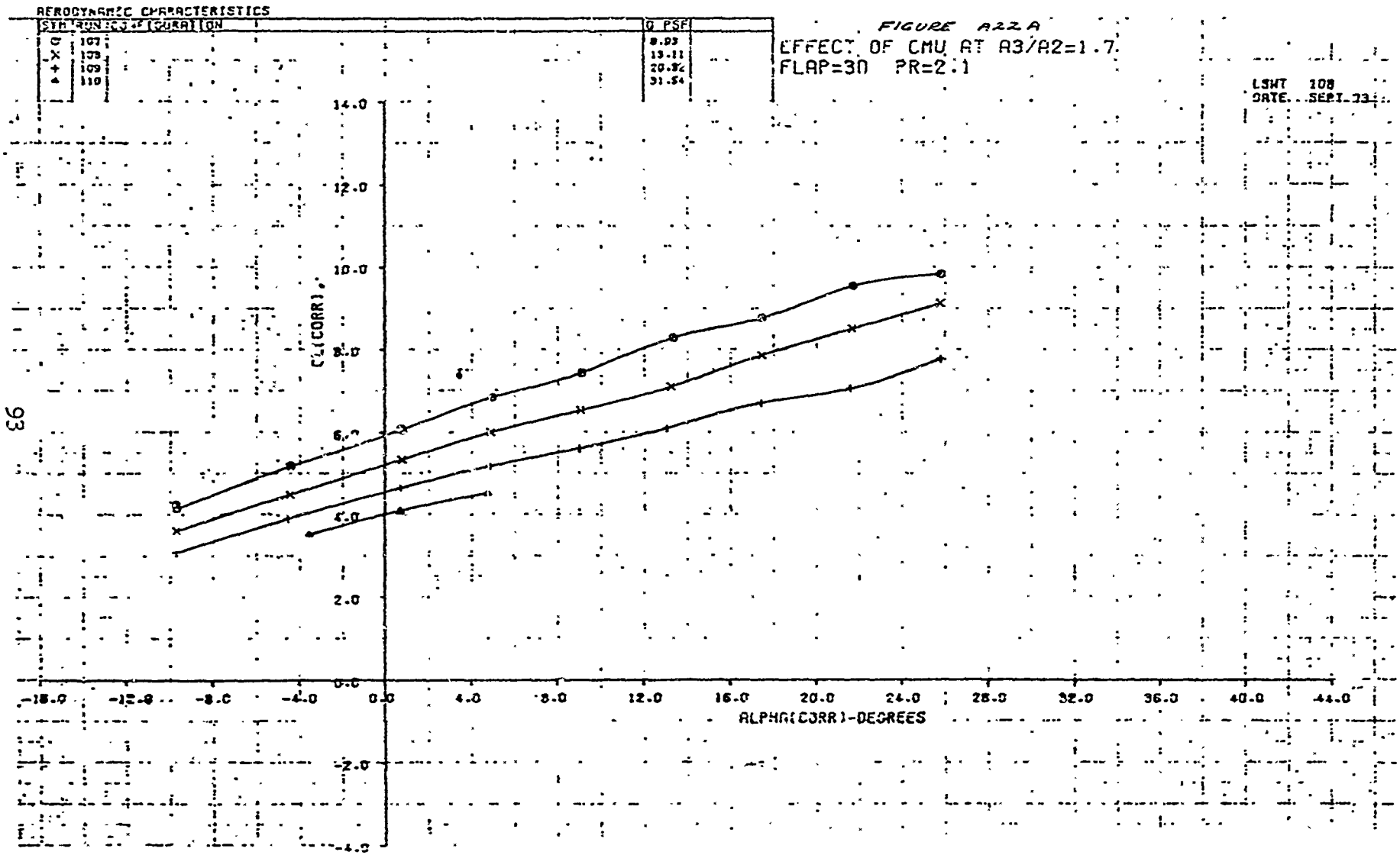
AERODYNAMIC CHARACTERISTICS
STH RUN CONFIGURATION
Q PSF
8.03
13.11
20.82
31.54
FIGURE A22A
EFFECT OF CMU AT A3/A2=1.7
FLAP=30 PR=2.1
LSWT 108
DATE SEPT 23
CL(CORR)
ALPHA(CORR)-DEGREES
14.0
12.0
10.0
8.0
6.0
4.0
2.0
0.0
-2.0
-4.0
-16.0
-12.0
-8.0
-4.0
0.0
4.0
8.0
12.0
16.0
20.0
24.0
28.0
32.0
36.0
40.0
44.0

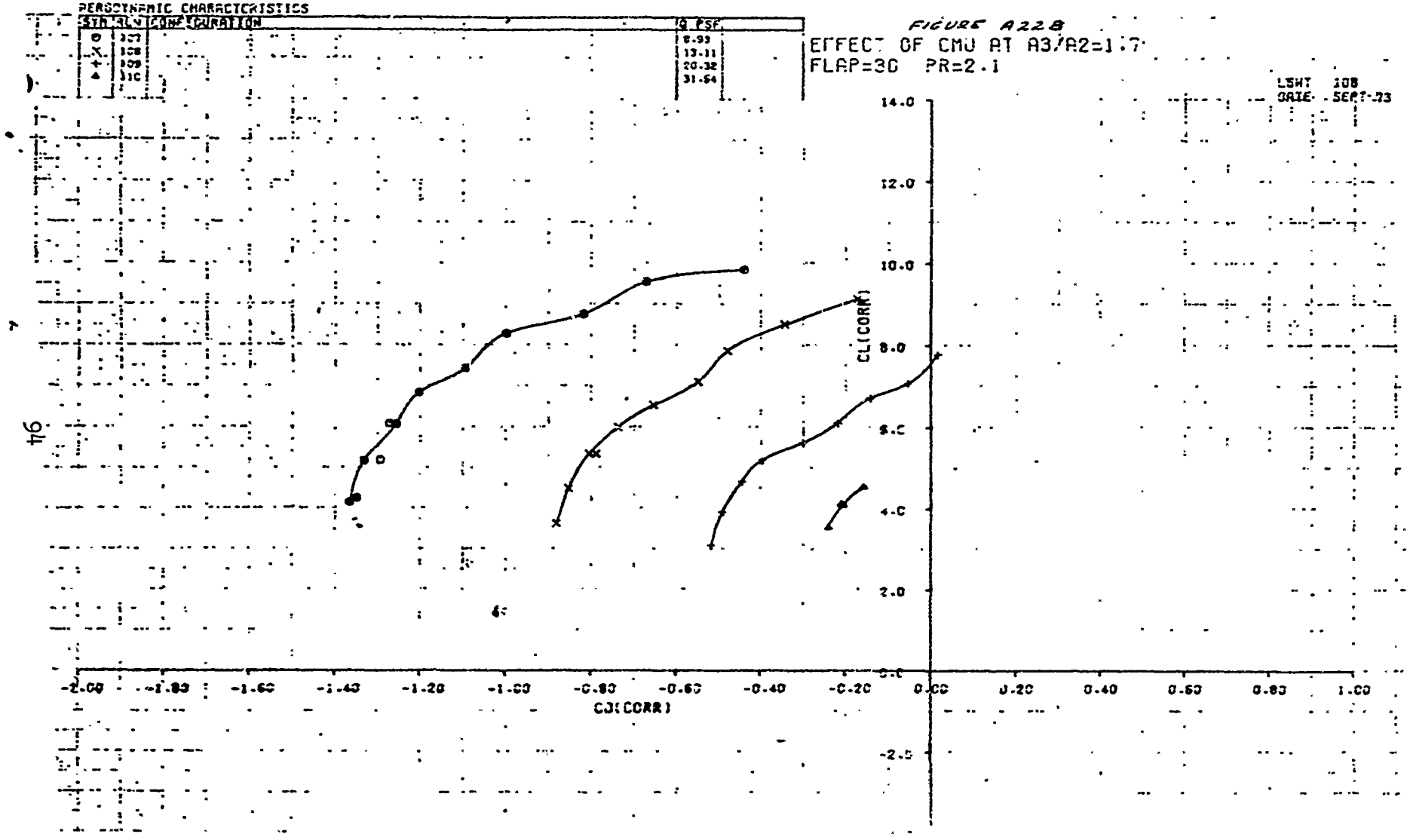
AERODYNAMIC CHARACTERISTICS
STN SLN CONFIGURATION
Q PSF
8.93
13.11
20.32
31.54
FIGURE A22B
EFFECT OF CMU AT A3/A2=1.7
FLAP=30 PR=2.1
LSHT 108
DATE SEPT-73
CL(CORR)
CJ(CORR)
14.0
12.0
10.0
8.0
6.0
4.0
2.0
0.0
-2.0
-1.80
-1.60
-1.40
-1.20
-1.00
-0.80
-0.60
-0.40
-0.20
0.00
0.20
0.40
0.60
0.80
1.00

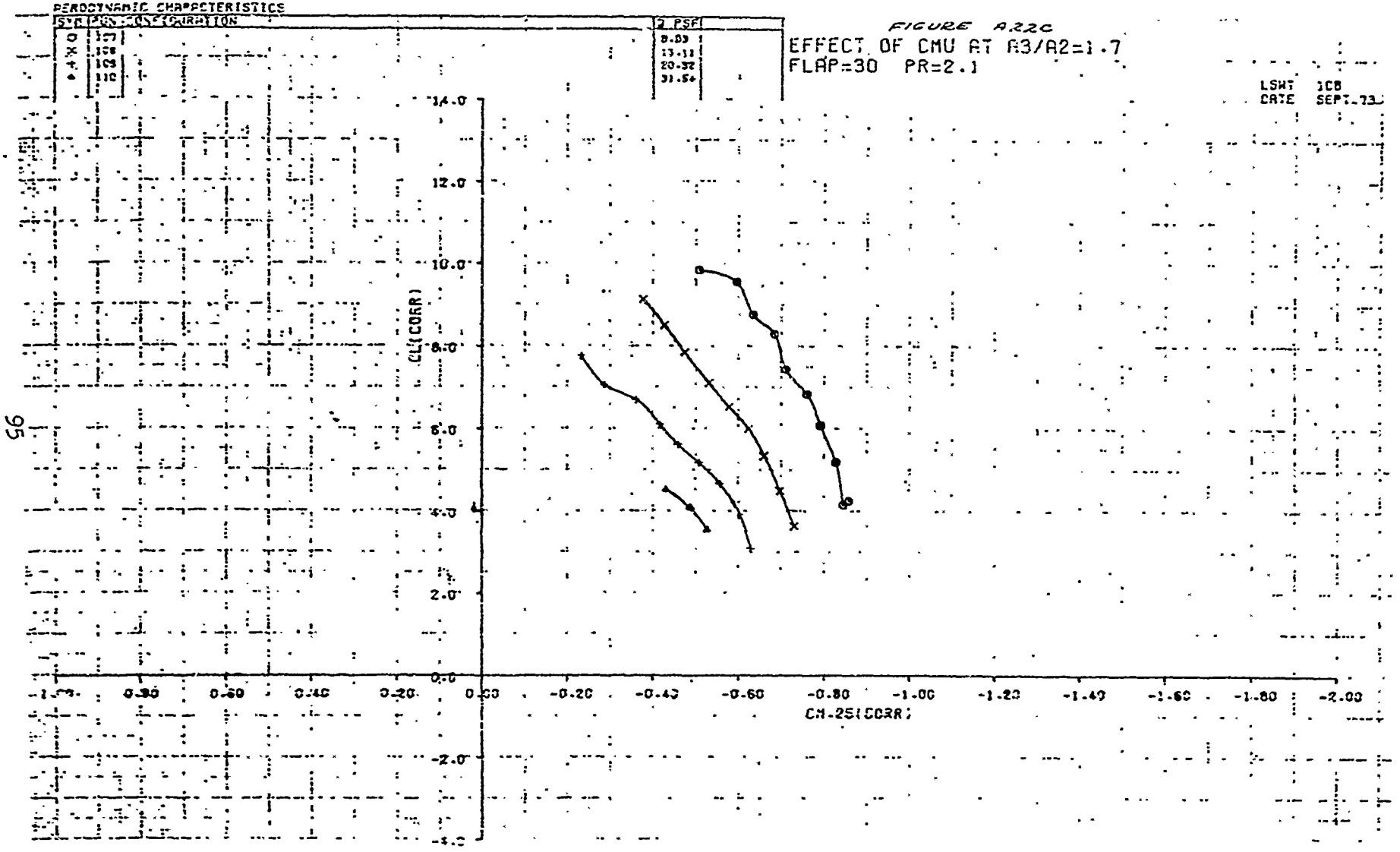

FIGURE A.22c

EFFECT OF CMU AT A3/A2=1.7
FLAP=30 PR=2.1

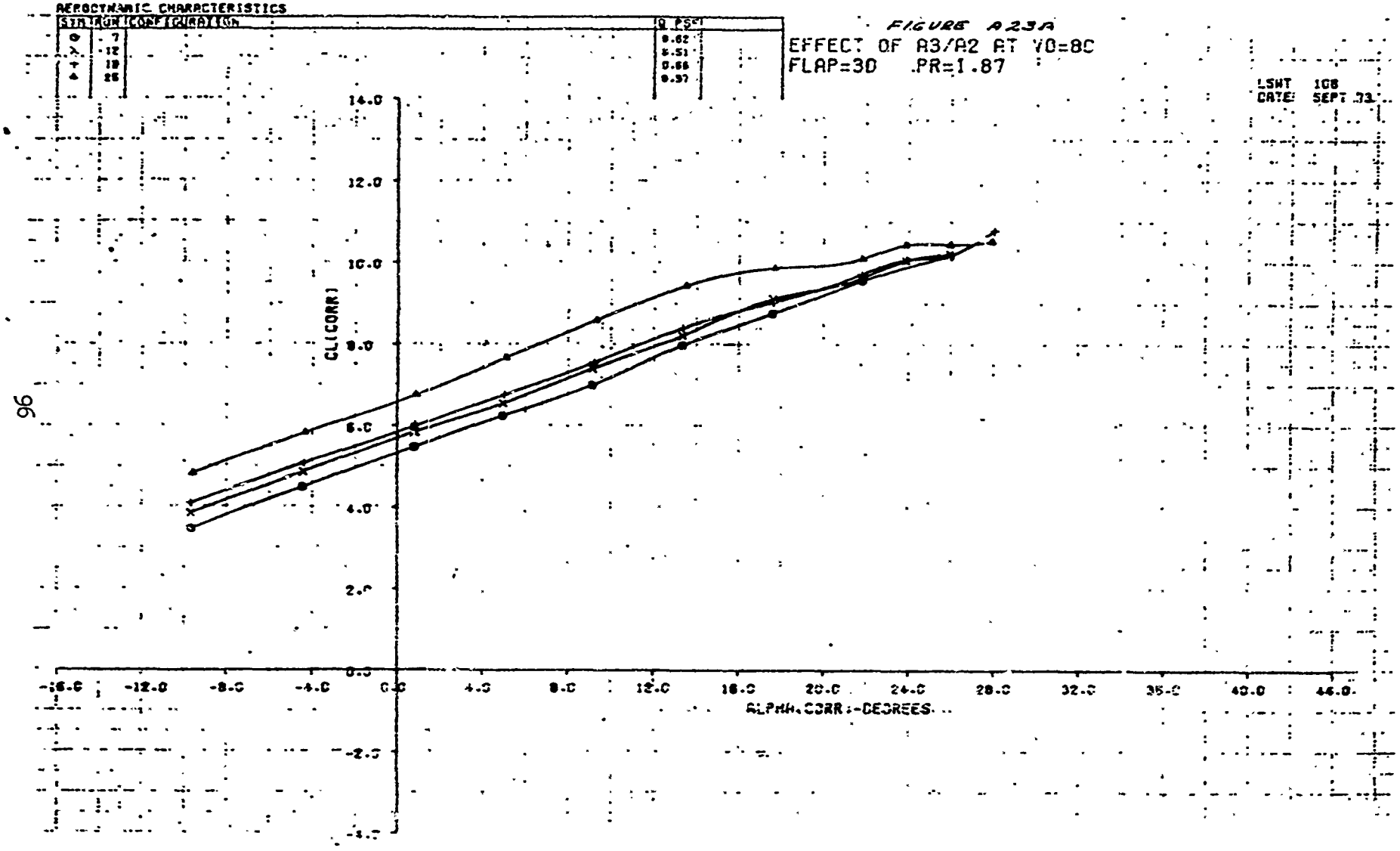
AERODYNAMIC CHARACTERISTICS
FIGURE A23A
EFFECT OF A3/A2 AT V0=8C
FLAP=30 .PR=1.87
LSWT 108
DATE SEPT 73
CL(CORR)
ALPHA,CORR:-DEGREES
14.0
12.0
10.0
8.0
6.0
4.0
2.0
0.0
-2.0
-4.0
-16.0
-12.0
-8.0
-4.0
0.0
4.0
8.0
12.0
16.0
20.0
24.0
28.0
32.0
36.0
40.0
44.0

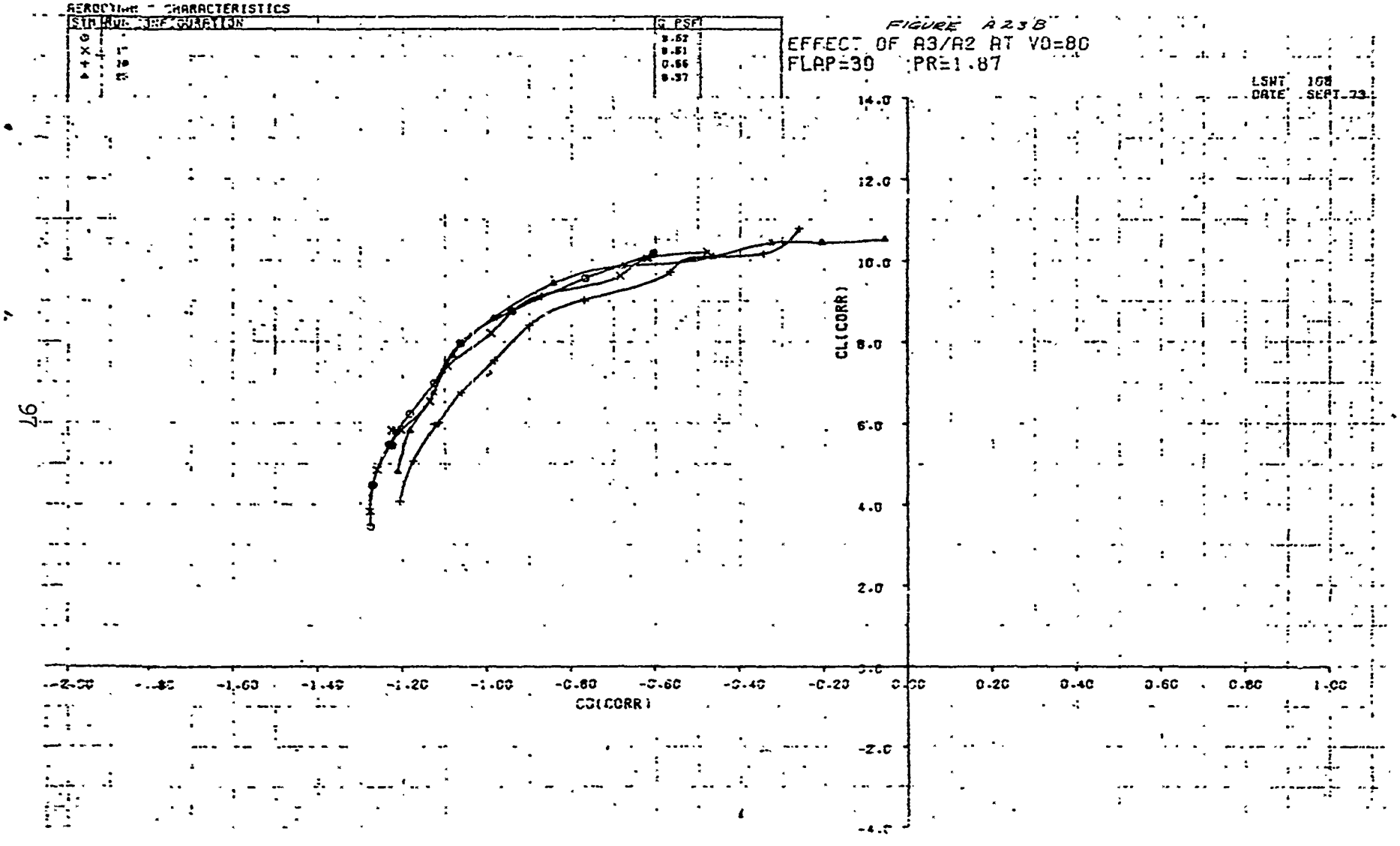
AERODYNAMIC CHARACTERISTICS
STABILIZER CONFIGURATION
Q PSF
9.52
9.51
0.66
9.37
FIGURE A23B
EFFECT OF A3/A2 AT V0=80
FLAP=30 PR=1.87
LSNT 168
DATE SEPT 23
14.0
12.0
10.0
8.0
6.0
4.0
2.0
-2.0
-4.0
CL(CORR)
-2.00
-1.80
-1.60
-1.40
-1.20
-1.00
-0.80
-0.60
-0.40
-0.20
0.00
0.20
0.40
0.60
0.80
1.00
CD(CORR)

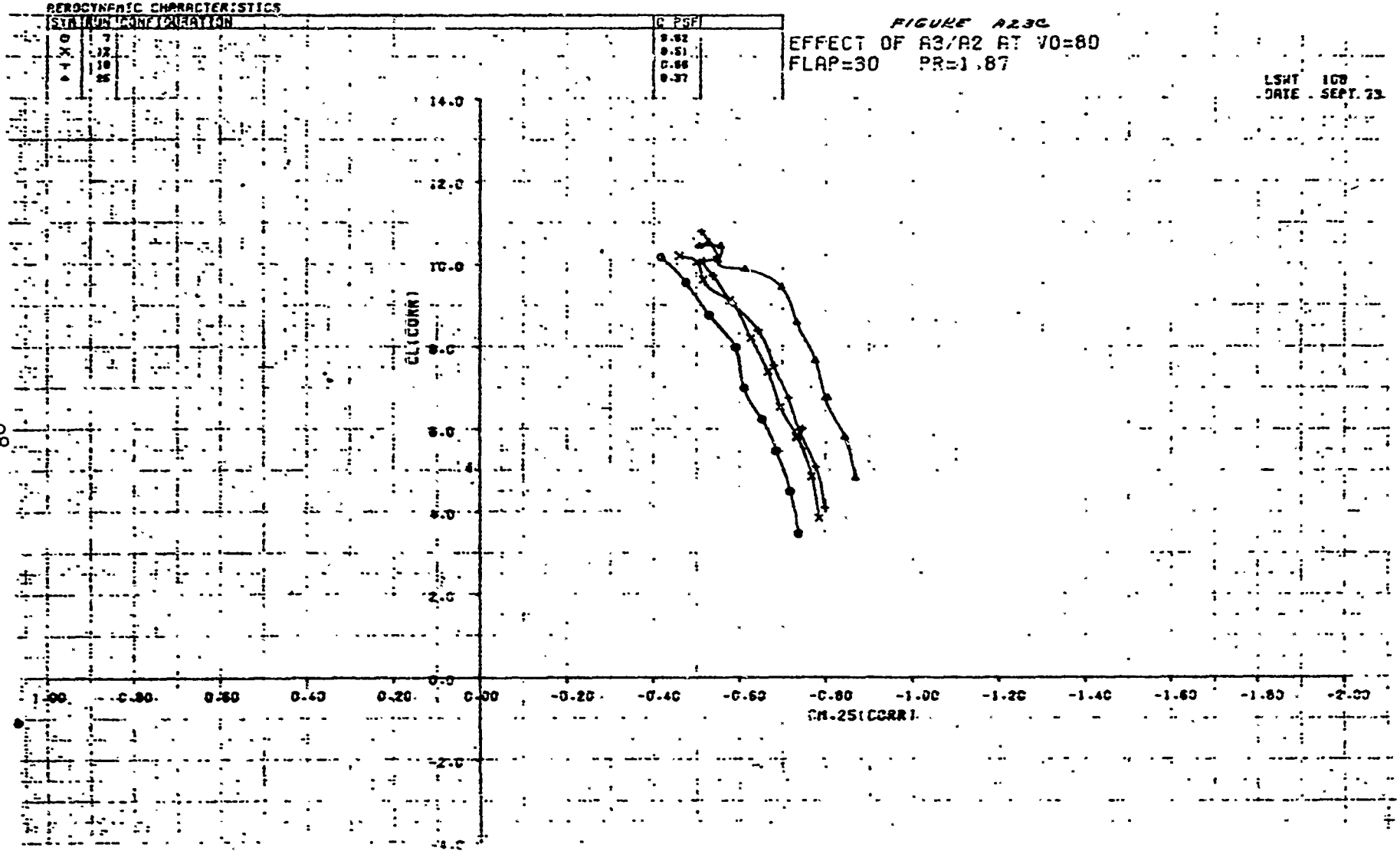
AERODYNAMIC CHARACTERISTICS
SYM RUN CONFIGURATION
Q PSF
FIGURE A23c
EFFECT OF A3/A2 AT V0=80
FLAP=30 PR=1.87
LSHT 100
DATE SEPT. 73
CL(CORR)
CM.25(CORR)
14.0
12.0
10.0
8.0
6.0
4.0
2.0
0.0
-2.0
-.80
-.60
-.40
-.20
0.00
-0.20
-0.40
-0.60
-0.80
-1.00
-1.20
-1.40
-1.60
-1.80
-2.00

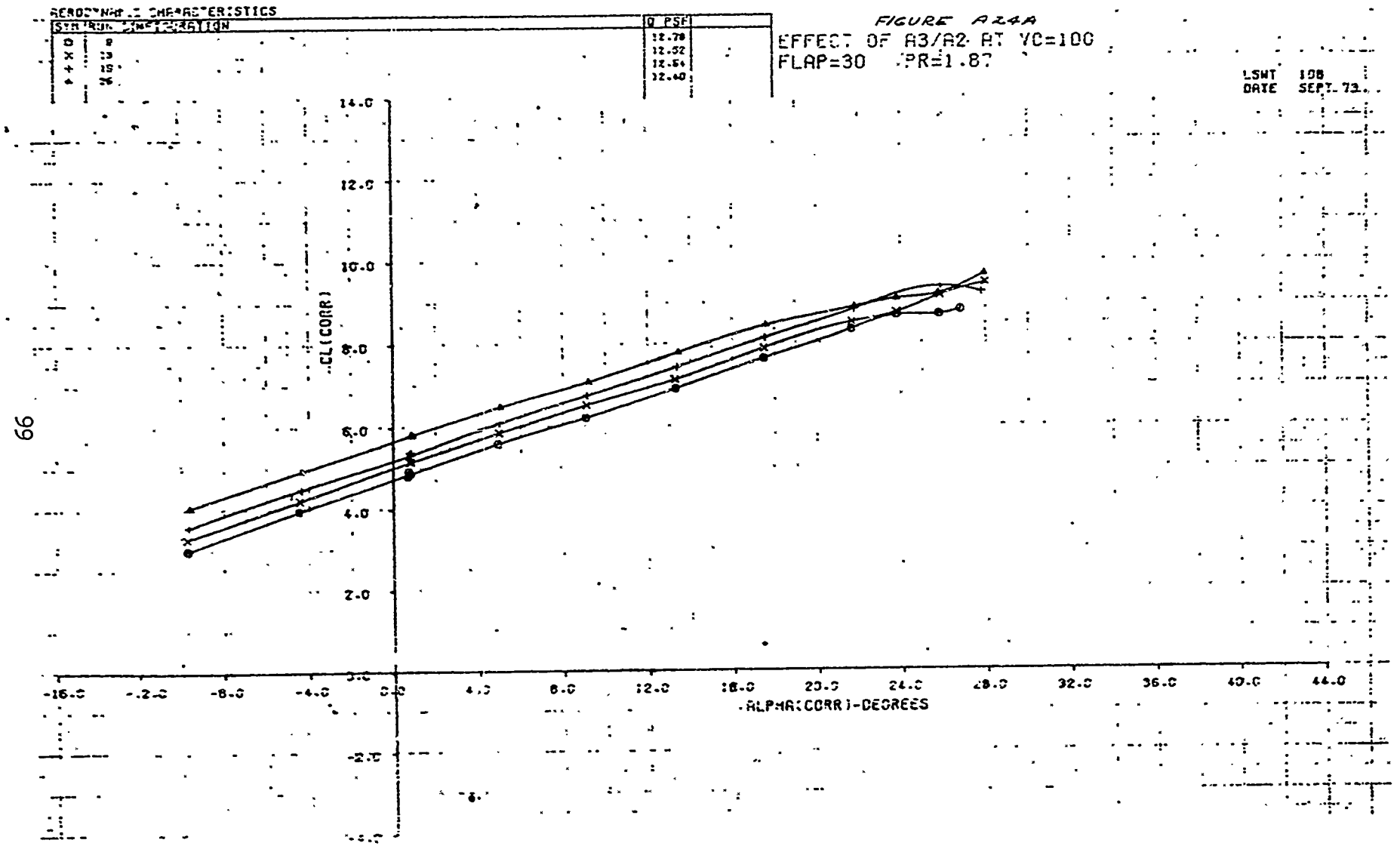
AERODYNAMIC CHARACTERISTICS
Q PSF
12.78
12.52
12.54
12.40
FIGURE A24A
EFFECT OF A3/A2 AT VC=100
FLAP=30 PR=1.87
LSWT 108
DATE SEPT. 73
14.0
12.0
10.0
8.0
6.0
4.0
2.0
-2.0
CL(CORR)
-16.0
-12.0
-8.0
-4.0
4.0
8.0
12.0
16.0
20.0
24.0
28.0
32.0
36.0
40.0
44.0
ALPHA(CORR)-DEGREES

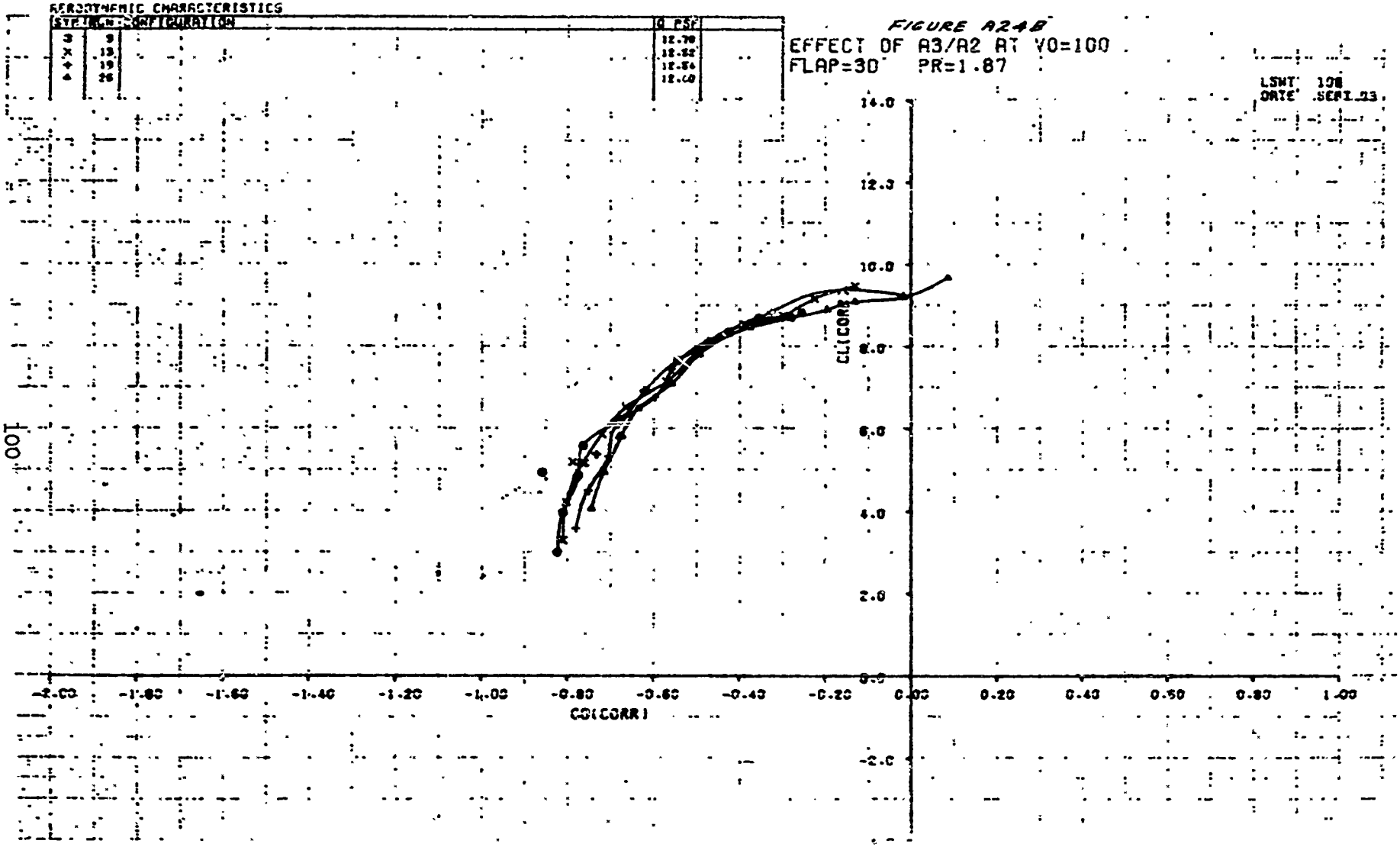
AERODYNAMIC CHARACTERISTICS
CONFIGURATION
Q PSF
12.70
12.52
12.54
12.60
FIGURE A24B
EFFECT OF A3/A2 AT V0=100
FLAP=30° PR=1.87
LSWT 198
DATE SEPT 73
CL(CORR)
CD(CORR)
14.0
12.0
10.0
8.0
6.0
4.0
2.0
0.0
-2.0
-2.00
-1.80
-1.60
-1.40
-1.20
-1.00
-0.80
-0.60
-0.40
-0.20
0.00
0.20
0.40
0.60
0.80
1.00

FIGURE A24C

EFFECT OF A3/A2 AT V0=100

FLAP=30 [illegible]=1.87

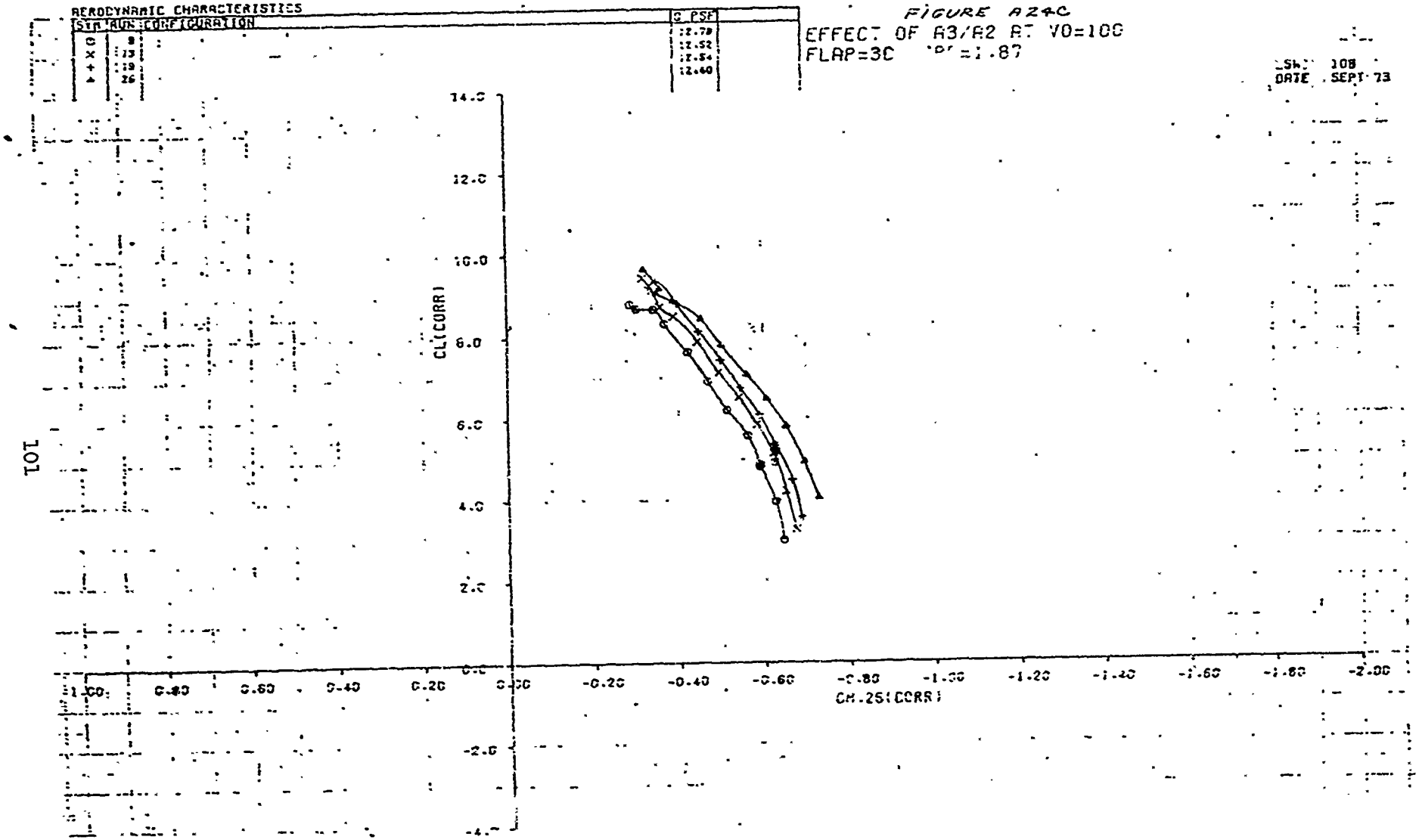

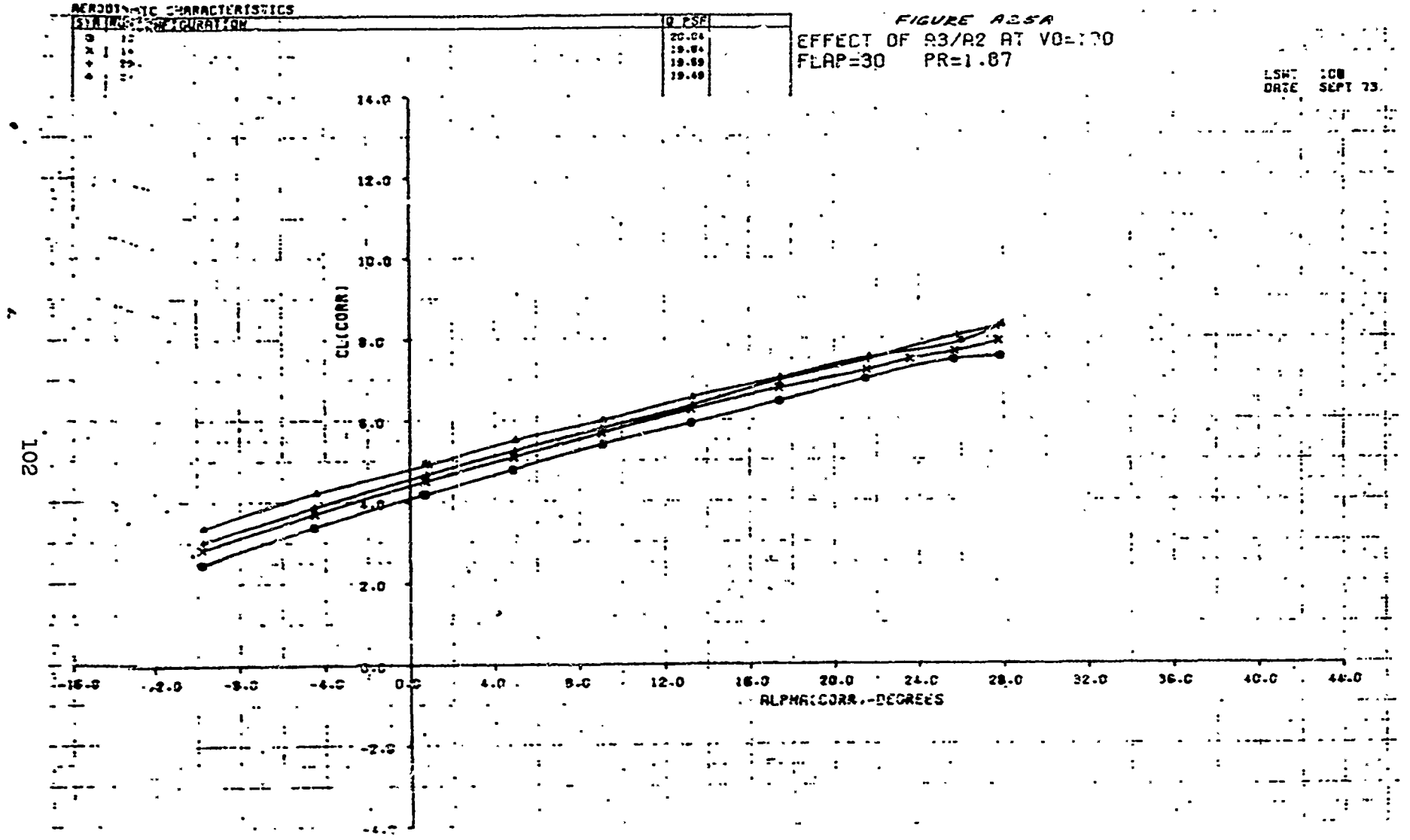
AERODYNAMIC CHARACTERISTICS
Q PSF
20.04
19.84
19.69
19.49
FIGURE A25A
EFFECT OF A3/A2 AT V0=170
FLAP=30 PR=1.87
LSHT :CB
DATE SEPT 73.
CL(CORR)
14.0
12.0
10.0
8.0
6.0
4.0
2.0
0.0
-2.0
-4.0
-16.0
-12.0
-8.0
-4.0
0.0
4.0
8.0
12.0
16.0
20.0
24.0
28.0
32.0
36.0
40.0
44.0
ALPHA(CORR.)-DEGREES

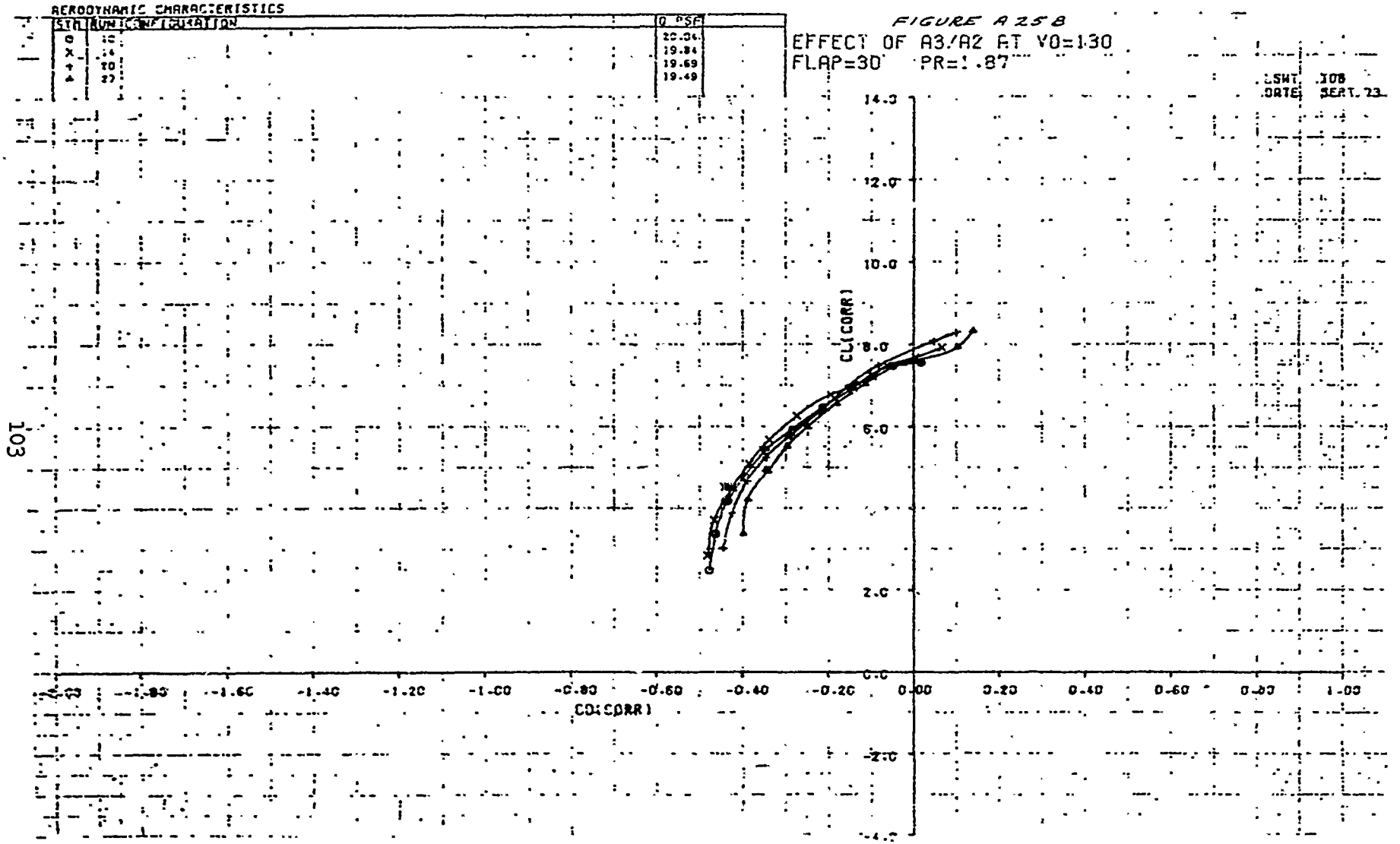
AERODYNAMIC CHARACTERISTICS
Q PSF
20.34
19.84
19.69
19.49
FIGURE A25B
EFFECT OF A3/A2 AT V0=130
FLAP=30 PR=1.87
LSHT
DATE SEPT. 23
14.0
12.0
10.0
8.0
6.0
2.0
0.0
-2.0
CL(CORR)
CD(CORR)
-0.20
0.00
0.20
0.40
0.60
1.00
103

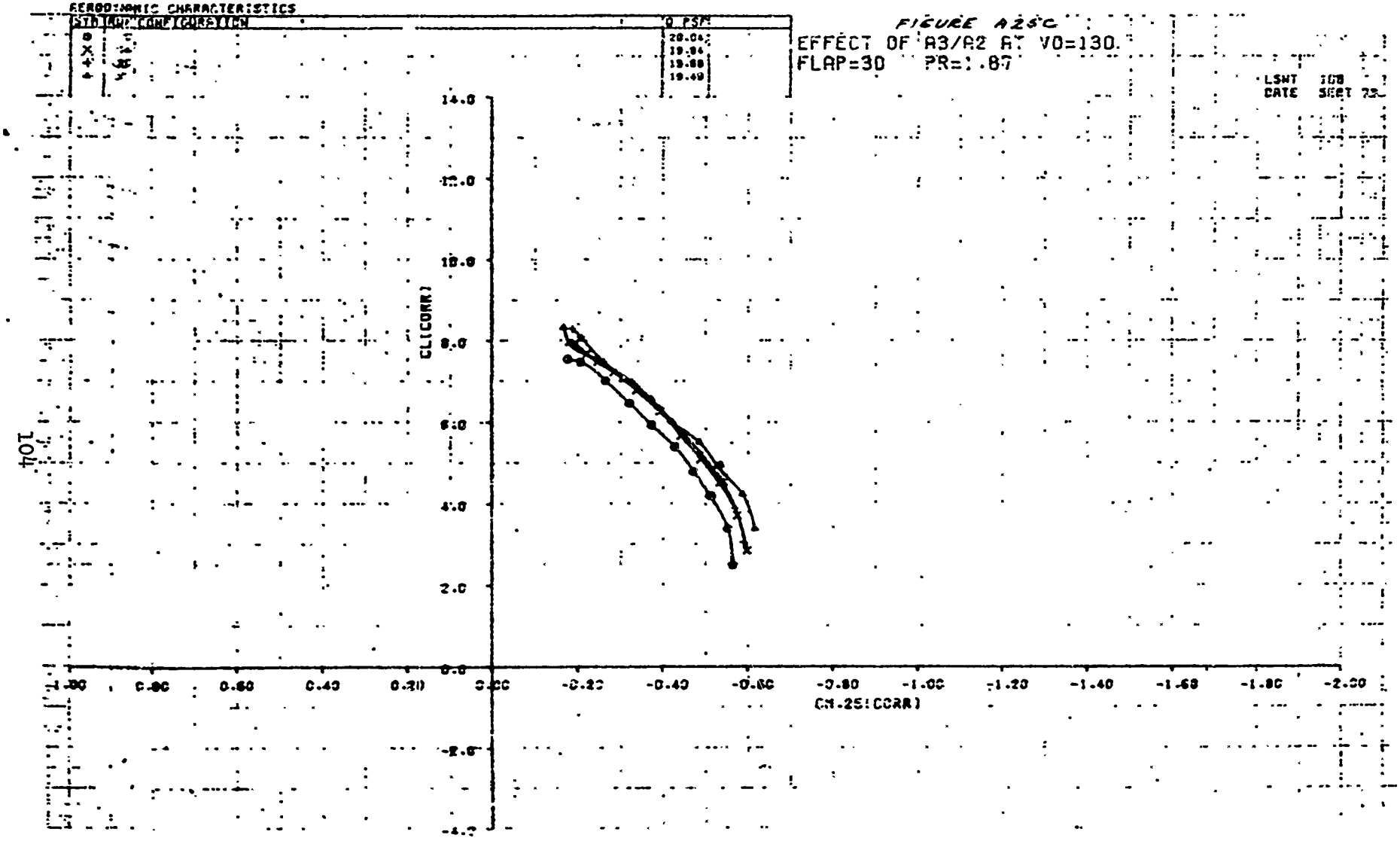
AERODYNAMIC CHARACTERISTICS
STD AIR CONFIGURATION
Q PSF
20.04
19.84
19.88
19.49
FIGURE A2SC
EFFECT OF A3/A2 AT V0=130.
FLAP=30 PR=1.87
LSHT 108
DATE SHEET 73
CL(CORR)
CM.25(CORR)
14.0
12.0
10.0
8.0
6.0
4.0
2.0
0.0
-2.0
-4.0
-0.20
-0.40
-0.60
-0.80
-1.00
-1.20
-1.40
-1.60
-1.80
-2.00

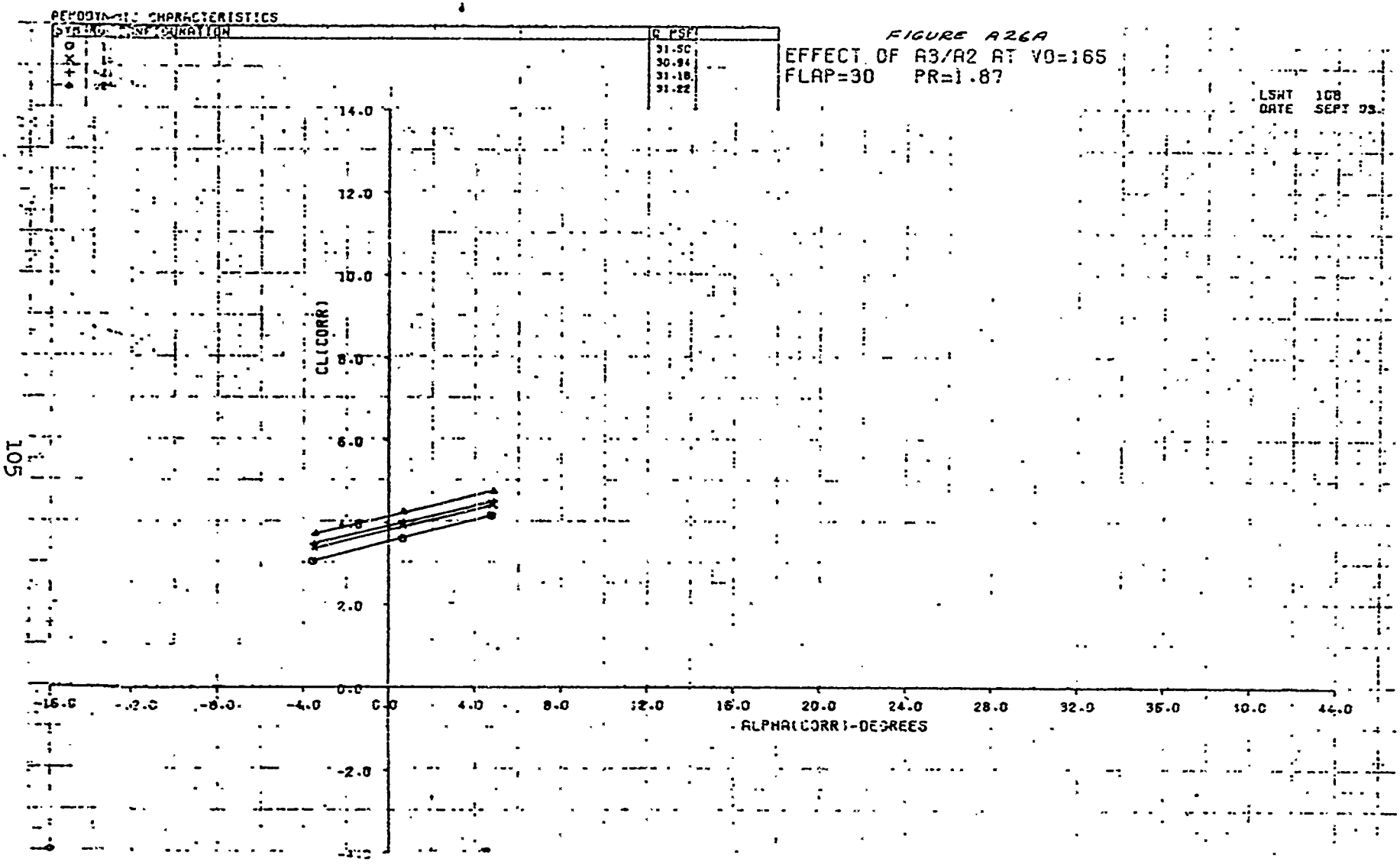
AERODYNAMIC CHARACTERISTICS
STATIC CONFIGURATION
Q PSF
31.50
30.94
31.18
31.22
FIGURE A26A
EFFECT OF A3/A2 AT V0=165
FLAP=30 PR=1.87
LSWT 108
DATE SEPT 78
105
CL(CORR)
14.0
12.0
10.0
8.0
6.0
4.0
2.0
0.0
-2.0
-16.0
-12.0
-8.0
-4.0
0.0
4.0
8.0
12.0
16.0
20.0
24.0
28.0
32.0
36.0
40.0
44.0
ALPHA(CORR)-DEGREES

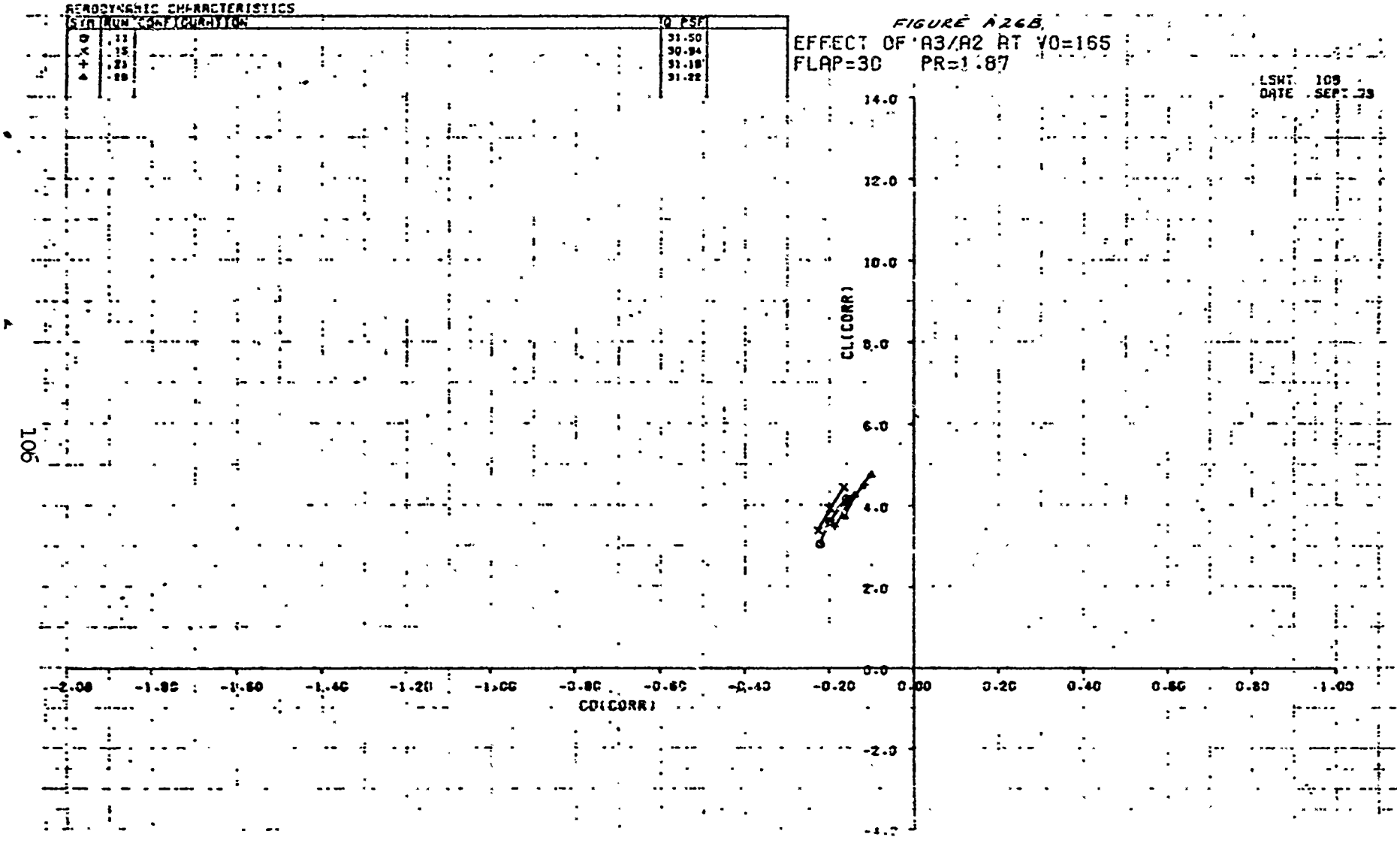
AERODYNAMIC CHARACTERISTICS
STA RUN CONFIGURATION Q PSF
0 .11 31.50
X .15 30.94
+ .23 31.18
4 .28 31.22
FIGURE A26B
EFFECT OF A3/A2 AT V0=165
FLAP=30 PR=1.87
LSHT 105
DATE SEPT 29
CL(CORR)
CD(CORR)
14.0
12.0
10.0
8.0
6.0
4.0
2.0
0.0
-2.0
-2.00
-1.80
-1.60
-1.40
-1.20
-1.00
-0.80
-0.60
-0.40
-0.20
0.00
0.20
0.40
0.60
0.80
1.00

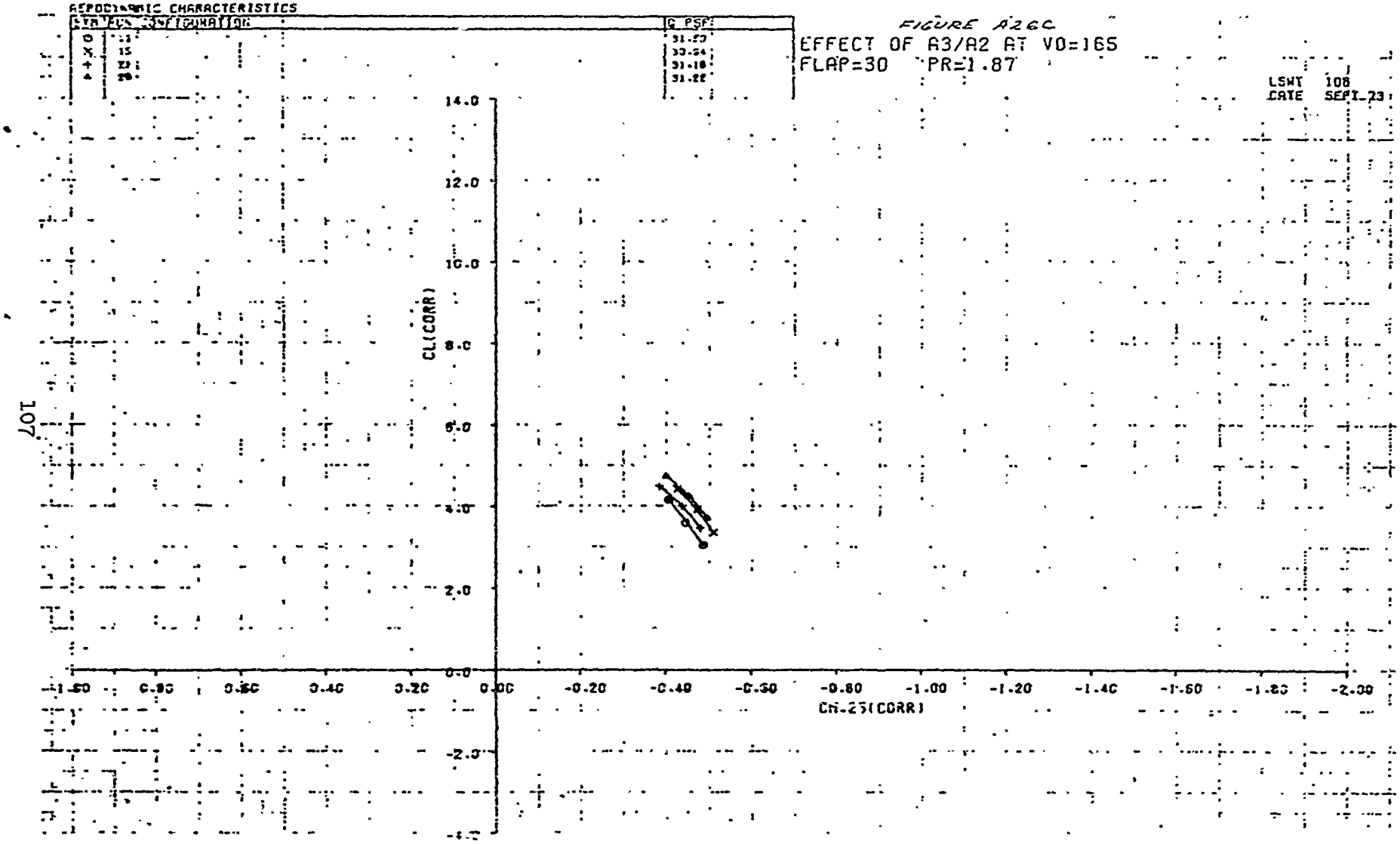
AERODYNAMIC CHARACTERISTICS
CONFIGURATION
Q PSF
31.53
33.84
31.18
31.22
FIGURE A26C
EFFECT OF A3/A2 AT V0=165
FLAP=30 PR=1.87
LSWT 108
DATE SEPT-23
107
CL(CORR)
14.0
12.0
10.0
8.0
6.0
4.0
2.0
0.0
-2.0
-1.60
-1.40
-1.20
-1.00
-0.80
-0.60
-0.40
-0.20
0.00
0.20
0.40
0.60
0.80
CM-25(CORR)
-2.00

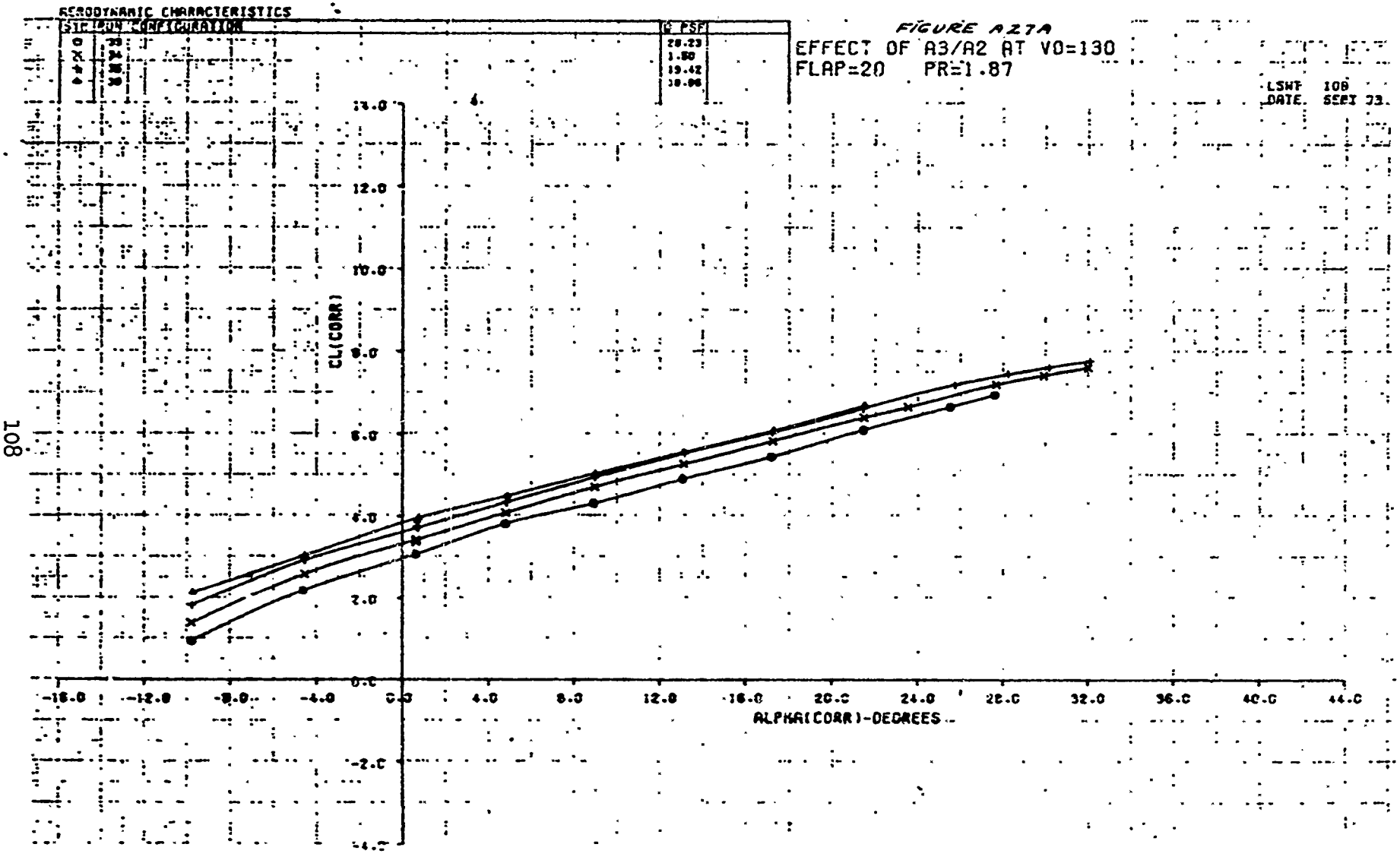
AERODYNAMIC CHARACTERISTICS
SECTION CONFIGURATION
Q PSF
28.23
1.80
19.42
10.06
FIGURE A27A
EFFECT OF A3/A2 AT V0=130
FLAP=20 PR=1.87
LSWT 108
DATE. SEPT 73.
CL(CORR)
ALPHA(CORR)-DEGREES
-16.0
-12.0
-8.0
-4.0
4.0
8.0
12.0
16.0
20.0
24.0
28.0
32.0
36.0
40.0
44.0
12.0
10.0
8.0
6.0
4.0
2.0
0.0
-2.0
-4.0

FIGURE A27B

EFFECT OF A3/A2 AT V0=130

FLAP=20 PR=1.87

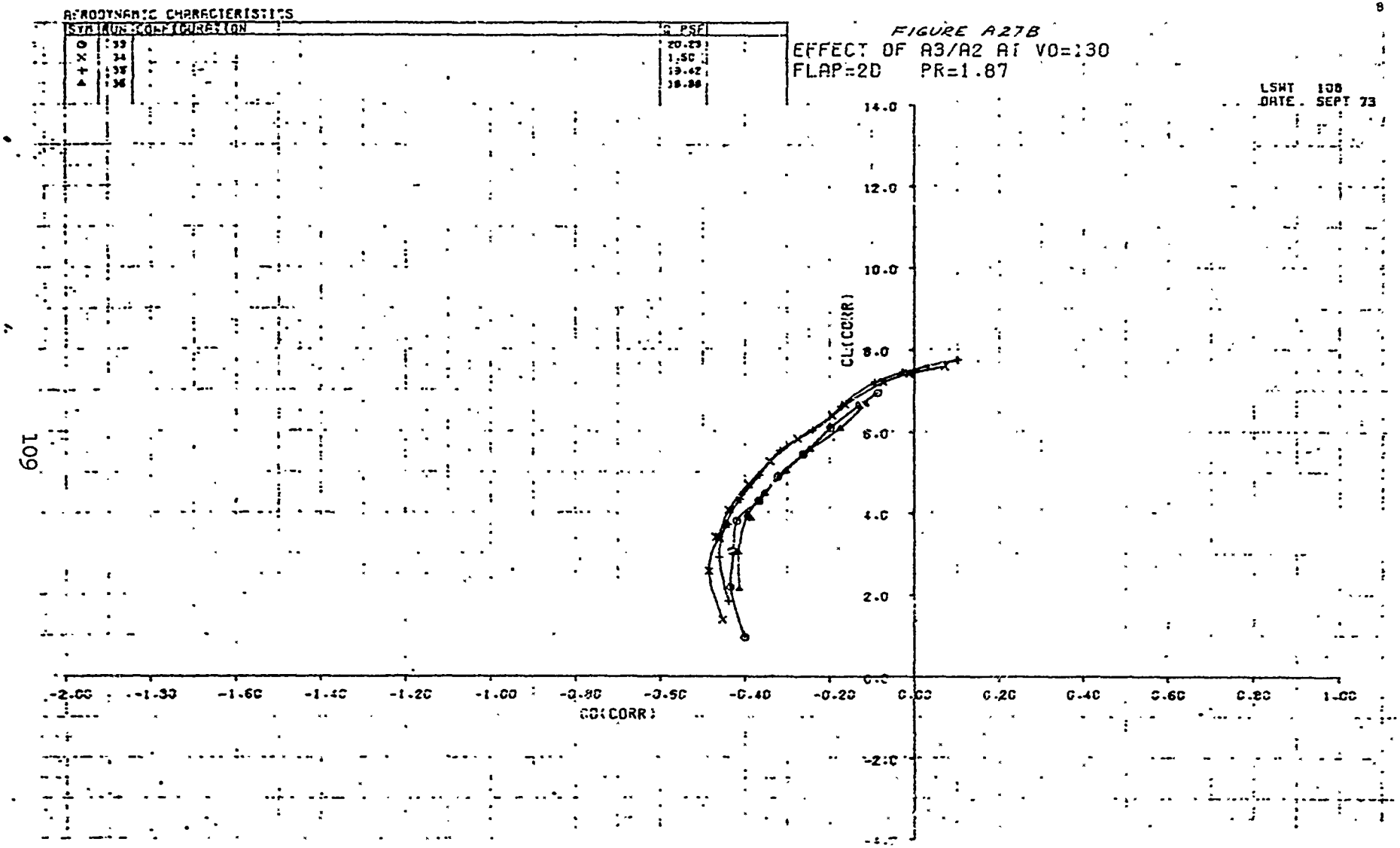

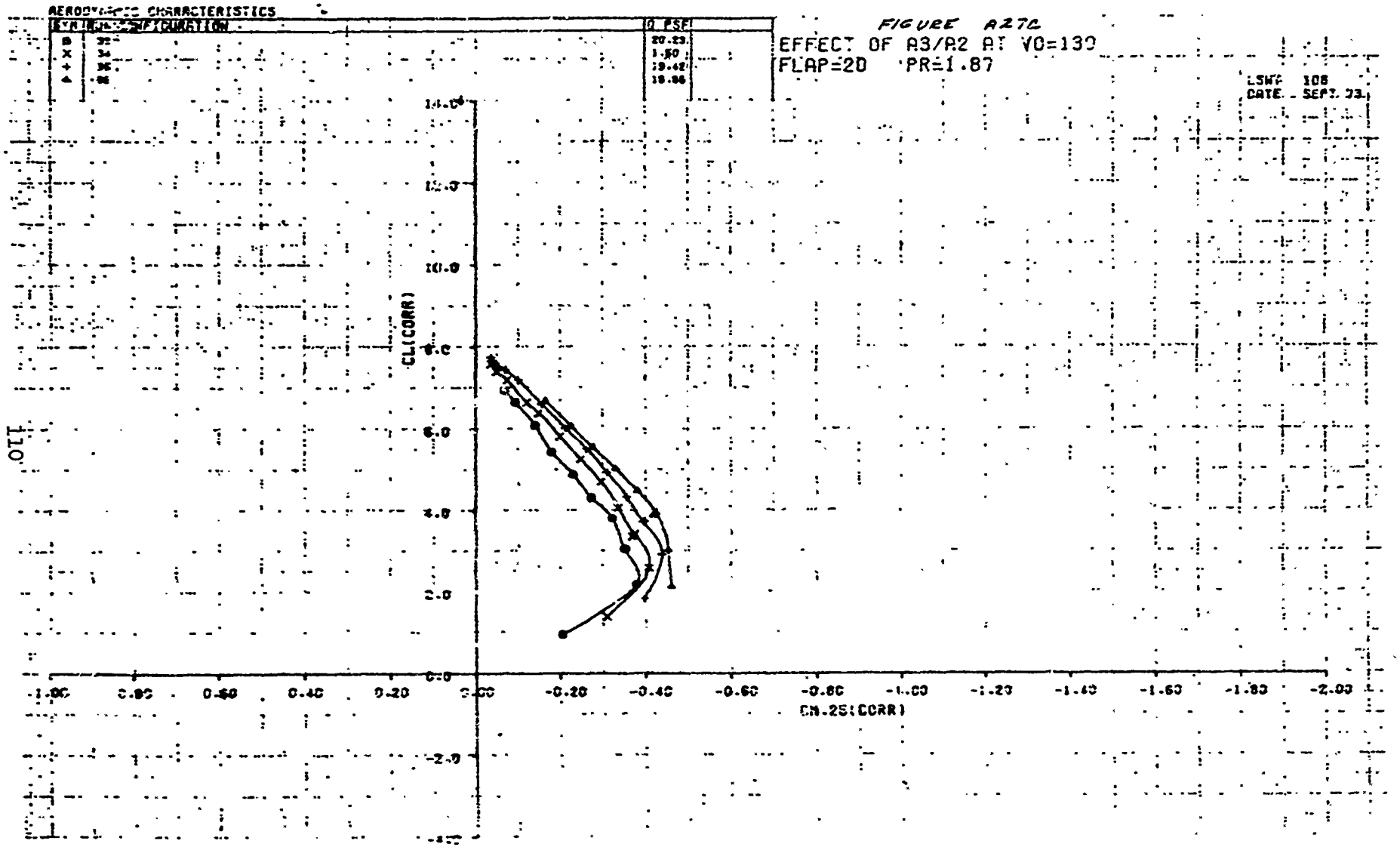
AERODYNAMIC CHARACTERISTICS
Q PSF
20.23
1.50
19.42
18.86
FIGURE A27C
EFFECT OF A3/A2 AT V0=130
FLAP=20 PR=1.87
LSWT 108
DATE SEPT. 73
CL(CORR)
CM.25(CORR)
110

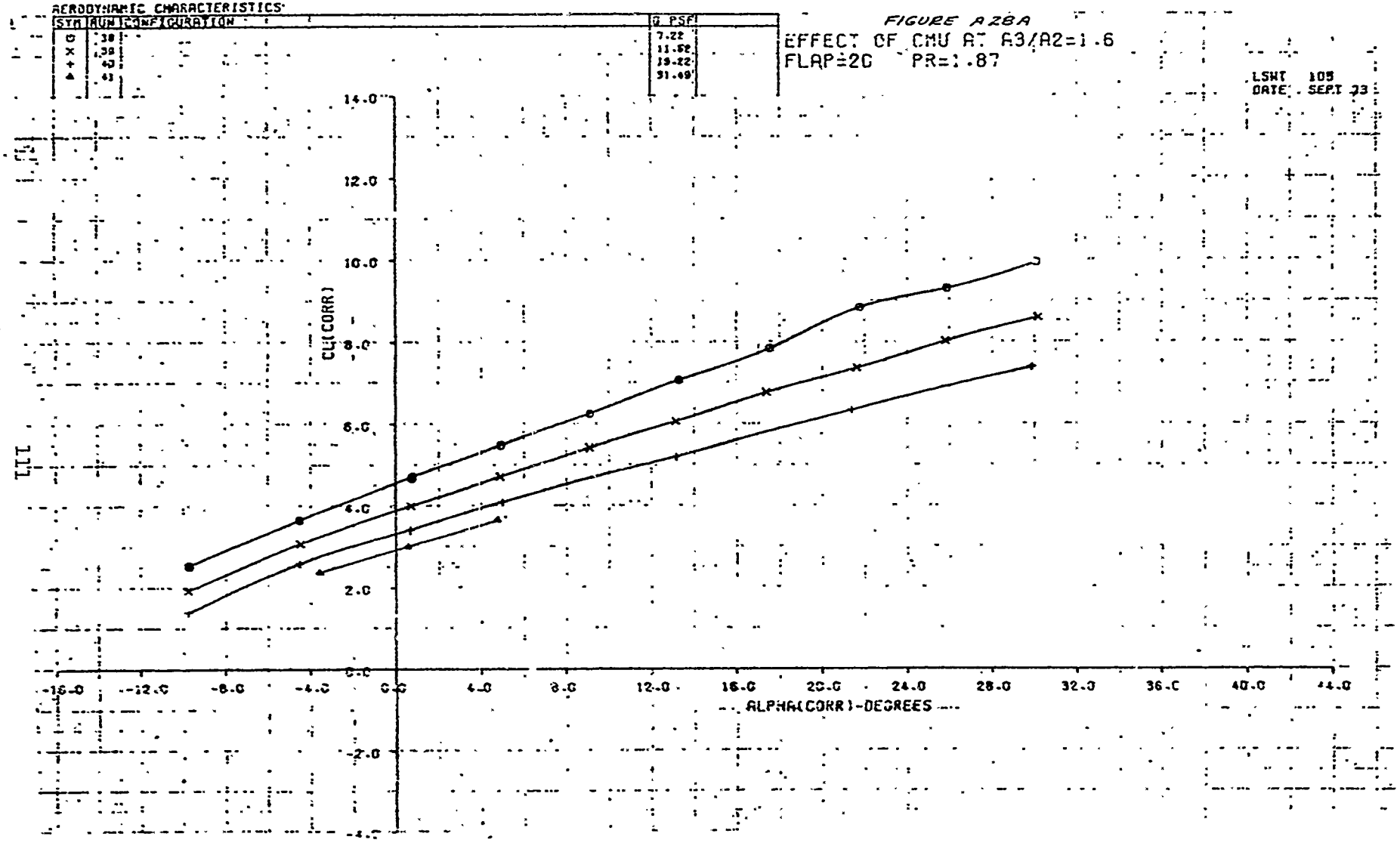
AERODYNAMIC CHARACTERISTICS
SYM | RUN | CONFIGURATION
Q PSF
7.22
11.52
19.22
31.69
FIGURE A2BA
EFFECT OF CMU AT A3/A2=1.6
FLAP=20 PR=1.87
LSWT 103
DATE SEPT 73
CL(CORR)
ALPHA(CORR)-DEGREES
14.0
12.0
10.0
8.0
6.0
4.0
2.0
0.0
-2.0
-16.0
-12.0
-8.0
-4.0
0.0
4.0
8.0
12.0
16.0
20.0
24.0
28.0
32.0
36.0
40.0
44.0

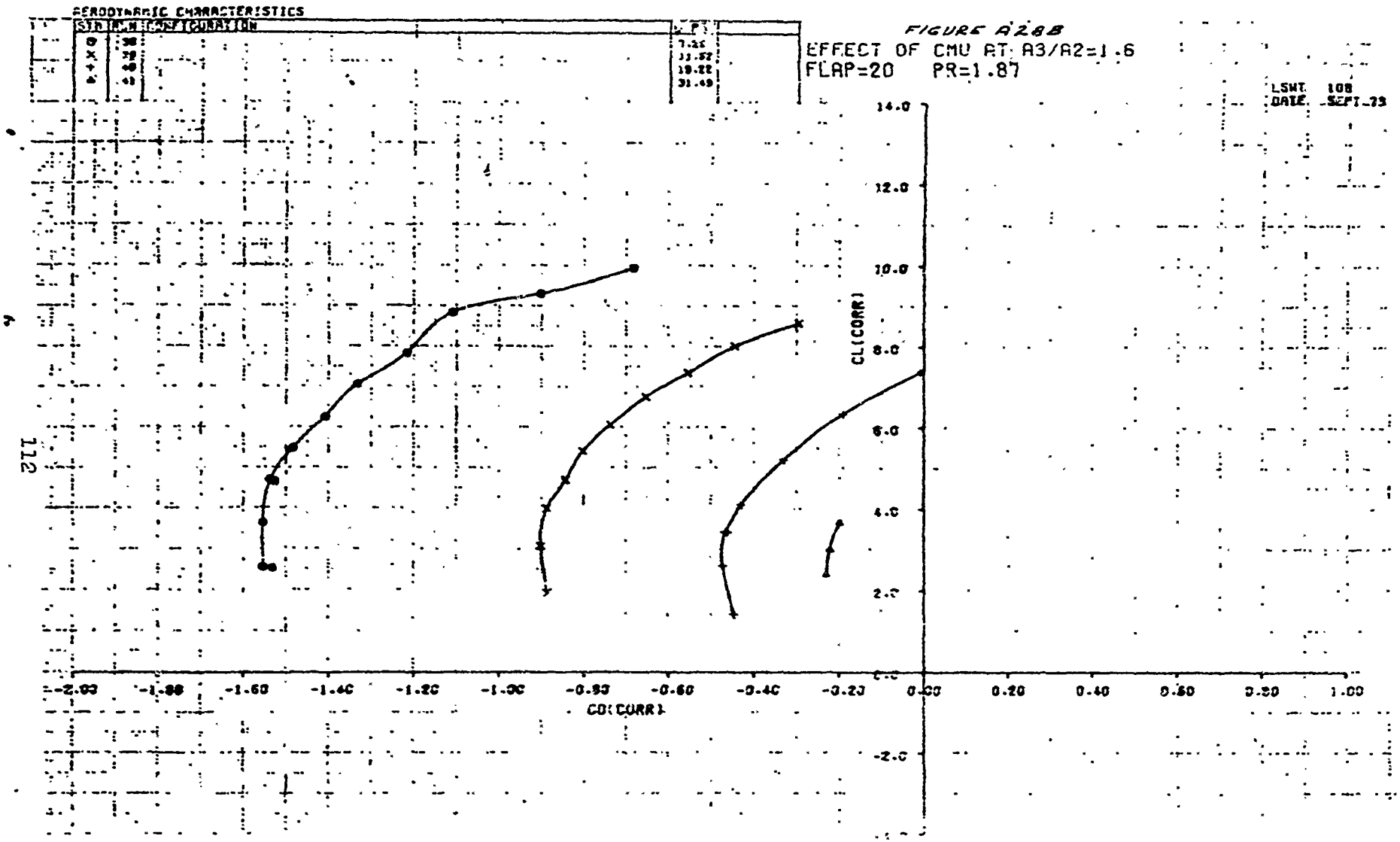

FIGURE A28B

EFFECT OF CMU AT A3/A2=1.6

FLAP=20 PR=1.87

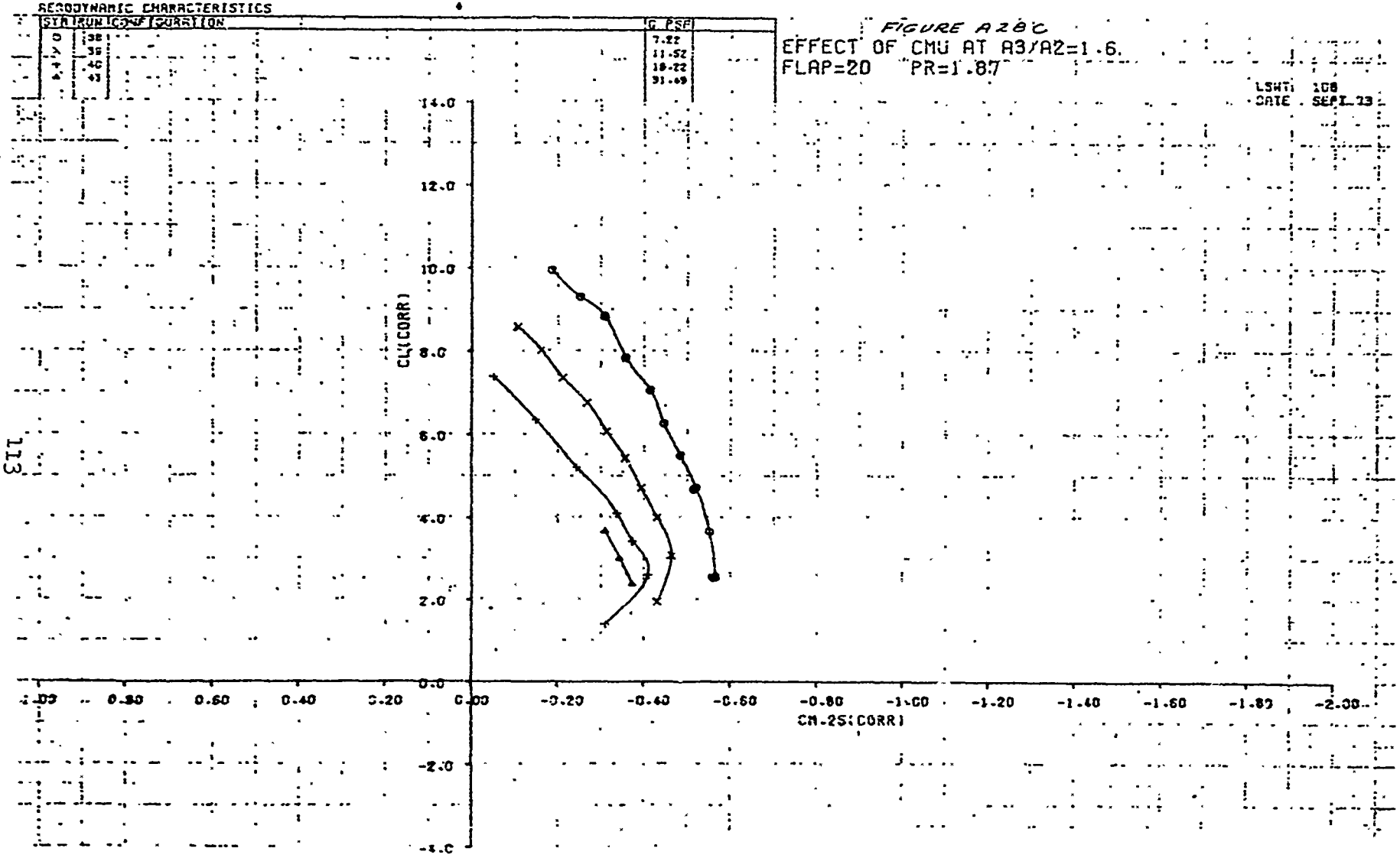

FIGURE A2&C

EFFECT OF CMU AT A3/A2=1.6.

FLAP=20 PR=1.87

LSHTI 108

DATE SEPT 73

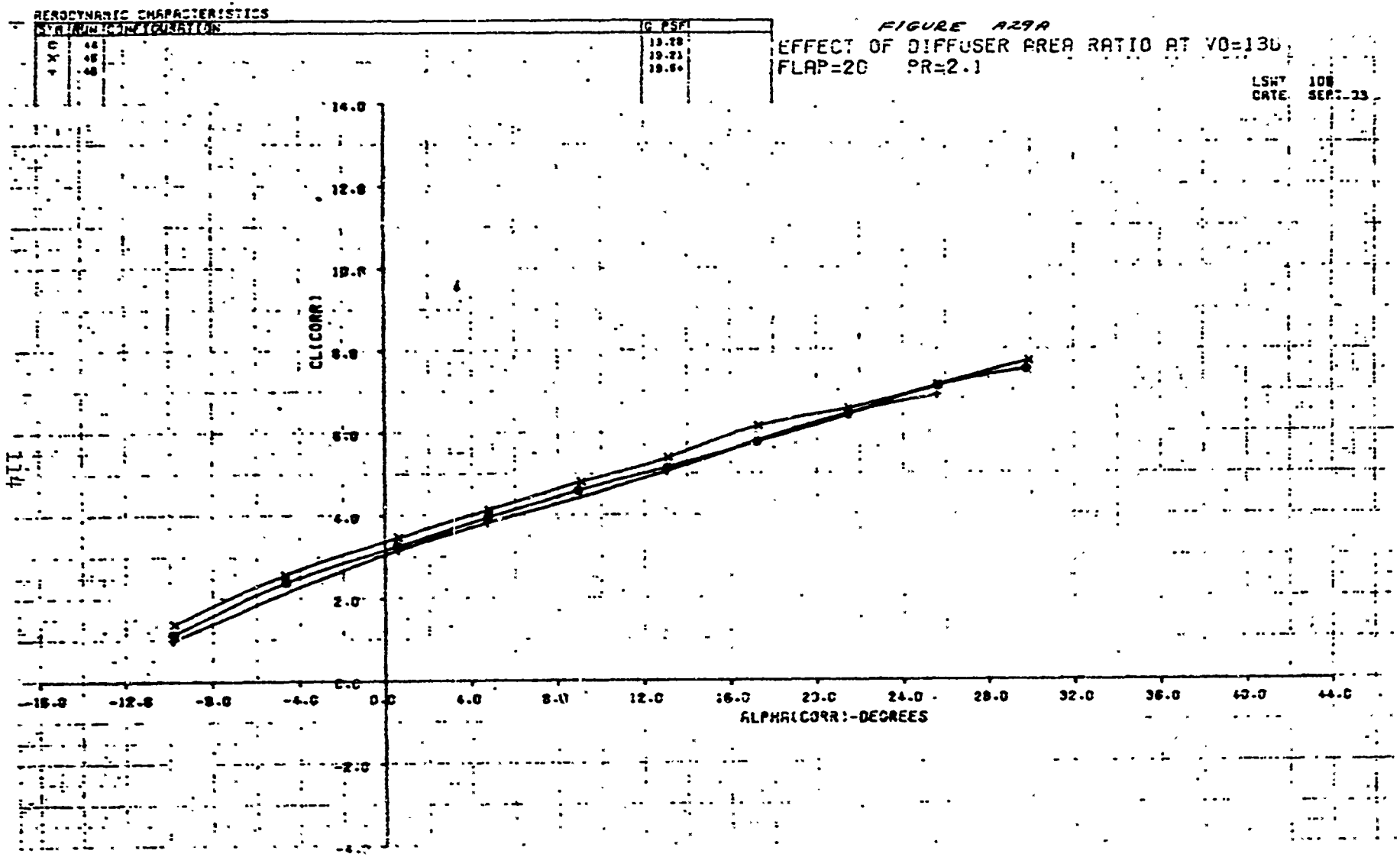

FIGURE A29A

EFFECT OF DIFFUSER AREA RATIO AT V0=130,
FLAP=20 PR=2.1

LSWT 108
DATE SEPT-23

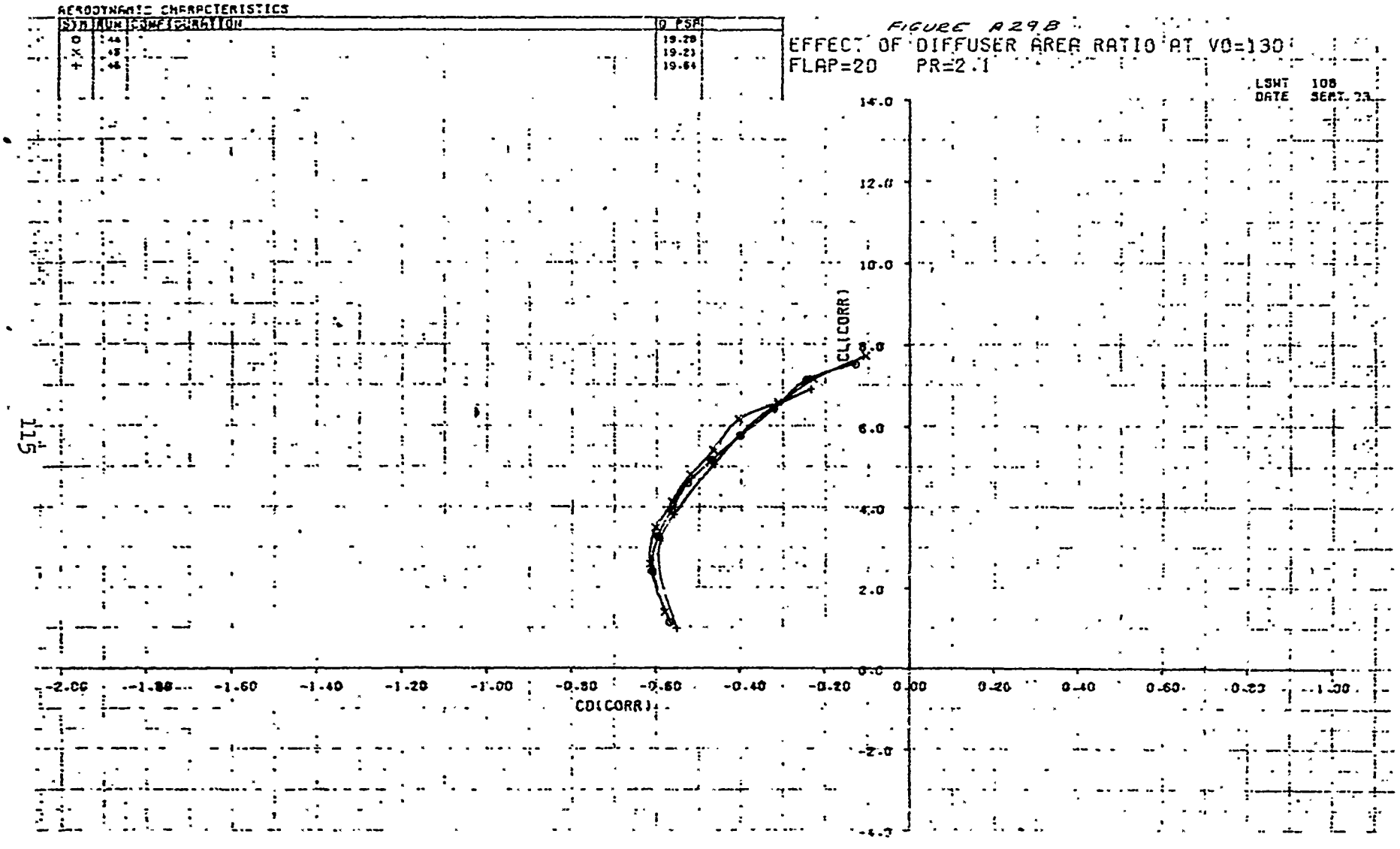
AERODYNAMIC CHARACTERISTICS
SYM RUN CONFIGURATION
Q PSF
19.29
19.23
19.64
FIGURE A29B
EFFECT OF DIFFUSER AREA RATIO AT V0=130
FLAP=20 PR=2.1
LSHT 108
DATE SEPT. 23
CL(CORR)
CD(CORR)
14.0
12.0
10.0
8.0
6.0
4.0
2.0
0.0
-2.0
-2.00
-1.80
-1.60
-1.40
-1.20
-1.00
-0.80
-0.60
-0.40
-0.20
0.00
0.20
0.40
0.60
0.80
1.00

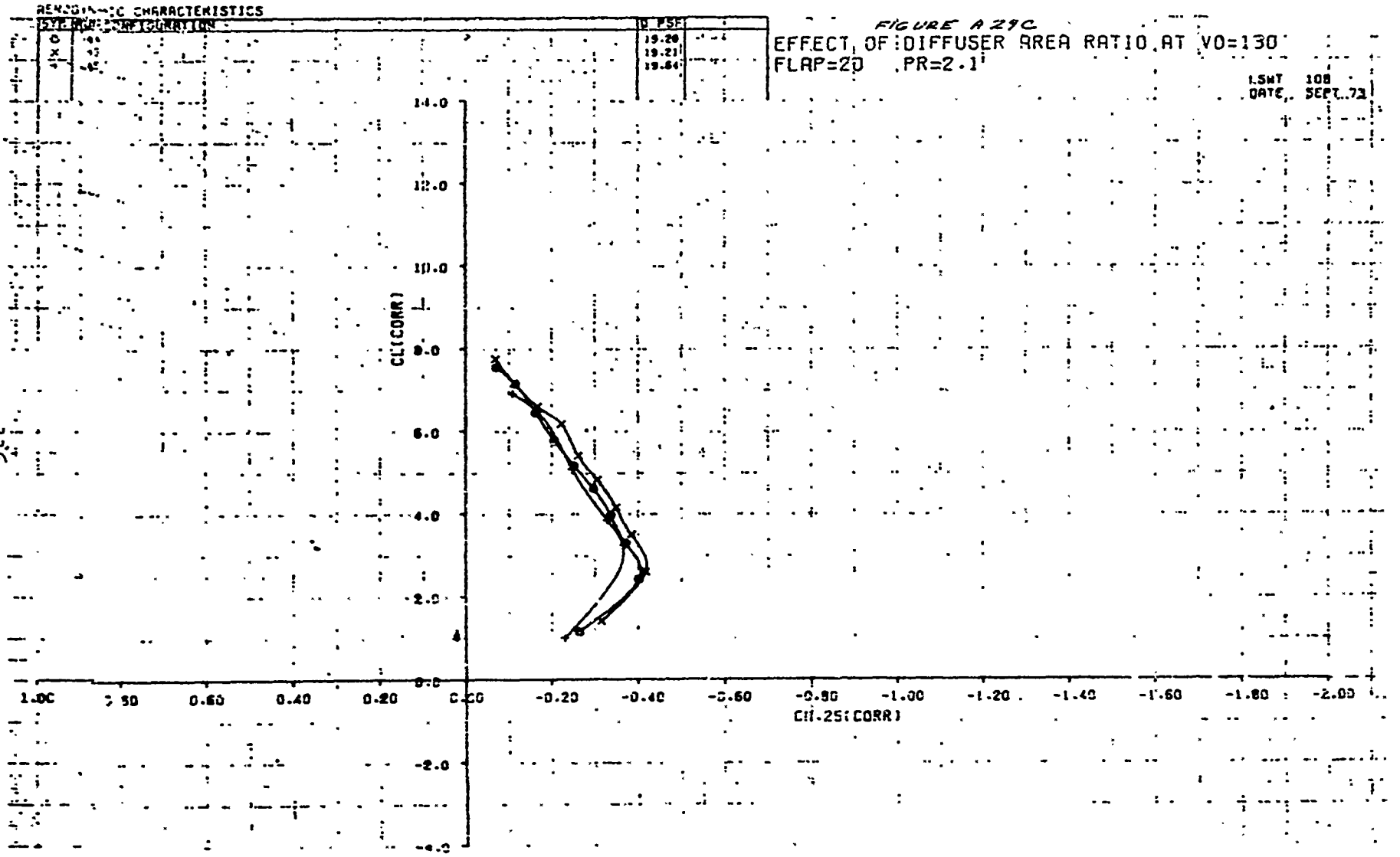
AERODYNAMIC CHARACTERISTICS
CONFIGURATION
Q PSF
19.20
19.21
19.64
FIGURE A 29C
EFFECT OF DIFFUSER AREA RATIO AT V0=130
FLAP=20 PR=2.1
LSHT 108
DATE, SEPT.73
CL(CORR)
CH.25(CORR)
14.0
12.0
10.0
8.0
6.0
4.0
2.0
-2.0
1.00
0.80
0.60
0.40
0.20
0.00
-0.20
-0.40
-0.60
-0.80
-1.00
-1.20
-1.40
-1.60
-1.80
-2.00

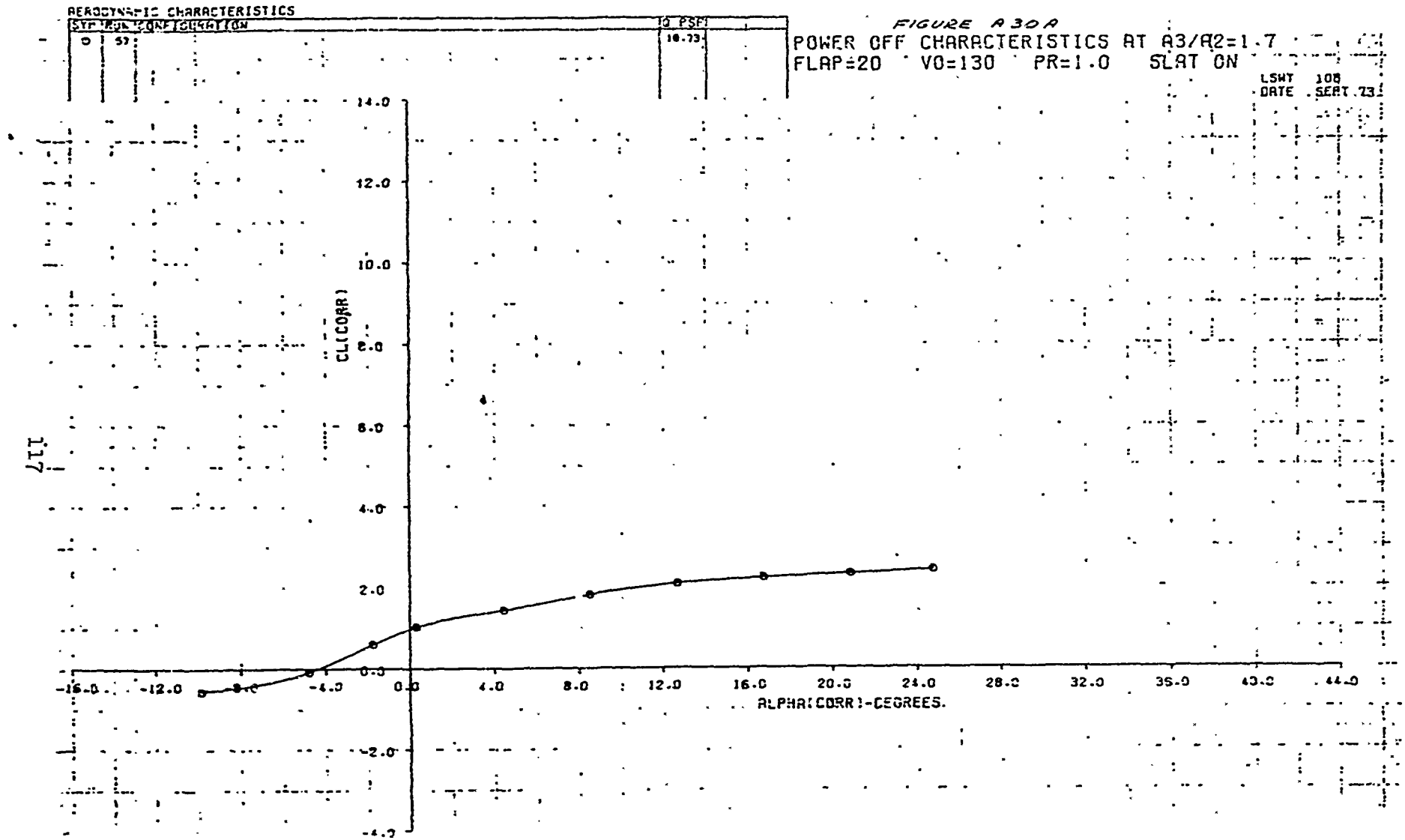

FIGURE A30A

POWER OFF CHARACTERISTICS AT A3/A2=1.7

FLAP=20 V0=130 PR=1.0 SLAT ON

LSWT 108
DATE SEAT 73

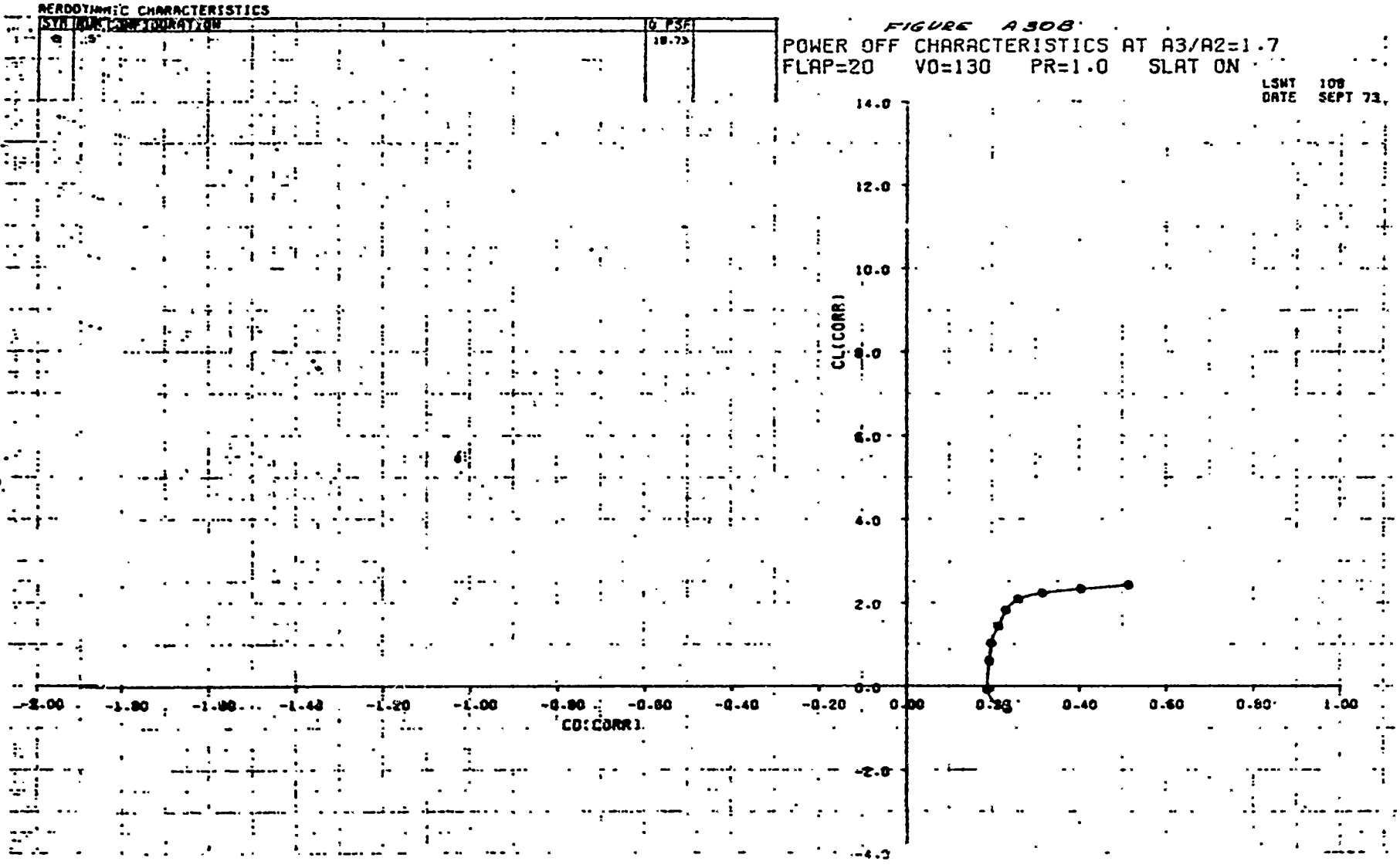
AERODYNAMIC CHARACTERISTICS
Q PSF
18.73
FIGURE A30B
POWER OFF CHARACTERISTICS AT A3/A2=1.7
FLAP=20 V0=130 PR=1.0 SLAT ON
LSWT 108
DATE SEPT 73
CL(CORR)
CD:CORR)
14.0
12.0
10.0
8.0
6.0
4.0
2.0
0.0
-2.0
-4.0
-2.00
-1.80
-1.60
-1.40
-1.20
-1.00
-0.80
-0.60
-0.40
-0.20
0.00
0.20
0.40
0.60
0.80
1.00

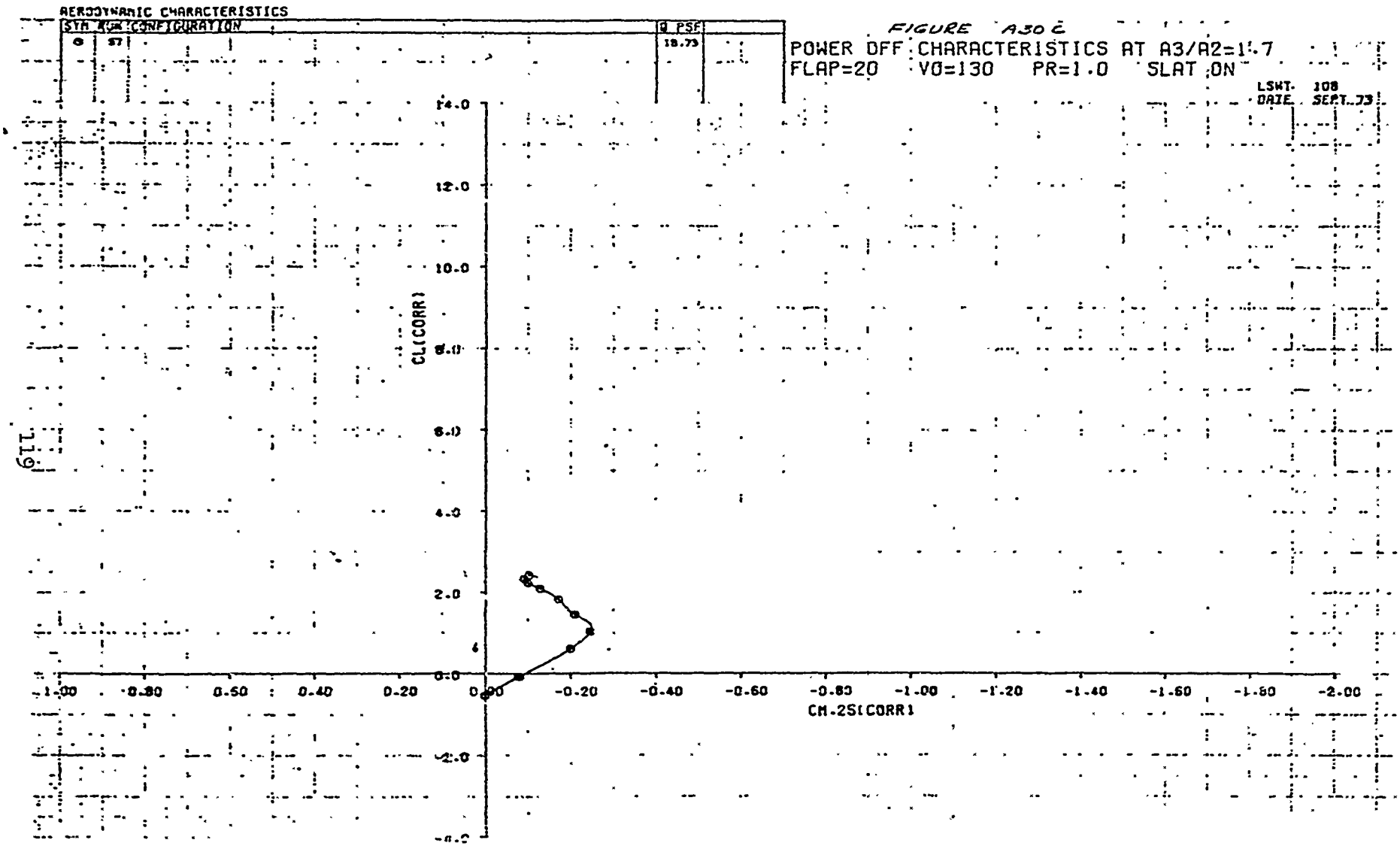
AERODYNAMIC CHARACTERISTICS
SYM CONFIGURATION
Q PSF
18.73
FIGURE A30 C
POWER OFF CHARACTERISTICS AT A3/A2=1.7
FLAP=20 V0=130 PR=1.0 SLAT ON
LSWT- 108
DATE SEPT.73
CL(CORR)
CM-2S(CORR)
14.0
12.0
10.0
8.0
6.0
4.0
2.0
0.0
-2.0
-1.00
-0.80
-0.60
-0.40
-0.20
0.00
-0.20
-0.40
-0.60
-0.80
-1.00
-1.20
-1.40
-1.60
-1.80
-2.00

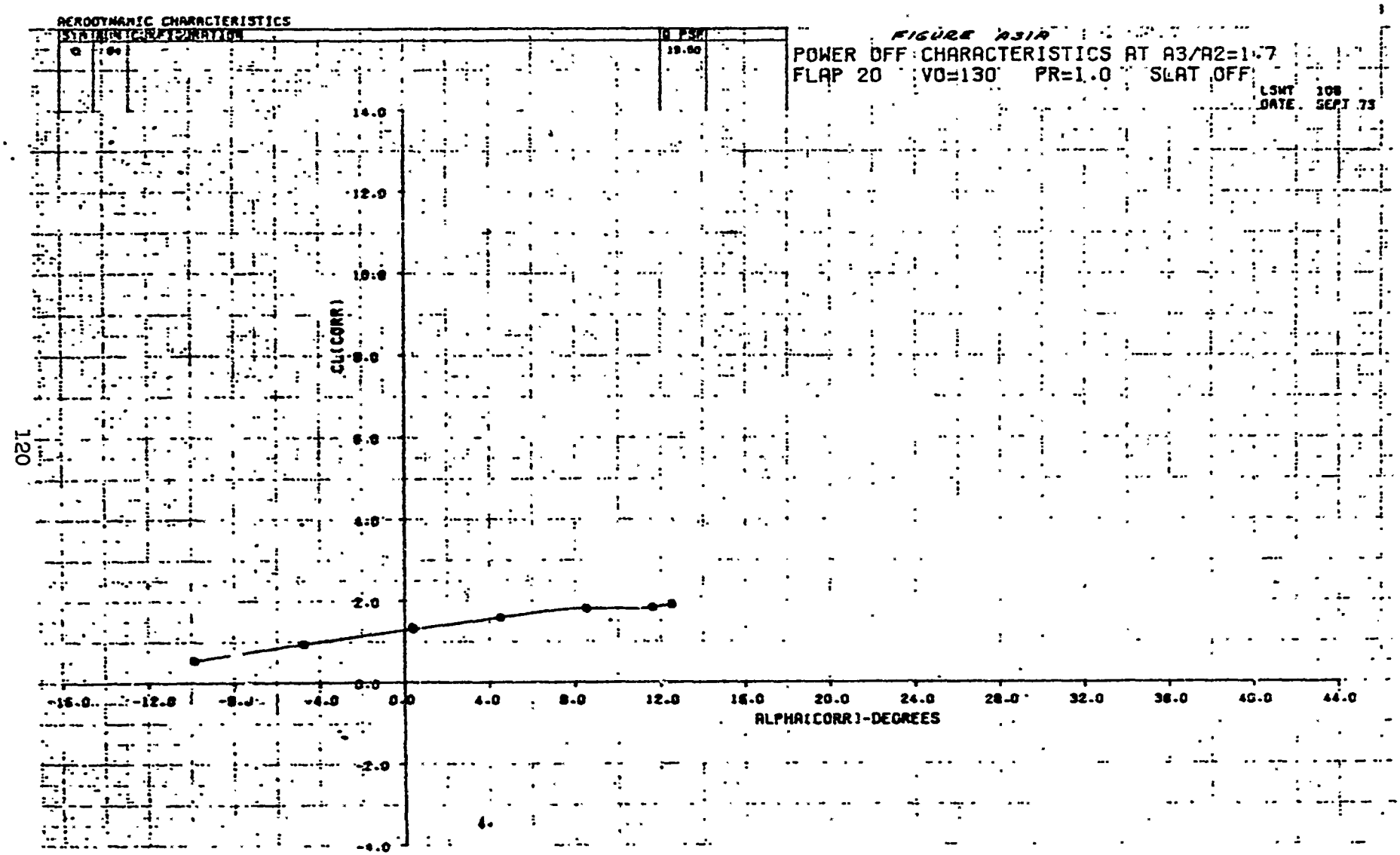
AERODYNAMIC CHARACTERISTICS
STABILITY AXIS
Q 7.00
Q PSF 19.00
FIGURE A31A
POWER OFF CHARACTERISTICS AT A3/A2=1.7
FLAP 20 VO=130 PR=1.0 SLAT OFF
LSWT 108
DATE SEPT 73
CL(CORR)
14.0
12.0
10.0
8.0
6.0
4.0
2.0
0.0
-2.0
-4.0
-16.0
-12.0
-8.0
-4.0
0.0
4.0
8.0
12.0
16.0
20.0
24.0
28.0
32.0
36.0
40.0
44.0
ALPHA(CORR)-DEGREES

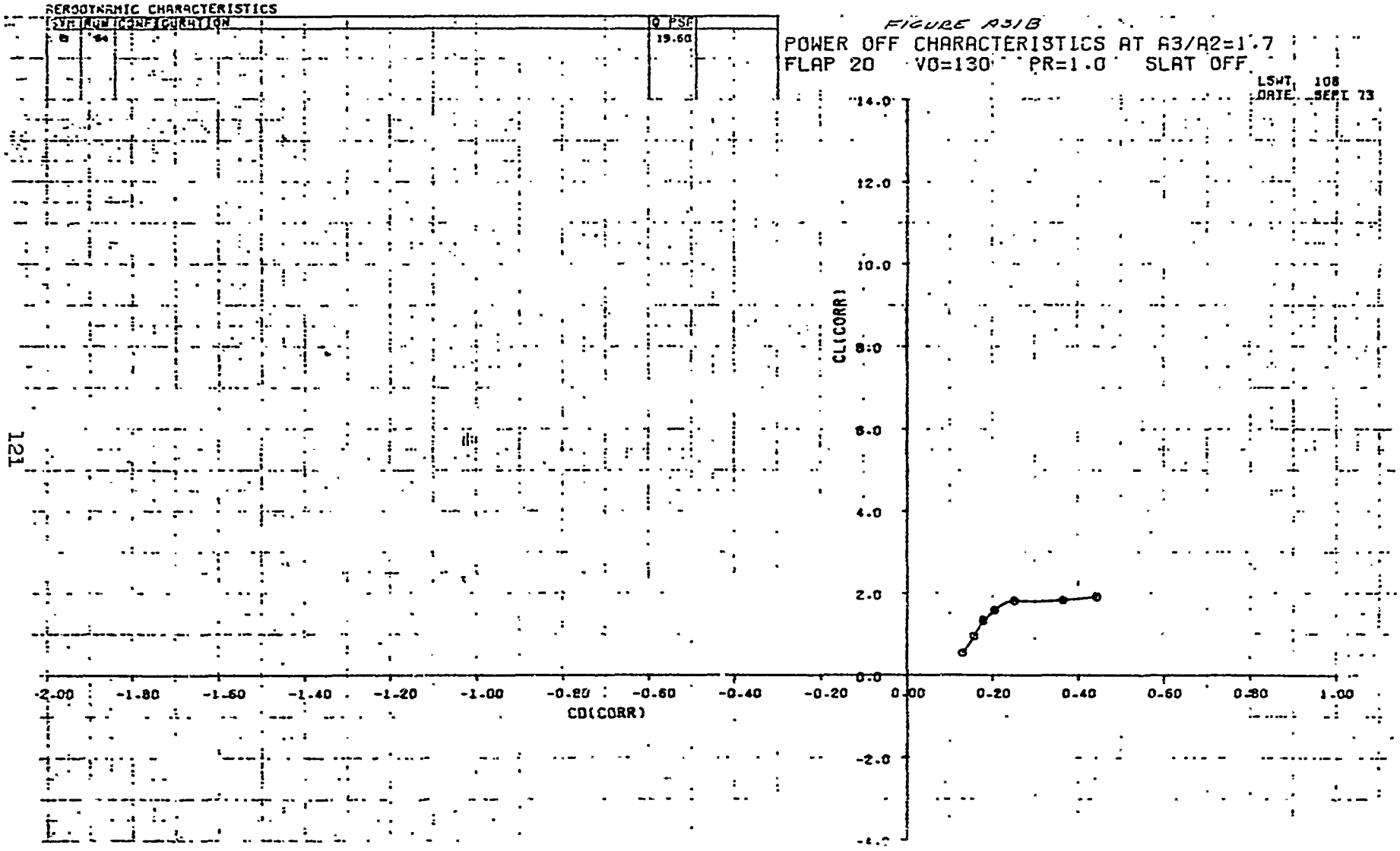

FIGURE A31B

POWER OFF CHARACTERISTICS AT A3/A2=1.7

FLAP 20 V0=130 PR=1.0 SLAT OFF

LSWT 108
DATE SEPT 73

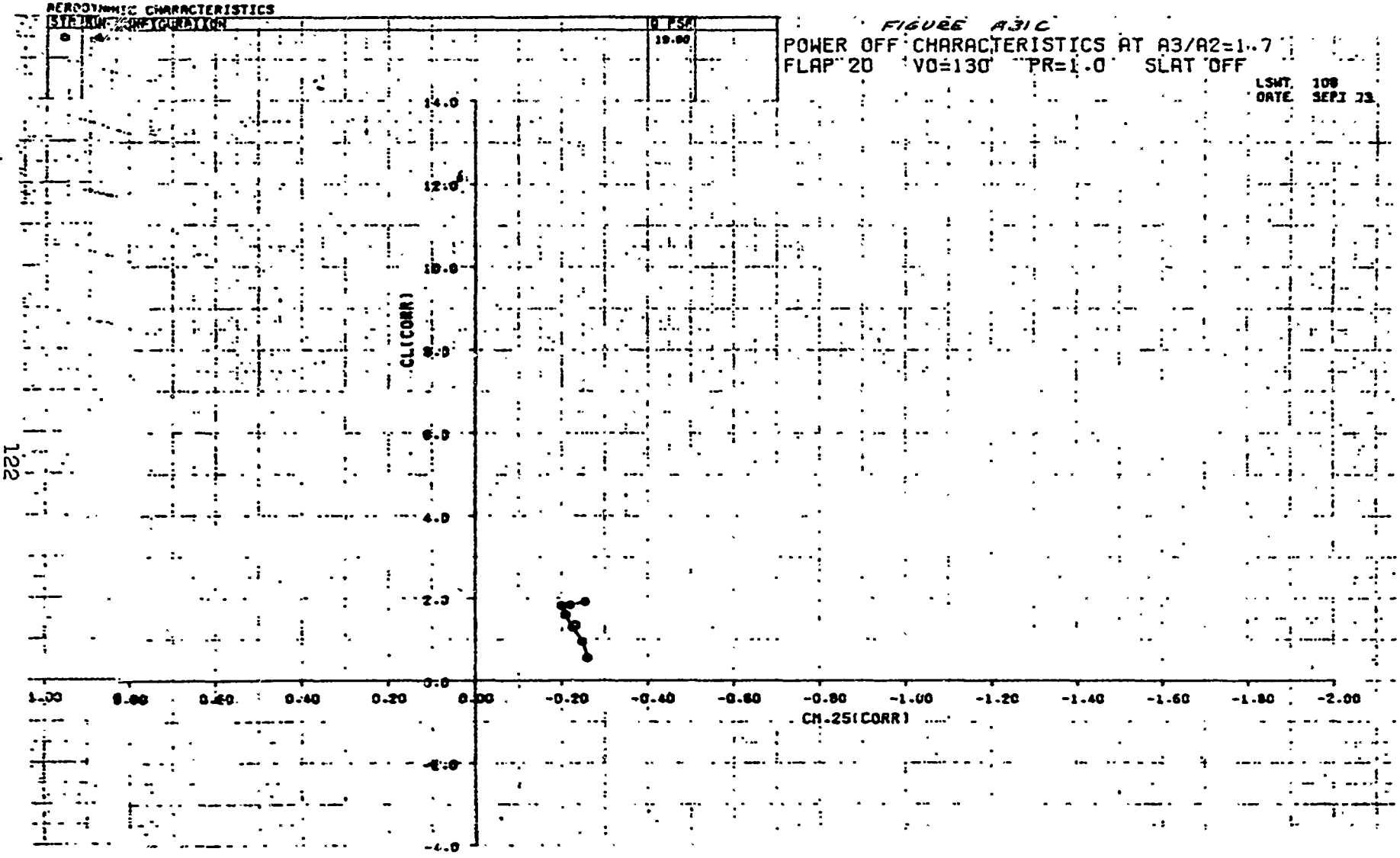
AERODYNAMIC CHARACTERISTICS
STETSON CONFIGURATION
0 PSF
19.00
FIGURE A31C
POWER OFF CHARACTERISTICS AT A3/A2=1.7
FLAP 20 VO=130 PR=1.0 SLAT OFF
LSWT. 108
DATE SEPT 73
CL(CORR)
14.0
12.0
10.0
8.0
6.0
4.0
2.0
0.0
-4.0
1.00
0.80
0.60
0.40
0.20
0.00
-0.20
-0.40
-0.60
-0.80
-1.00
-1.20
-1.40
-1.60
-1.80
-2.00
CM.25(CORR)

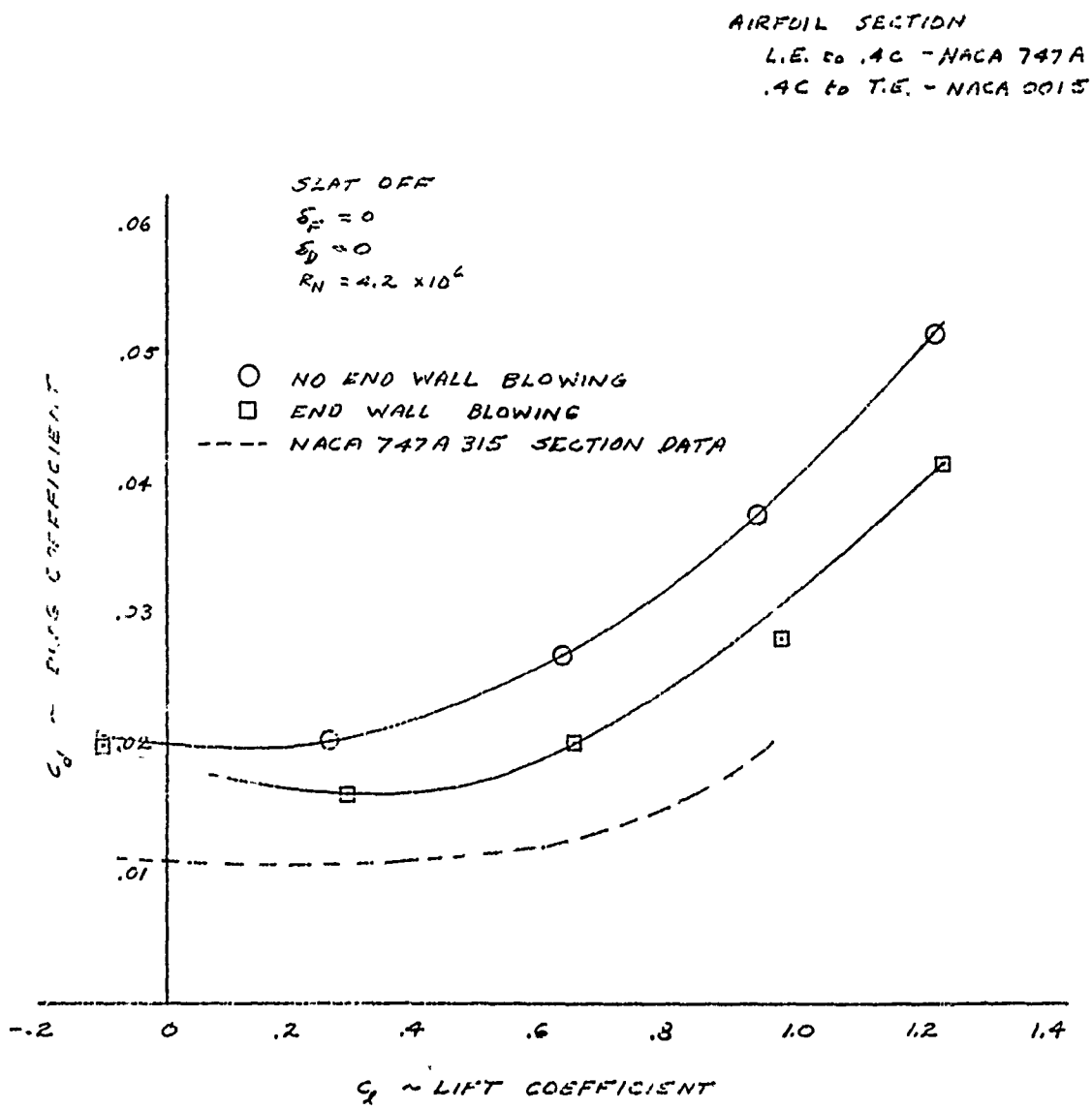

FIGURE 86. CTA 2D CLEAN WING DRAG CHARACTERISTICS

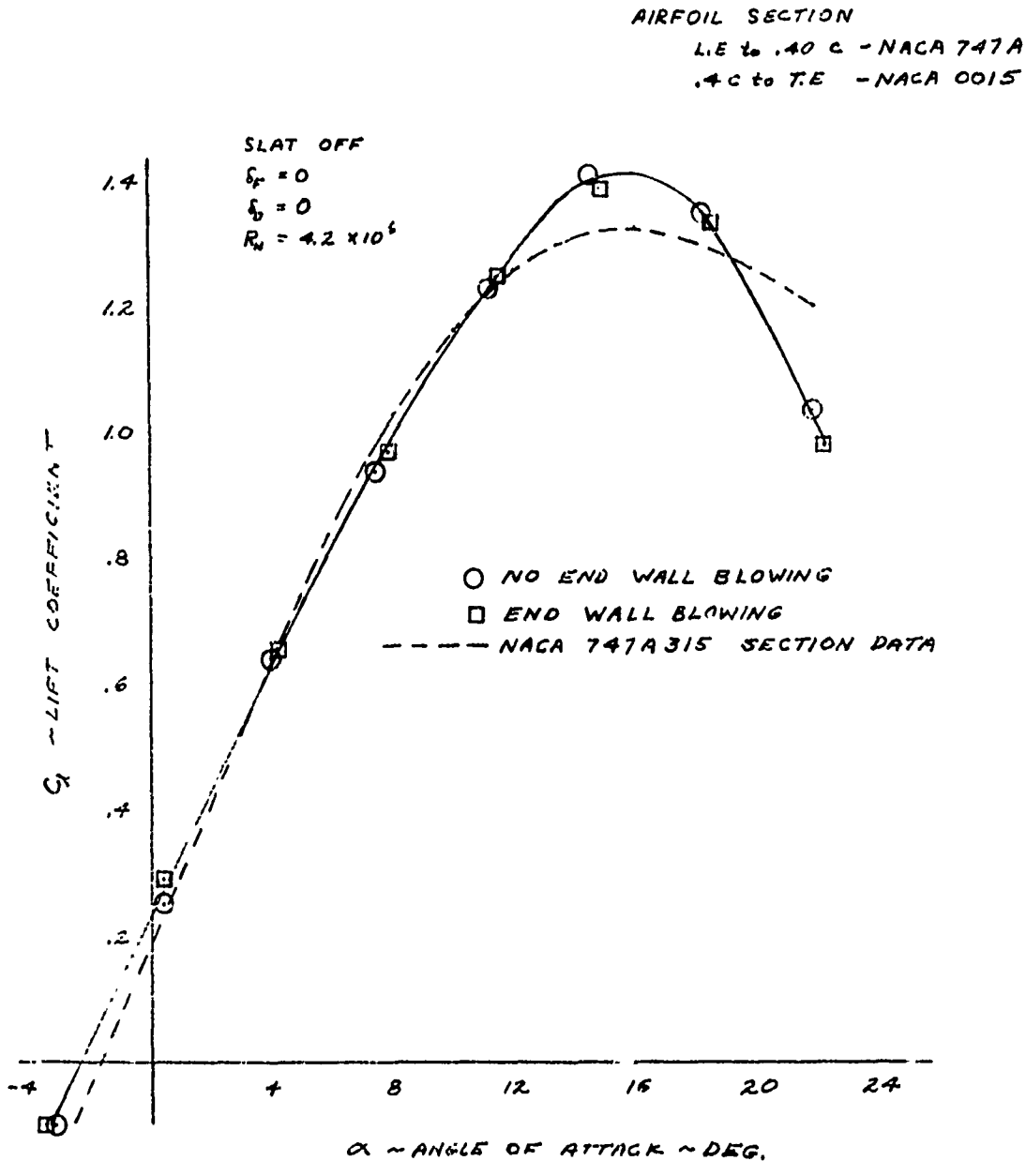

FIGURE 87. CTA 2D CLEAN WING LIFT CHARACTERISTICS

SLAT OFF
$\delta_F = 0$
$\delta_D = 0$
$R_N = 4.2 \times 10^6$

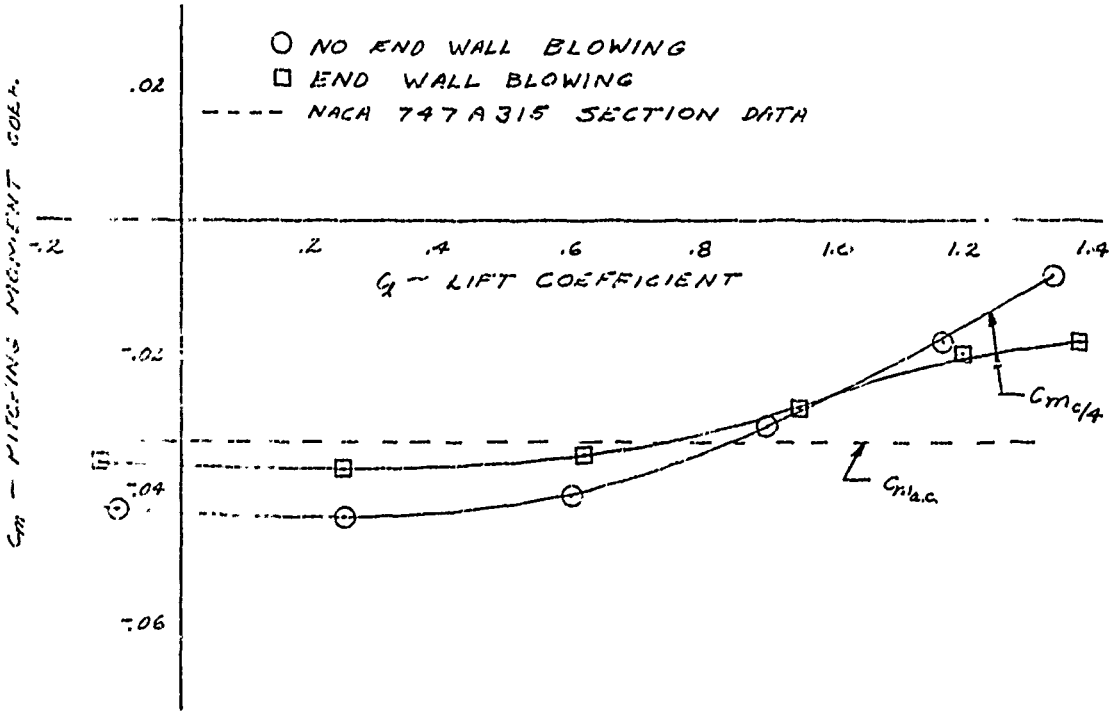

FIGURE 88. CTA 2D CLEAN WING PITCHING MOMENT

APPENDIX B

DETERMINATION OF EJECTOR NOZZLE PERFORMANCE

There has been much confusion concerning the values of the geometric and effective primary nozzle areas, how they were determined, and how they influenced the value of the inlet area ratio (A_1/A_o). This note explains the origin and gives an explanation of the following three sets of primary nozzle area values.

A) The final set of pretest predictions
B) A set of values for a typical test as they appear on the test data printout sheet.
C) The post test assessment of the most probable actual values of each number in the set.

Also shown for reference are the results for the hypermixing nozzles, both FDL and ARL sizes, during calibration and selected test.

The values shown are defined as follows.

I. NOZZLE DEFINITIONS

A. Primary Nozzle Geometric Exit Area (AG)

1. Hypermixing Nozzles

For the hypermixing nozzles this value is the sum total of the exit areas of each of the six exit openings. Each area is defined as the opening length times the width. The width of the opening nearest the nozzle base is defined as in sketch a) and the width of the remaining openings are defined as shown in sketch b).

2. Inlet Blowing Slot

The inlet slot nozzle area is, strictly speaking, not the exit area but the slot throat area which is 0.156 inches (1/2 spacer washer diameter) back from the nozzle exit plane. The area is defined as the spacer thickness times the ejector span minus the sum of all the spacer diameters.

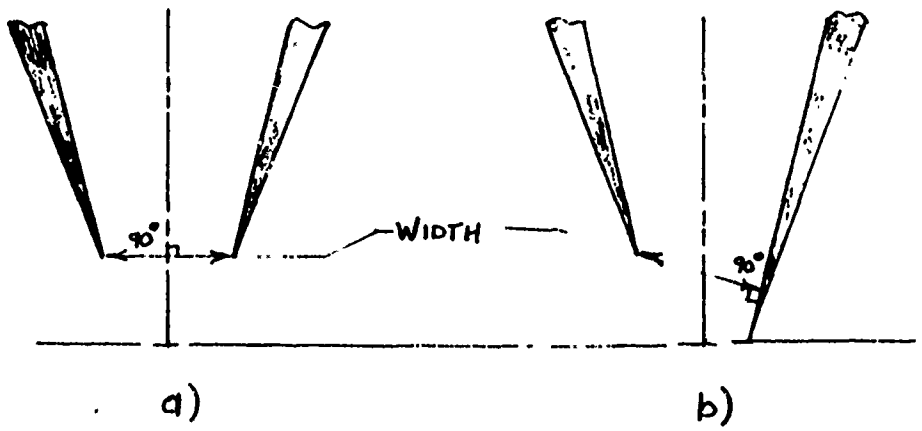

HYPERMIXING NOZZLE EXIT WIDTH

3. Diffuser Blowing Slot

The diffuser slot nozzle area is defined as the ejector span times the slot width. Although there is no good way to confirm it, the diffuser nozzles are designed so that the minimum slot width occurs at the nozzle exit plane.

B. Primary Nozzle Effective Exit Area (A_o)

The effective area of each primary nozzle is defined as the nozzle throat area required to pass the same flowrate for a flow expanding isentropically from the nozzle plenum conditions to an ambient back pressure. The location in the plenum at which the total temperature and pressure is measured is undefined and the location at which the ambient back pressure is measured is also undefined. The details of the instrumentation locations and method of computing effective area for the wind tunnel test program are reported in Section VI.

C. Nozzle Coefficients, C_D, C_V, C_C

These coefficients are the classic nozzle discharge, velocity, and contraction coefficients and are related as follows.

$$C_D = C_V \times C_C$$

The discharge coefficient is defined as,

$$C_D \equiv \frac{A_o}{A_G} .$$

The velocity coefficient (C_V), known as the nozzle efficiency (η_N) by ARL, is defined as follows:

$$\eta_N \equiv \frac{F}{\dot{m} V_e'} \doteq \frac{V_e}{V_e'} = C_V$$

F = measured thrust of a single isolated nozzle

$\dot{m}$ = measured mass flowrate through the nozzle

V_e' = isentropic exit velocity based on the ratio of the nozzle plenum (total) pressure to the ambient back pressure.

V_e = actual mean nozzle exit velocity.

The approximately equal symbol is replaced by an equal symbol for cases where the nozzle exit flow is perfectly expanded (pc = pa).

D. Secondary Stream Inlet Area (A_1)

The area available to the secondary stream at the ejector inlet is difficult to determine exactly. The value A_1 which approximates this area very closely has been defined, by mutual agreement between FDL and BELL, as follows,

$$A_1 = A_{inlet} - A_{o_{inlet}} - A_{o_{HYP}}.$$

A_{inlet} = inlet area as defined in the following paragraph

$A_{o_{inlet}}$ & $A_{o_{HYP}}$ = Effective areas of the inlet slot primary nozzle and the hypermixing nozzles, respectively.

The inlet area is defined as the rectangular area lying in the plane passing through the exits of all the hypermixing nozzles. The length of the rectangle is the full ejector span (end plate to end plate). The width is measured from the nozzle base plate to the point where the exit plane intercepts the aft inlet surface.

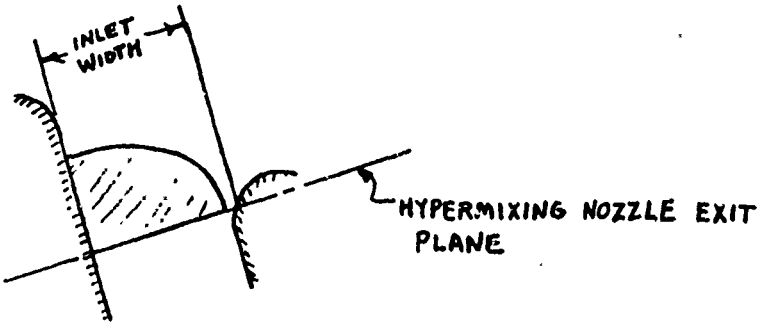

II. NOZZLE AREAS AS DETERMINED FROM TEST RESULTS

A. Pre-test Data Set

An inlet area ratio (A_1/A_o) of 15 was requested by FDL as this value was representative of a group of designs in which they had a current interest and for which no test data existed.

To achieve this value four steps were taken

1) The value of the effective area of the two existing slot nozzles was estimated.

2) Using the estimated slot nozzle effective areas the required hypermixing nozzle effective area was computed from the following equation.

$$A_{o_{HYP}} = A_{inlet} - A_{o_{inlet}} - 15\,(A_{o_{inlet}} + A_{o_{diffuser}})$$

3) The hypermixing nozzle discharge coefficient was estimated and the required geometric area computed.

4) A method of assembling the hypermixing nozzles which would produce the desired geometric area was devised.

Starting with step 1) the existing diffuser slot nozzle effective area was estimated. This nozzle had not been changed since the 1972 Bell IR&D wind tunnel test program so it was decided we would use the effective area as determined in that program. A typical value of 3.10 in^2 was selected based on the performance of this nozzle, during run 66-2 (1972) in particular. This run was chosen because the ejector performed well, the pressure ratio was high (PR = 1.73 in flap plenum) and the value of A_{OD} was near the mean value observed during this test series. The geometric area of this nozzle was computed as follows, based on the dimensions shown on the model drawings.

$$A_G = (0.05)(76.5) = 3.825 \text{ inches}$$

(0.05): Slot Width; (76.5): Ejector Span

The observed discharge coefficient was computed to be,

$$C_D = \frac{3.10}{3.825} = 0.810$$

which seemed to be a reasonable value.

The effective area of the inlet slot could not be determined from the 1972 IR&D tests because a leak from this nozzle had invalidated the measured air flowrate data. In this case the geometric area was computed first.

$$A_G + 0.020\,(76.5 - (51)(.3125)) = 1.21 \text{ in}^2$$

0.020: Spacer Thickness; 76.5: Nozzle Span; 51: No. of spacers; .3125: Spacer Diameter (5/16" washer)

A value of C_D of 0.90 was assumed based on past experience with slot nozzles..

The effective area was then computed.

$$A_{o_{inlet}} = (0.90)(1.21) = 1.09 \text{ in}^2$$

Moving on to step 2) the inlet area was computed based again on dimensions taken from the model drawing in accordance with the definition of inlet area given previously.

$$A_{inlet} = (5.15)(76.5) = 393.98 \text{ in}^2$$

The required hypermixing nozzle effective area was then computed. However, when the computation was made an effective area of 1.17 (not 1.09) was used for the inlet slot nozzle. This was because spacing washers having a 7/16" diameter (instead of 5/16" and .024" thick instead of .020" thick) were called out on the drawings in existence at the time this calculation was made.

$$A_{o_{HYP}} = \frac{393.98 - 1.17 - 15\ (1.17 + 3.10)}{16}$$

$$= 20.54 \text{ in}^2$$

Proceeding to step 3) the hypermixing nozzle discharge coefficient was estimated. This was based on the past performance of the ARL hypermixing nozzle as it was known in March 1970. First the geometric area was computed using the dimensions obtained from Bell Drawing 2445-976020. This value was computed as,

$$A_G = 0.579 \text{ in}^2/\text{nozzle}.$$

The computations used in determining this area are presented in Table X.

OPENING	$\bar{\theta}$	SIN θ	SIN $\frac{1}{2}\theta$	COS $\frac{1}{2}\theta$	W INCHES	L INCHES	AREA INCHES^2
1 (TIP)	14	.24192	.12187	.99255	.113	.784	0.0887
2	15	.25882	.13053	.99144	.115	.768	0.0883
3	16	.27564	.13917	.99027	.117	.768	0.0896
4	18	.30902	.15643	.98769	.120	.768	0.0922
5	19	.32557	.16505	.98629	.122	.768	0.0935
6 (BASE)	22	.19438 = TAN $\phi/2$			.1292	.984	0.1271
						TOTAL =	0.5794 = A_G

ALL DIMENSIONS TAKEN FROM DWG. BELL 2445-976020

$$W = 0.088 + (2)(0.106 \times \text{TAN}(\theta/2)) \quad \text{, OPENING 1}$$

$$W = \left(\frac{0.106}{\text{Cos}\,\theta/2} + \frac{0.044}{\text{SIN}\,\theta/2} \right) \text{SIN}\,\theta \quad \text{, OPENINGS 2-6}$$

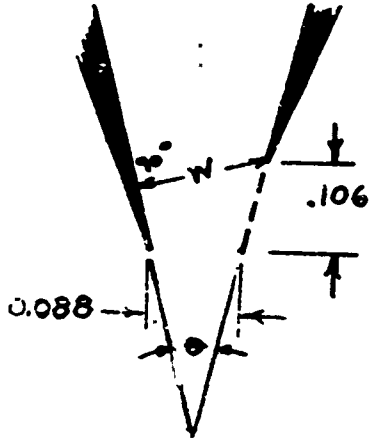

TABLE X

HYPERMIXING NOZZLE GEOMETRIC AREA

The effective area of these nozzles was stated by ARL to be 0.486 in^2 in July 1971 and 0.477 in March 1972 during discussions with G. Salter. Based on these discussions, a value of 0.48 in^2 was assumed. The resulting C_D;

$$C_D = \frac{0.48}{0.58} = 0.828$$

was also assumed to apply to the large exit FDL nozzles. The required geometric area was then determined to be;

$$A_{G_{HYP}} = 20.54/.828 = 24.81 \text{ in}^2$$

$$A_{G_{HYP}} = 24.81/30 = 0.827 \text{ in}^2/\text{nozzle}$$

Completing the set of pre-test predictions, a value of C_C of 1.00 was assumed for the hypermixing nozzles, that is no separation was assumed at any of the spacers or turning radii into the hypermixing nozzle. The final estimate of inlet area ratio was,

$$A_1/A_o = \frac{393.98 - 1.09 - 20.54}{20.54 + 1.09 + 3.10} = \frac{372.35}{24.73} = 15.06$$

and was considered close enough to the desired value of 15.

Step 4) involved scaling up existing drawings for the ARL nozzles and then building a suitable fixture to hold the exit at the proper dimensions as it was being assembled. It was subsequently determined that both of these procedures were done incorrectly but this will be discussed later.

B. Typical Test Data Set

The values of effective area did not vary widely from test to test except in the case of clearly identified equipment failures. The values did vary slightly however, so for the sake of this example all data in this set will be taken from a specific run. The run selected was 3-3. The primary nozzle pressure ratios were as follows.

PR = 1.869 Hypermixing
= 1.851 Inlet slot
= 1.834 Diffuser slot

The computed values of A_o based on the measured test data for air flowrate, total pressure and total temperature are shown in Table XI.

The values of geometric area were assumed to be the same as those determined in the pre-test estimates. They are shown in parenthesis because they were not actually determined during the course of the tests.

The values of the apparent discharge coefficients are also shown in parenthesis in Table I. These were determined by dividing the effective areas of the nozzles as determined by testing, by the geometric values determined before the tests.

C. Post Test Assessment

The test results deviated significantly from the pre-test predictions requiring a post test evaluation to assess the reasons for the deviations and to estimate the most probable values of the nozzle areas and discharge coefficients.

The most obviously unusual result seen in the data set for test 3-3 was the top slot discharge coefficient of 1.22. This value was always greater than one, being on the average about 1.16 (1.40/1.21 = 1.16). This problem is discussed in Section V and is attributed to leakage. No evidence exists that A_G was other than its design value of 1.21. The probable value of C_D of 0.85 has been selected based on Figure 8 of Reference 5. The slot flow Reynolds Number ranged between 1.28 and 1.51 x 10^4, and the L/D = 50 curve was selected as the most representative of the inlet slot. The product of the design geometric area (1.21) and the assumed C_D (.85) yields the estimated effective area, A_o (1.03).

DATA SET	NOZZLE TYPE	A_G * IN.^{2}	C_D	A_o * IN.^{2}	A_1 IN.^{2}	A_1/A_o	C_V	C_c
PRE-TEST	HYPER	24.81	.828	20.54			~.828	~1.00
	INLET	1.21	.900	1.09			.90	1.00
	DIFFUSER	3.825	.810	3.10			.81	1.00
	TOTAL			24.73	372.35	15.06		
TYPICAL TEST RUN 3-3	HYPER	(24.81)	(0.608)	15.09				
	INLET	(1.21)	(1.22)	1.48				
	DIFFUSER	(3.825)	(0.865)	3.31				
				19.88	377.41	18.98		
POST TEST ASSESMENT	HYPER	19.81	.772	15.30				
	INLET	1.21	.850	1.03				
	DIFFUSER	4.36	.700	3.06				
				19.39	377.64	19.48		
					OR			
					366.16	18.88		
FDL NOZZLE CALIBRATION	HYPER	16.71	0.918	15.33				
		[.557]		[.511]				
ARL NOZZLE CALIB. (PR=1.42)	HYPER	.579 (1)	0.696	.403				
		.528 (2)	0.763					
ARL NOZZLE TYPICAL TEST RUN 59-1, PR=1.55	HYPER			.375 (3)				

(1) A_G BASED ON DWG (2) A_G BASED ON FDL MEASUREMENT (3) DECREASES WITH INCREASING PR & TIME.

* VALUE FOR 30 NOZZLES, EXCEPT FOR [BRACKETED] VALUES WHICH ARE SINGLE NOZZLE VALUES

TABLE XI

NOZZLE EFFECTIVE AREA

An evaluation of the diffuser slot data as well as on-site inspection during the test program indicated that there was on occasion a leak from the flap plenum through the sealed flap upper surface blowing slot. The average value of the diffuser slot effective area, immediately after the flap slot was resealed, was 3.06. Post test inspection revealed, however, that the diffuser slot gap was not 0.05 inches as had been thought but varied along its length between the values of 0.051 and 0.064 being most generally 0.057 inches. The true geometric area of this nozzle was re-estimated as 4.36 inches^2 (0.057 x 76.5). The resulting discharge coefficient of 0.70 is considerably less than the value of 0.86 which would be predicted on the basis of the data in reference 5. This low value of discharge coefficient is thought to be the result of the pressure losses at the nozzle inlet. This is also discussed briefly in Section IV.

The most important and unfortunately the most difficult data to interpret concerns the hypermixing nozzles. The main reason the resulting ejector inlet area ratio (A_1/A_o) was closer to 19 than the predicted value of 15 stemmed from the fact that the hypermixing nozzle effective area was on the average only 74.5% (15.30/20.54 or .510/.685) of the design value.

The reason for the low effective area of these nozzles is primarily a consequence of the geometric area being made too small. This was due in large part to a drawing and manufacturing error and is suspected by Bell of being due in part to an erroneous data base upon which the estimate of the hypermixing nozzle discharge coefficient was based. Three values are in question, related as shown below.

$$C_D = A_o/A_G$$

There is general agreement between wind tunnel tests and ARL calibration concerning the value of A_o. The values determined

for A_G by Bell and FDL differ significantly however, leading to widely differing values of C_D.

	Bell	FDL
A_G	.660	.557 in^2 (X30 = values in table B-2)
C_D	.772	.918

The Bell value of geometric area was computed based on a measurement of the nozzle assembly tool and the method of construction. The FDL value is based on direct measurement but the procedure is unknown. Direct measurement would normally provide the more credible value, but the measurement is difficult and the resulting Bell value for C_D seems more in line with the other experimental results. The FDL findings concerning the flow separation at the alteration dividers would seem to indicate that the value of C_D would be less than 0.918.

The determination of the proper C_D value for these nozzles has also been complicated by the calibration of the ARL nozzles and the test nozzles of reference 5. When this data is added the range of possible C_D values for the hypermixing nozzles ranges between the limits of:

$$.65 < C_d < .92$$

The only means of resolving this dilemma appears to be the development of an accurate way of determining nozzle geometric area, then applying this method to a sample of both the FDL and BELL nozzles used in the 1973 CTA-2D wind tunnel model, and then using the areas so determined to recompute the C_D values.

Finally, two values of inlet secondary flow area (A_1) are shown. One represents the case where the aft inlet is in its design position. The smaller value represents the final configuration after the aft inlet rotated until it touched the hypermixing nozzle tips.

VIII REFERENCES

1. Benedict, Robert P., "Fundamentals of Temperatures, Pressure, and Flow," John Wiliy & Sons, Inc., 1959.
2. Alan Pope, "Wind Tunnel Testing," John Wiliy & Sons, Inc., Second Edition 1954.
3. Anon.; "Low Speed Wind Tunnel User Manual," Lockheed-Georgia Company, Report No. ER-11000, May 1970.
4. "Fluid Meters, Their Theory and Applications," Report of ASME Research Committee on Fluid Meters, 5th Edition, 1959.
5. Peschke, W. "Advanced Ejector Thrust Augmentation Study-Mass Entrainment of Axisymmetric and Rectangular Free Jets" Technical Report AFFDL-TR-73-55, April 1973.